Hydrogeologic Investigation, Water Chemistry Analysis, and Model Delineation of Contributing Areas for City of Tallahassee Public-Supply Wells, Tallahassee, Florida

By J. Hal Davis and Brian G. Katz

Prepared in cooperation with the
City of Tallahassee

Scientific Investigations Report 2007-5070

U.S. Department of the Interior
U.S. Geological Survey

U.S. Department of the Interior
DIRK KEMPTHORNE, Secretary

U.S. Geological Survey
Mark D. Myers, Director

U.S. Geological Survey, Reston, Virginia: 2007

For product and ordering information:
World Wide Web: http://www.usgs.gov/pubprod
Telephone: 1-888-ASK-USGS

For more information on the USGS--the Federal source for science about the Earth, its natural and living resources, natural hazards, and the environment:

World Wide Web: http://www.usgs.gov
Telephone: 1-888-ASK-USGS

Suggested citation:
Davis, J.H., and Katz, B.G., 2007, Hydrogeologic Investigation, Water Chemistry Analysis, and Model Delineation of contributing Areas for City of Tallahassee Public-Supply Wells, Tallahassee, Florida: U.S. Geological Survey Scientific Investigations Report 2007-5070, 67 p.

Contents

Figures

Tables

Conversion Factors

Multiply	By	To obtain
	Length	
inch (in.)	2.54	centimeter
inch (in.)	25.4	millimeter
foot (ft)	0.3048	meter
mile (mi)	1.609	kilometer
	Area	
square mile (mi^2)	2.590	square kilometer
	Flow rate	
gallon per minute (gal/min)	0.06309	liter per second
inch per year (in/yr)	25.4	millimeter per year
	Hydraulic conductivity	
foot per day (ft/d)	0.3048	meter per day
	Transmissivity*	
foot squared per day (ft^2/d)	0.09290	meter squared per day
	Temperature	

Degrees Fahrenheit (°F) may be converted to degrees Celsius (°C) as follows: °C = (°F-32)/1.8

Abbreviations and Acronyms

cm^3	cubic centimeter
mg/L	milligram per liter
mL	milliliter
TU	tritium unit
µg/L	microgram per liter

Ar	Argon
CO2	Carbon dioxide
CFC	Chlorofluorocarbon
FDEP	Florida Department of Environmental Protection
^3H	Tritium
^3He	Helium-3
$^3He_{trit}$	Tritiogenic helium-3
^4He	Helium-4
N_2	Nitrogen
Ne	Neon
P	Tetrachloroethylene
SF_6	Sulfur hexafluoride
TDCZ	Time-dependent capture zones
USGS	U.S. Geological Survey

Vertical coordinate information is referenced to the North American Vertical Datum of 1988 (NAVD 88).

Historical data were collected and stored as National Geodetic Vertical Datum of 1929 (NGVD 29).

Horizontal coordinate information is referenced to the North American Datum of 1983 (NAD 83).

Altitude, as used in this report, refers to distance above the vertical datum.

*Transmissivity: The standard unit for transmissivity is cubic foot per day per square foot times foot of aquifer thickness [$(ft^3/d)/ft^2$]ft. In this report, the mathematically reduced form, foot squared per day (ft^2/d), is used for convenience.

Hydrogeologic Investigation, Water Chemistry Analysis, and Model Delineation of Contributing Areas for City of Tallahassee Public-Supply Wells, Tallahassee, Florida

By J. Hal Davis and Brian G. Katz

Abstract

Ground water from the Upper Floridan aquifer is the sole source of water supply for Tallahassee, Florida, and the surrounding area. The City of Tallahassee (the City) currently operates 28 water-supply wells; 26 wells are distributed throughout the City and 2 are located in Woodville, Florida. Most of these wells yield an ample supply of potable water; however, water from several wells has low levels of tetrachloroethylene (PCE). The City removes the PCE from the water by passing it through granular-activated carbon units before distribution. To ensure that water-supply wells presently free of contamination remain clean, it is necessary to understand the ground-water flow system in sufficient detail to protect the contributing areas.

Ground-water samples collected from four public-supply wells were analyzed for tritium (^3H), chlorofluorocarbons (CFCs), and sulfur hexafluoride (SF_6). Using data for the CFC compounds, apparent ground-water ages ranged from 7 to 31 years. For SF_6, the apparent ages tended to be about 5 to 10 years younger than those from CFCs. Apparent ages based on the tritium/tritiogenic helium-3 ($^3H/^3He_{trit}$) method ranged from 26 to 33 years. The three dating methods indicate that the apparent age of ground water generally decreases from northern to southern Leon County. This southward trend of decreasing ages is consistent with increasing amounts of recharge that occur as ground water moves from north to south.

The ground-water age data derived by geochemical and tracer analyses were used in combination with the flow model and particle tracking to determine an effective porosity for the Hawthorn clays and Upper Floridan aquifer. The effective porosities for the Upper Floridan aquifer that resulted in best model matches were averaged to produce an effective porosity of 7 percent, and the effective porosities for the Hawthorn clays that resulted in a match were averaged to produce an effective porosity of 22 percent.

Probabilistic contributing areas were determined for 26 City wells using MODFLOW and MODPATH. For each probabilistic contributing area delineated, the model was run 100 times and the results were analyzed statistically. For each of the 100 runs, a different hydraulic conductivity for each of the zones was assigned to the Upper Floridan aquifer. The hydraulic conductivities were generated randomly assuming a lognormal probability distribution; the mean of the distribution was equal to the hydraulic conductivity from the calibrated model.

The 5-year time-dependent capture zones (TDCZs), assuming effective porosities of 0.1, 1, and 7 percent for four representative wells, were delineated. The higher probabilities of capture (greater than 40, 60, and 80 percent) were similar for all effective porosities, and the TDCZ delineated using a 7-percent porosity was slightly smaller; the lower probabilities of capture (greater than 10 and 20 percent) showed a large range of variability.

Introduction

Ground water from the Upper Floridan aquifer is the sole source of water supply for Tallahassee, Florida, and the surrounding area. The City of Tallahassee (the City) currently operates 28 water-supply wells; 26 are distributed throughout the area and 2 are located in Woodville, Florida. Most of these wells yield an ample supply of potable water; however, tetrachloroethylene (PCE) has been detected in water from several wells in concentrations in the low microgram per liter range. The City removes the PCE by passing the water through granular-activated carbon filtration units before distribution. The presence of PCE was first detected in the late 1980s and is attributed to past disposal practices of dry cleaners, service stations, and other businesses within the downtown area. To ensure that water-supply wells, presently free of contamination, remain clean, it is necessary to protect the part of the aquifer from which the wells derive water. Such areas were delineated for five representative City wells by Davis (1996) in a cooperative study between the City, the U.S. Geological Survey (USGS), and the Florida Department of Environmental Protection (FDEP).

The contributing area to a well encompasses the entire part of the aquifer from which the well derives water. If the entire contributing area for a well is delineated, then the size and shape of the contributing area is predominately a function of the recharge rate to the aquifer, the permeability of the aquifer, and the pumping rate of the well. If the delineation of a contributing area is restricted to a zone that will provide water to the well within a set time period, then the porosity must be included in the calculation. This set time period will be designated as the time-dependent capture zone (TDCZ) for the wells in this report.

Purpose and Scope

This report presents the results of a ground-water modeling study to define the contributing areas for 26 City water-supply wells. Additionally, various TDCZs were delineated for representative wells. The porosity, used to delineate some of the TDCZs, was estimated by using various ground-water age dating techniques and comparing these ages to model simulations. The delineation of the contributing areas for the two Woodville wells was not done because the results of ongoing studies south of the City should provide for a more accurate delineation in the near future. The combination of ground-water age dating and model simulation allows for a more accurate prediction of porosity, which is a difficult parameter to estimate for all ground-water models.

Description of Study Area

The study area, as defined by the extent of the regional model, includes about 11,000 mi^2 in north-central Florida and southwestern Georgia (fig. 1). The topography within the study area is characterized by rolling hills and land-surface altitudes that range from 0 ft in the southern part to about 350 ft above NGVD 29 in the northern part. The study area is defined by the major ground-water flow boundaries of the regional ground-water flow system and encompasses the entire recharge area for ground water that moves beneath Leon County (fig. 1). The climate is humid subtropical with relatively high rainfall. The average annual temperature in Tallahassee is 67° F, and the average annual precipitation is about 66 in/yr. The City water-supply wells are widely spread out and are generally located close to the areas being served (fig. 2). All 28 wells are interconnected through distribution lines.

Approach

The contributing areas were delineated using an existing ground-water flow model (Davis, 1996) that was updated with additional data for this study. The additional data consisted of ground-water samples collected from wells and analyzed to determine their age using various isotopes and tracers. The age of ground water, in the context of this report, is the period of time that has passed since recharge occurred. Generally, this period will consist of the time it takes ground water to move through the surficial and Upper Floridan aquifers to a well. The ground-water age data were then used in combination with the model to determine the effective porosity of the aquifer to determine TDCZs for some wells.

Geologic and Hydrologic Framework

This section describes the relation of geologic units, hydrogeologic units, and model layers in north-central Florida and southwestern Georgia. The ground-water flow system, long-term water-level trends, and recharge to the Upper Floridan aquifer and porosity development in the study area also are described.

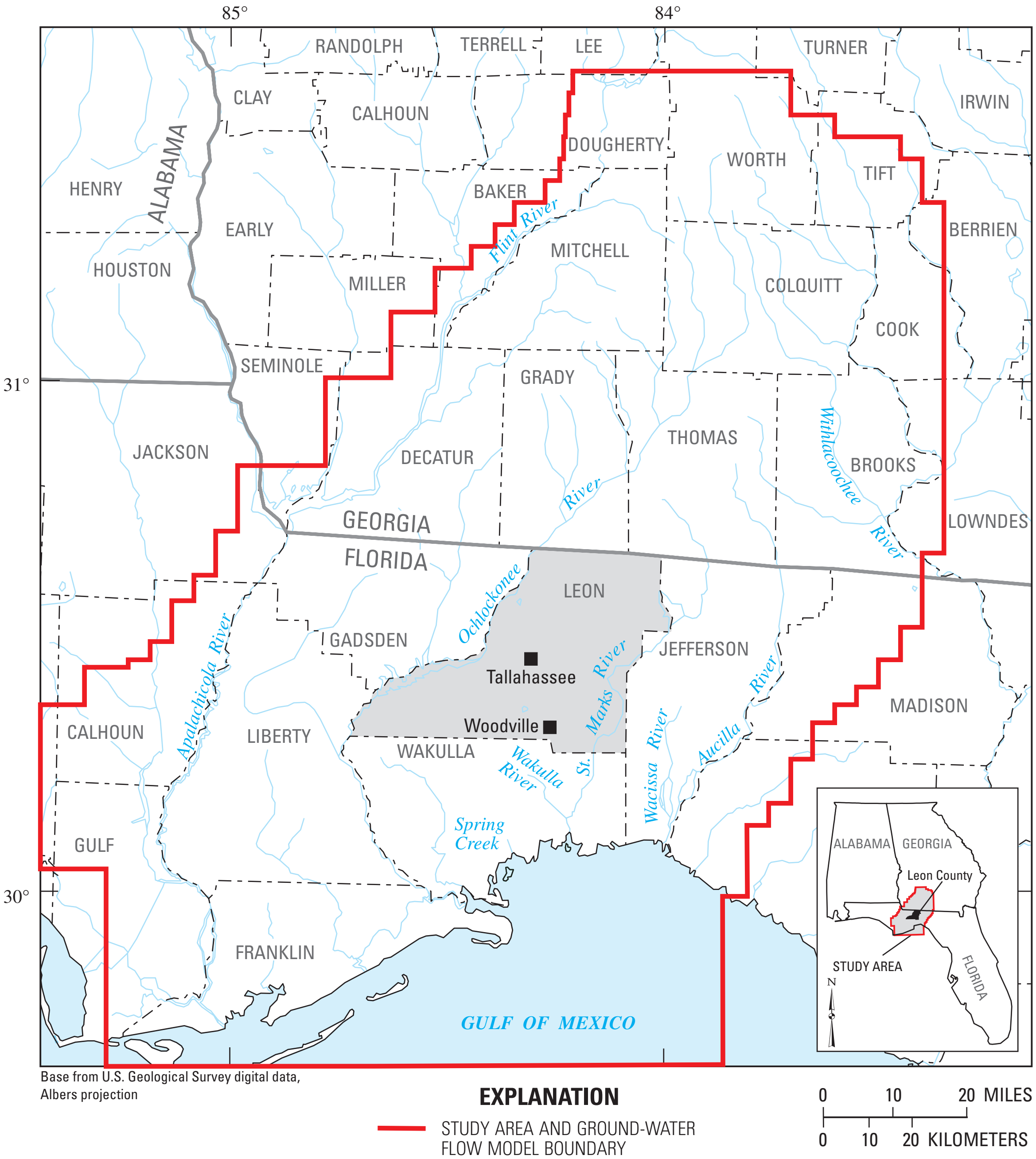

Figure 1. Study area in north-central Florida and southwestern Georgia.

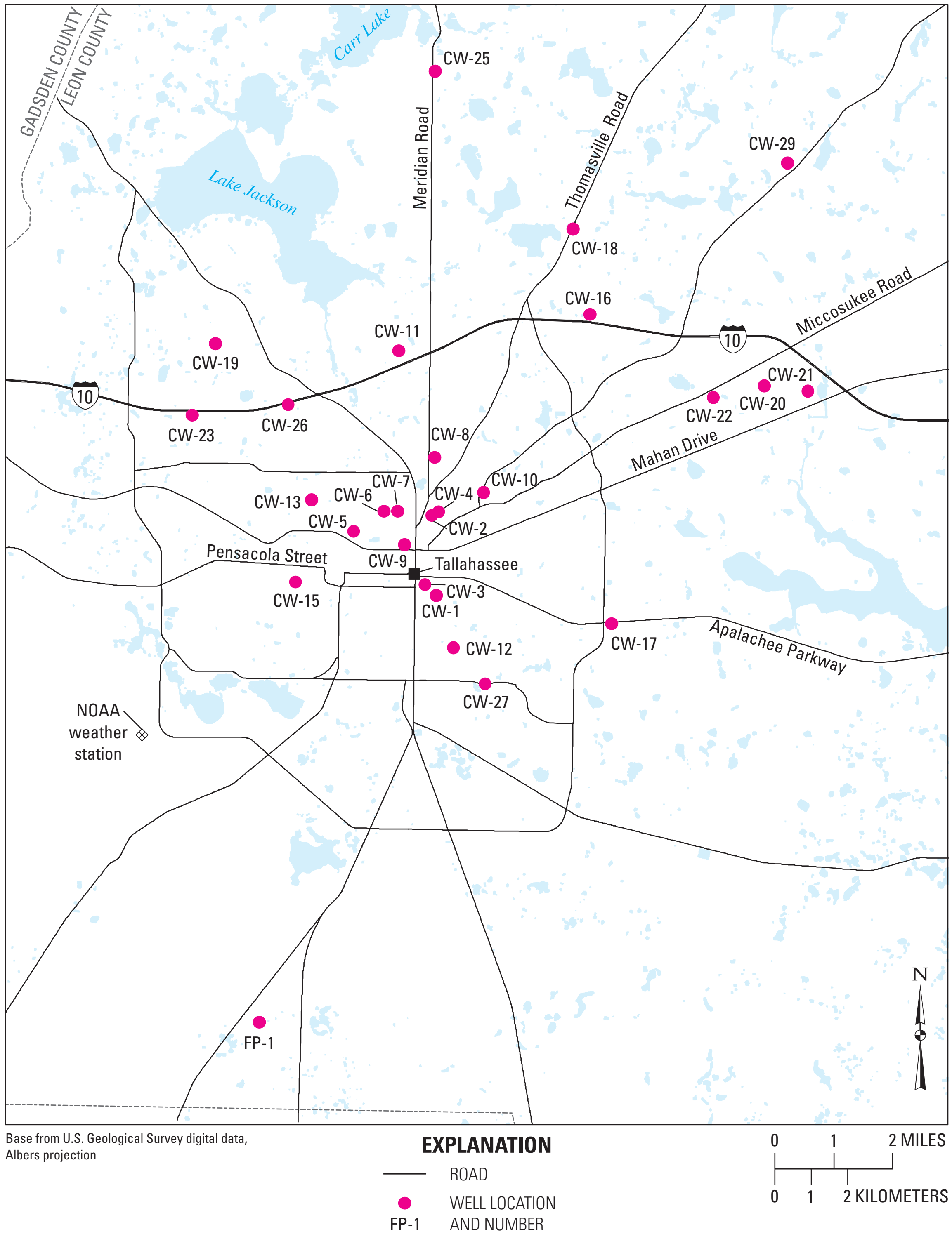

Figure 2. Location of the City of Tallahassee water-supply wells and National Oceanographic Atmospheric Administration monitoring station.

Geologic Setting

The study area is underlain by sedimentary rocks of Tertiary through Quaternary age that consist of limestone, dolostone, clay, and sand of varying degrees of lithification (Miller, 1986). These rock units generally slope downward toward the south and the Gulf of Mexico. A list of geologic units, their relation to the principal hydrogeologic units (aquifers and confining units), and corresponding model layers are shown in figure 3, and a generalized geohydrologic section is shown in figure 4. The geologic descriptions in this section are based on work by Miller (1986) unless otherwise cited.

Lithologic Units and Description

The Paleocene-age Clayton Formation underlies the entire study area and consists of a massive calcareous marine clay in the southern part of the study area. Northward, the formation grades to a fine- to medium-grained glauconitic sand and clayey sand with smaller amounts of medium- to dark-gray clay and generally has low permeability. The Eocene-age sediments can be subdivided into the Oldsmar and Avon Park Formations and the Ocala Limestone. The Oldsmar Formation underlies the entire study area, but consists of permeable limestones only in Wakulla, Leon, Jefferson,

SYSTEM	SERIES	FORMATION	HYDROGEOLOGIC UNIT	MODEL LAYERS: Davis (1996)	MODEL LAYERS: This Study
QUATERNARY	HOLOCENE	Undifferentiated deposits	Water-table aquifer	Layer 1	Layer 1
QUATERNARY	PLEISTOCENE	Undifferentiated terrace and shallow marine deposits	Water-table aquifer	Layer 1	Layer 1
TERTIARY	PLIOCENE	Citronelle Formation Miccosukee Formation Jackson Bluff Formation	Water-table aquifer / Hawthorn clays	Layer 1 / Low vertical conductance between layers 1 and 2	Layer 1 / Layer 2
TERTIARY	MIOCENE	Hawthorn Group	Hawthorn clays	Low vertical conductance between layers 1 and 2	Layer 2
TERTIARY	MIOCENE	Chattahoochee and St. Marks Formations	Upper Floridan aquifer	Layers 2 and 3	Layers 3 and 4
TERTIARY	OLIGOCENE	Suwannee Limestone	Upper Floridan aquifer	Layers 2 and 3	Layers 3 and 4
TERTIARY	EOCENE	Ocala Limestone	Upper Floridan aquifer	Layers 2 and 3	Layers 3 and 4
TERTIARY	EOCENE	Avon Park Formation	Upper Floridan aquifer	Layers 2 and 3	Layers 3 and 4
TERTIARY	EOCENE	Oldsmar Formation	Upper Floridan aquifer	Layers 2 and 3	Layers 3 and 4
TERTIARY	PALEOCENE	Clayton Formation	Low-permeability sediments	No-flow boundary	No-flow boundary

Figure 3. Relation of geologic units, hydrogeologic units, and model layers in north-central Florida and southwestern Georgia.

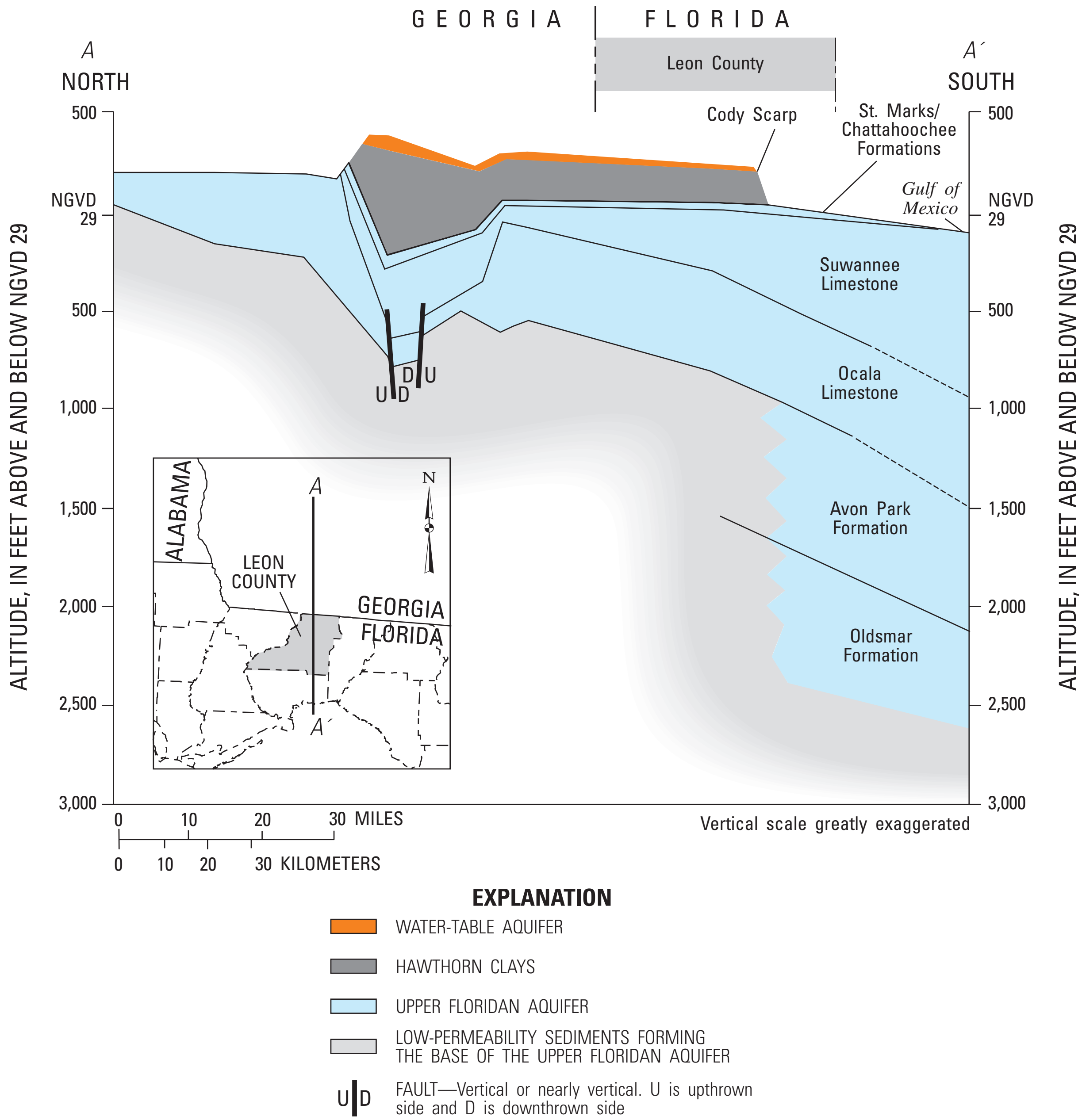

Figure 4. Generalized hydrogeologic section showing aquifer and geologic formations of the Upper Floridan aquifer in north-central Florida and southwestern Georgia.

Taylor, and Madison Counties, Florida. To the north, in Georgia, the Oldsmar becomes less permeable, grading from limestone to argillaceous limestone and from calcareous clay into glauconitic calcareous sand. The Avon Park Formation consists of a permeable and relatively pure limestone only in parts of Wakulla, Leon, Jefferson, Taylor, and Madison Counties. The Ocala Limestone is permeable through the entire study area and ranges in thickness from about 200 ft in the northern part of the study area to about 500 ft in Leon and Wakulla Counties. The Suwannee Limestone generally consists of two permeable rock types: a highly vuggy limestone, and a finely pelletal limestone. The thickness of the Suwannee Limestone reaches a maximum of about 600 ft in the southwestern part of the study area and thins to less than 100 ft in the southeastern and northern parts where the limestone crops out.

The Miocene-age sediments can be subdivided into the St. Marks Formation, Chattahoochee Formation, and Hawthorn Group. The St. Marks Formation is a predominantly fine- to medium-grained, silty to sandy limestone that has undergone degrees of secondary dolomitization (Hendry and Sproul, 1966). The Chattahoochee Formation is primarily a dolostone containing quartz sand, clay, calcite, limestone, chert, mica, heavy minerals, phosphate, and fossils (Huddlestun, 1988). The permeability of the St. Marks and Chattahoochee Formations ranges from highly permeable to relatively impermeable. The Hawthorn Group is predominantly sand and clay; subordinate components include dolomite, dolostone, calcite, limestone, phosphorite, phosphate, silica in the forms of claystone, chert, and siliceous microfossils, feldspar, heavy minerals, carbonaceous material and lignite, zeolites, and fossils (Huddlestun, 1988). The total thickness of the Miocene sediments ranges from about 0 to 350 ft, and these sediments crop out to the north (fig. 4).

The Pliocene-age sediments can be subdivided into several formations including the Jackson Bluff Formation, the Miccosukee Formation, and the Citronelle Formation. The Jackson Bluff and Citronelle Formations are present only in the southwestern part of the study area. The Jackson Bluff Formation is composed of clayey sands and sandy clays that are macrofossiliferous; the Miccosukee Formation is composed of interbedded and cross-bedded clays, silts, sands, and gravels of varying coarseness and mixtures (Hendry and Sproul, 1966). The Citronelle Formation is composed of medium to coarse sand containing many stringers of gravel and a few thin clay beds. Sediments of the Hawthorn Group and the overlying clay, silts, and sandy clays of the Miccosukee and Jackson Bluff Formations form a continuous low-permeability hydrogeologic unit that is referred to in this report as the Hawthorn clays.

Pleistocene-age sediments consist of medium- to coarse-grained, tan, white, and brown sand that locally contains trace amounts of carbonaceous material and shell fragments. The Holocene deposits include thin sand and gravel accumulations deposited mostly adjacent to streams, estuaries, and lagoons. The Citronelle Formation, together with the Pleistocene- and Holocene-age sediments, form the highly permeable water-table aquifer, which overlies the Hawthorn clays.

Depositional and Structural History

A broad band of low-permeability limestones extends diagonally across the entire study area (fig. 5). These limestones were deposited in a deep-water marine channel, named the Suwannee Straits, which extended from the Gulf of Mexico to the Atlantic Ocean in pre-Miocene times (Bush and Johnston, 1988). The limestones were deposited as a fine-grained mud with low original porosity. North and south of the Suwannee Straits, limestones were deposited in a shallow warm sea similar to the present-day Bahamas and had a relatively high porosity. During Miocene and later times, most of the study area was covered by silt and clay sediments carried southward by rivers draining the Appalachian Mountains. The thickest deposits of the Hawthorn clays accumulated in the Suwannee Straits, and thinner deposits accumulated north and south of the straits (fig. 5).

Hydrologic Setting

Aquifers in the study area include the water-table aquifer and the Upper Floridan aquifer. These two aquifers are separated by the Hawthorn clays (figs. 3-5). Small amounts of water, usually for domestic supply, are produced from sandy units within the Hawthorn clays.

The water-table aquifer lies within the shallow sediments exposed at land surface and yields only small amounts of water when pumped, and thus, is rarely utilized. The depth to the water generally is only a few feet below land surface. Transmissivity ranges from very low where the sediments are fine grained, to moderately high where substantial thicknesses of sand and gravel are present. The water-table aquifer is present where substantial thicknesses of the Hawthorn sediments are present.

The Hawthorn clays overlie and, in some areas, confine the Upper Floridan aquifer. These sediments are several hundred feet thick in the southwestern, central, and northeastern parts of the study area and are thin to absent in the south-central and northwestern parts of the study area (fig. 5).

The Upper Floridan aquifer is part of the Floridan aquifer system that is present in Florida and parts of Georgia, South Carolina, and Alabama, and is utilized for municipal, industrial, agricultural, and domestic water supply. Where transmissivities are high, the Upper Floridan aquifer generally yields large quantities of potable water. Miller (1986) defined the Floridan aquifer system as a vertically continuous sequence of carbonate rocks of generally high permeability that are hydraulically connected to varying degrees and whose permeability is, in general, an order of magnitude to several orders of magnitude greater than those of the rocks that bound the system. Within the study area, the Upper Floridan aquifer includes all or parts of the Oldsmar Formation, Avon Park Formation, Ocala Limestone, Suwannee Limestone, St. Marks Formation, and Chattahoochee Formation (figs. 3 and 4).

The Upper Floridan aquifer is delineated based on permeability characteristics of the rocks (Miller, 1986); therefore, neither the top nor bottom of the aquifer necessarily conforms to formation or time-stratigraphic boundaries. Bush and Johnston (1988) conducted an investigation of the entire Floridan aquifer system and observed that carbonate rocks are nearly always characterized by an uneven distribution of permeability. Throughout much of the area where the Upper Floridan aquifer is present,

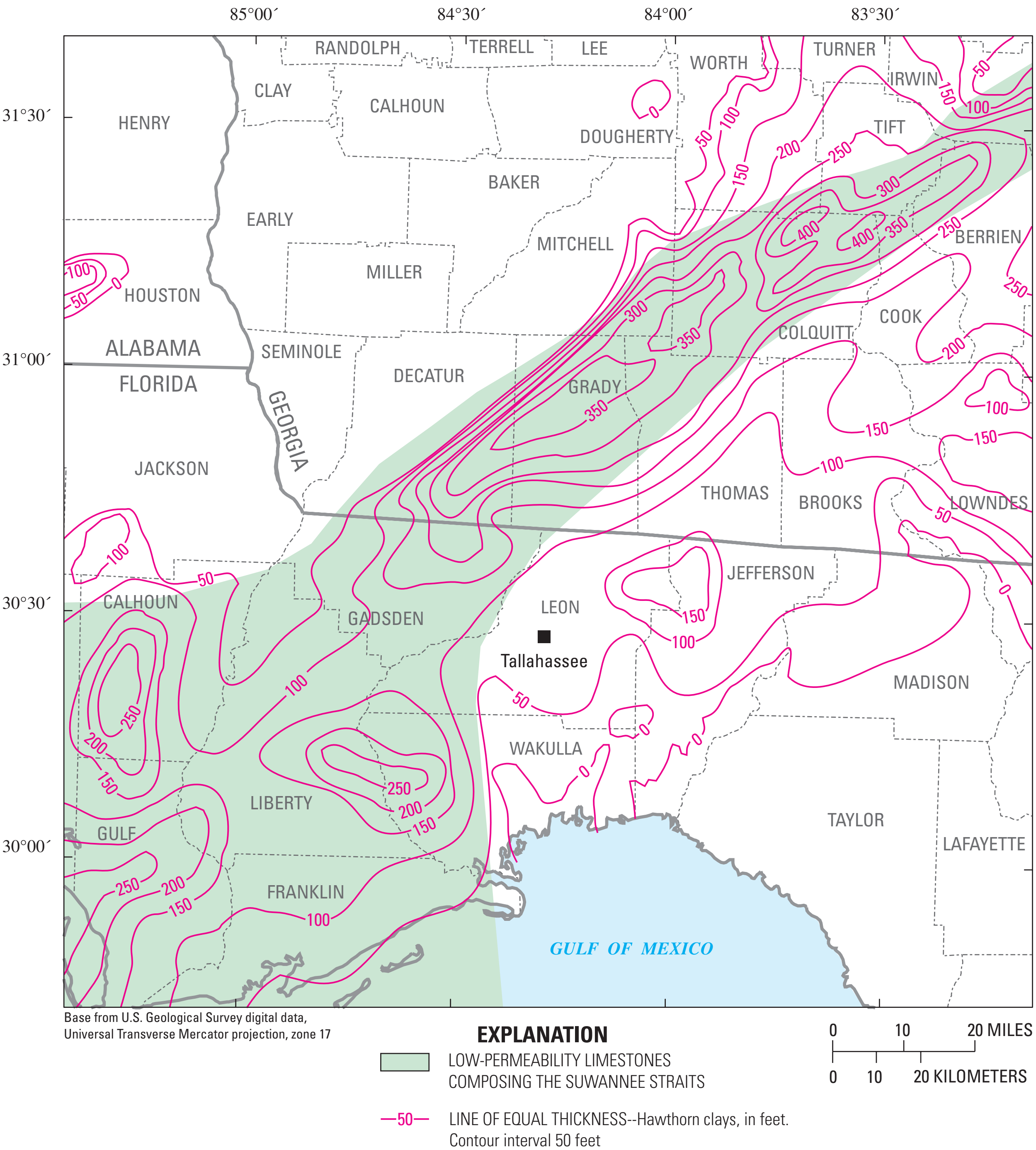

Figure 5. Location of the Suwannee Straits and lines of equal thickness of the Hawthorn clays.

the water-bearing openings consist of one or more of the following: (1) openings in loosely cemented fossil hashes that are similar to the interstices of sands, (2) mosaics of many fractures and solution-widened joints, and (3) solution cavities ranging in size from less than 1 ft to tens of feet or greater. Large solution cavities generally are present near large springs and some sinkholes where dissolution of the limestone is greatest. In areas away from the large solution openings, the first two conditions dominate. The transmissivity of the Upper Floridan aquifer is directly related to the thickness and lithology of the overlying low-permeability sediments. Thinner and more permeable overlying sediments allow greater rates of infiltration and increased dissolution of the limestones. The removal of these low-permeability sediments from some areas during Pleistocene time is largely responsible for the current distribution of karst, and thus, the current distribution of transmissivity. Values of transmissivity determined by aquifer tests for the Upper Floridan aquifer vary greatly in the study area, ranging from 1.3×10^3 to 1.3×10^6 ft^2/d (Davis, 1996).

Ground-Water Flow System

A potentiometric-surface map of the Upper Floridan aquifer (fig. 6) was constructed using ground-water level data collected from 274 wells during a period, October 21 to November 8, 1991 (Davis 1996), when water levels generally were lower than average. A ground-water divide extends diagonally from southwest to northeast across the study area. North of the divide, ground water moves eastward toward the Flint River. South of the divide, ground water moves south toward several large springs. The springshed for Wakulla and Spring Creek Springs is delineated by the orange box in figure 6.

Stream-discharge measurements were taken at seven locations on November 1, 1991, concurrently with the previously discussed ground-water level measurements (Davis, 1996). Rivers in the study area were at baseflow conditions during field-data collection as a result of several months of low rainfall. Baseflow conditions were indicated by constant and low river stages in the Withlacoochee, St. Marks, Aucilla, and Apalachicola Rivers (Davis, 1996).

Long-Term Water-Level Trends

Within the study area, the Upper Floridan aquifer is in a state of dynamic equilibrium in which there have been no known long-term changes in the potentiometric surface, although its water levels have fluctuated seasonally and yearly in response to variations in rainfall. Water levels in Leon County increase during extended periods of high rainfall and slowly decrease during periods of low rainfall. The hydrograph of two wells located within the City, one at Florida State University and one at Lafayette Park, is shown in figure 7. Both wells show an increase in water levels after substantial periods of rainfall and a slow decrease during periods of below-average rainfall. Hydrographs from wells located in Wakulla County, Florida, and in Seminole, Decatur, Miller, Mitchell, and Dougherty Counties, Georgia, show the same lack of long-term change. Additionally, Bush and Johnston (1988) found no evidence for a net decline between the estimated predevelopment potentiometric surface and the observed potentiometric surface in May 1980.

Recharge to the Upper Floridan Aquifer and Porosity Development

The recharge rate to the Upper Floridan aquifer is highly variable spatially due to the geology. Where the Hawthorn clay layer is thick (fig. 5), rainfall runs off and the water is carried to streams and rivers that discharge to the Gulf of Mexico, resulting in low recharge rates to the aquifer. The effect of the clay thickness on surface streams can readily be discerned (fig. 8): where the clay exceeds about 100 ft, there is a well-developed stream network; where the thickness of the clay is between 100 and 50 ft, streams are fragmented and flow into closed basins or sinkholes; and where the clay thickness is less than 50 ft, few streams exist. Recharge is lower and the circulation of ground water in the Upper Floridan aquifer is slower below the thicker clay deposits, resulting in ground water that is in contact with the aquifer longer and has higher concentrations of dissolved solids than ground water in areas overlain by thinner clays.

In karst aquifers, secondary effective porosity development is varied and hard to predict on a small scale. The limestones within the Suwannee Straits presumably were deposited with a low primary effective porosity and, because the thick overlying clay layer restricts the circulation of ground water through this feature, the effective porosity remains low. North and south of the Suwannee Straits, the primary effective porosity of the limestone at the time of deposition was high, the clay layer was thin or absent, and dissolution by circulating ground water further enhanced and increased the secondary effective porosity.

In southernmost Leon and Wakulla Counties, an extensive underwater cave system has developed that conducts water to Wakulla Springs (figs. 6 and 8). The cave system is accessible through numerous sinkholes and has been mapped by cave divers. Ames Sink and Fisher Creek Sink were found through dye tracer tests to be hydraulically connected to Wakulla Springs (Hazlett and Kincaid, 2004), indicating that a cave system may connect both of these sinks directly to Wakulla Springs. South of the Cody Scarp in the Wakulla Springs area, the potentiometric surface is relatively flat even though the aquifer is covered only by a thin veneer of sand that allows for high rates of recharge (fig. 6). North of the Cody Scarp, the potentiometric surface rises steadily from about 20 to 90 ft above NAVD 1988 even though the aquifer is covered

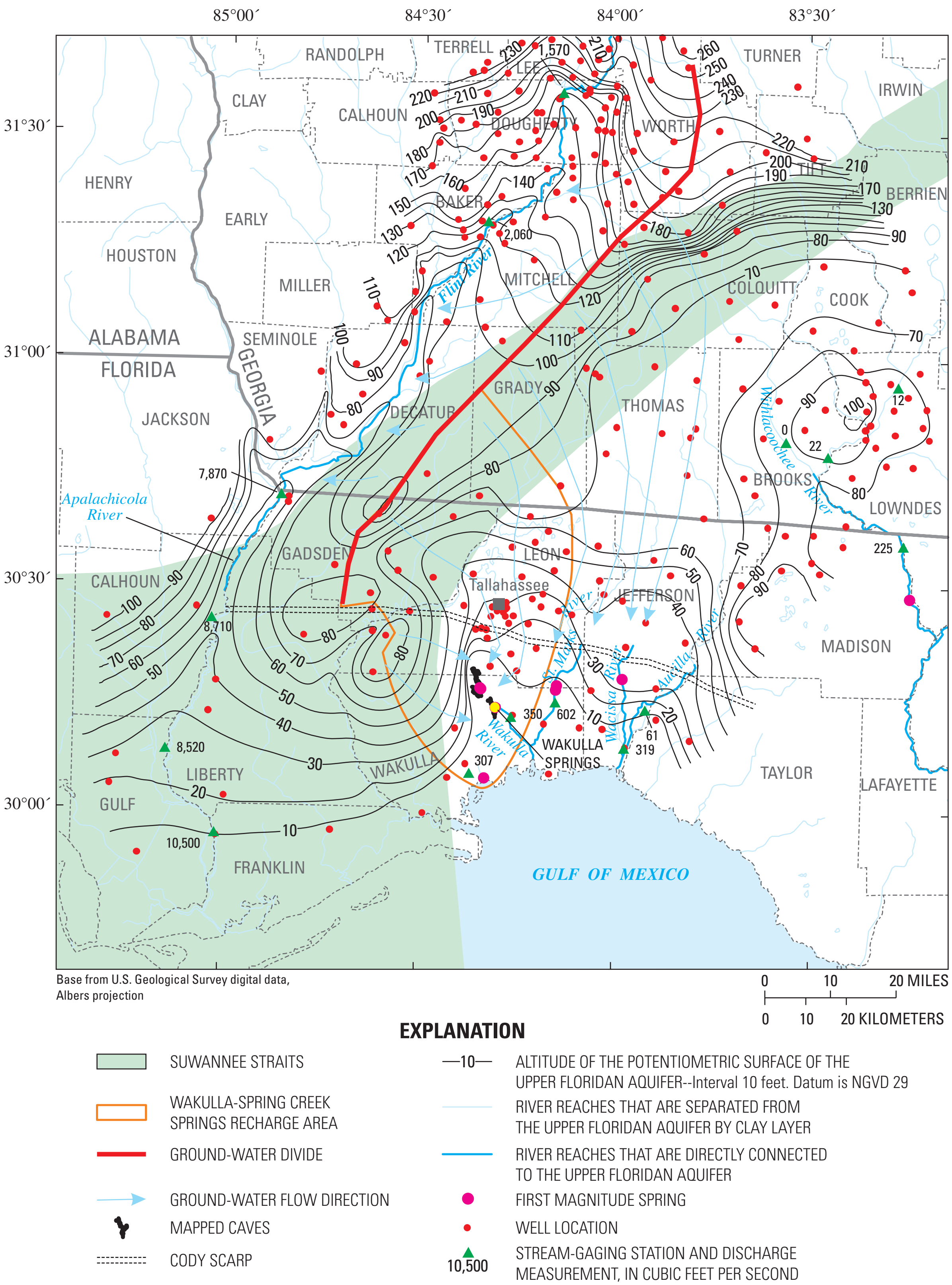

Figure 6. Altitude of the potentiometric surface of the Upper Floridan aquifer from October 21 to November 8, 1991, and stream-discharge measurements on November 1, 1991.

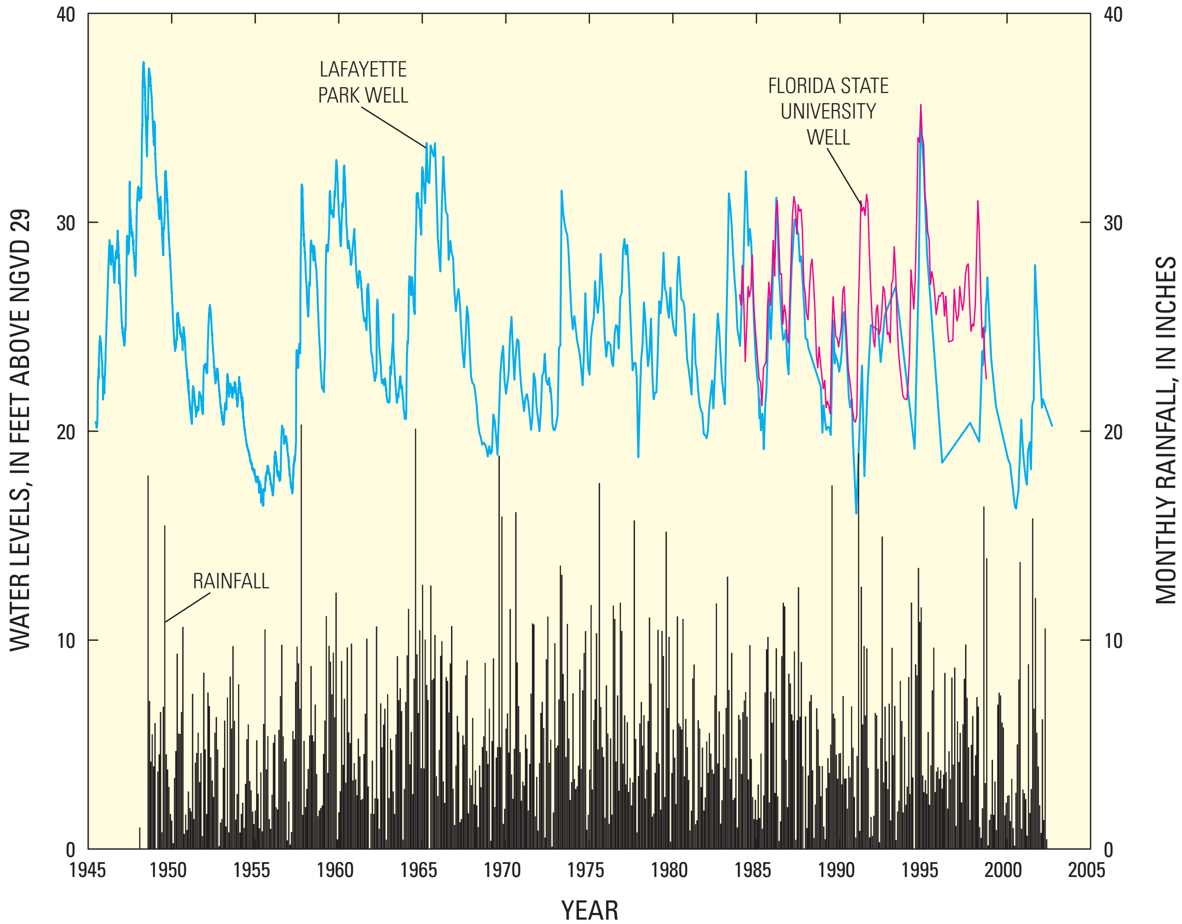

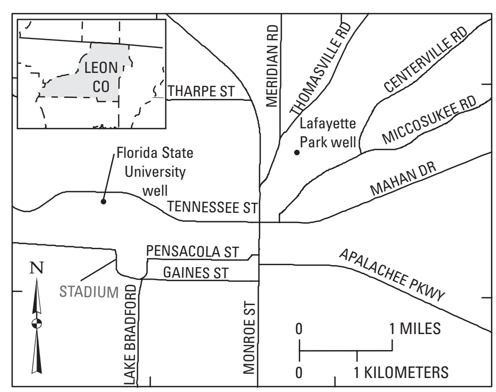

Figure 7. Long-term water levels at two wells in Tallahassee and rainfall over time.

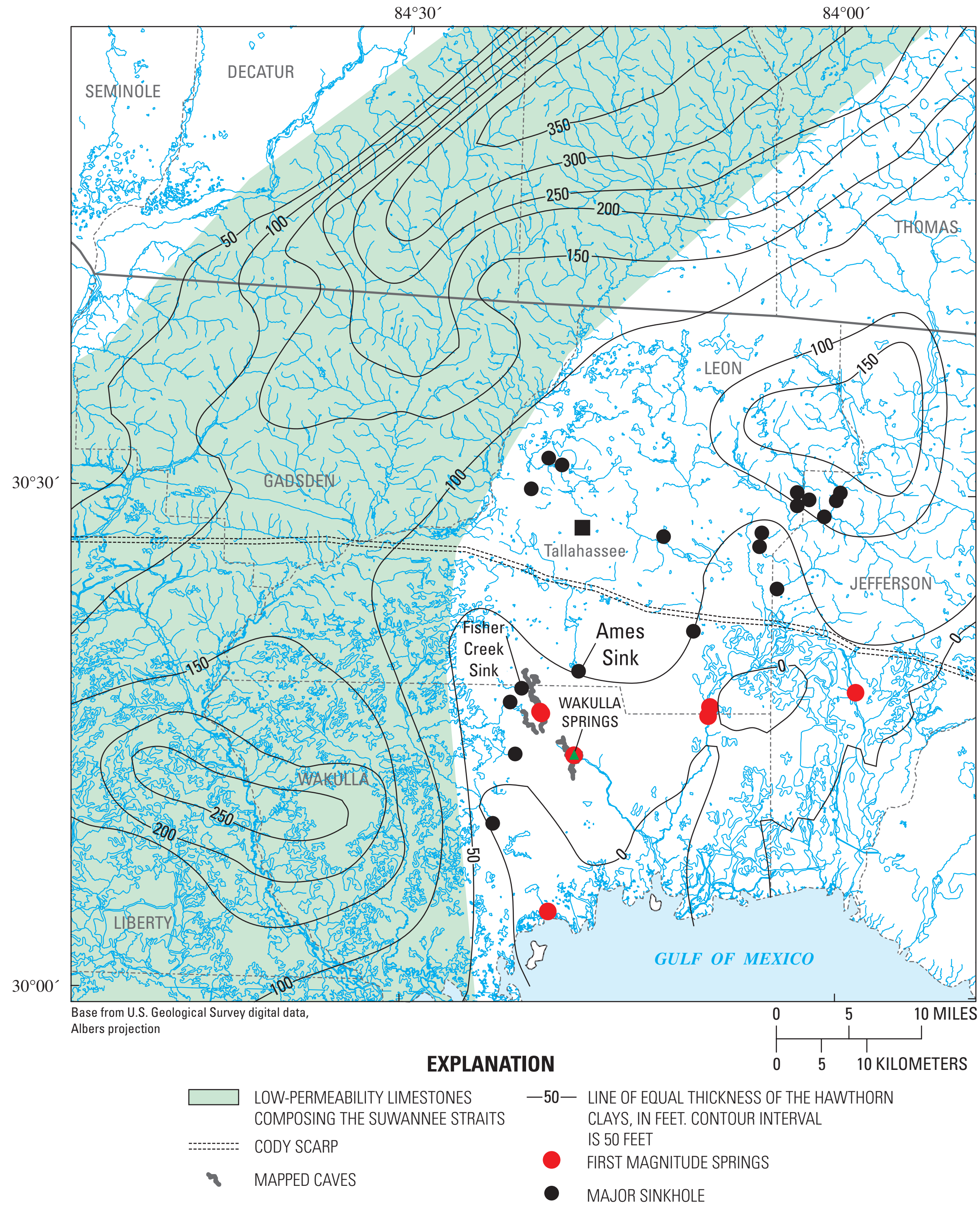

Figure 8. Location of the Suwannee Straits, Cody Scarp, and Hawthorn clays in and near Leon County.

by clay that restricts the rate of recharge. This steadily rising potentiometric surface probably indicates that the permeabilities to the north of the scarp are lower than those to the south. The type of large caves that are present near Wakulla Springs (and probably Ames Sink) probably do not extend north of the Cody Scarp or beneath Tallahassee. Upgradient from the scarp, the secondary effective porosity development may consist of only numerous smaller fractures and dissolutions along bedding planes.

The caliper log from a 600-ft-deep Lafayette Park well shows the effect of secondary dissolution (fig. 9) with numerous small openings present in the upper two-thirds of the borehole. The large opening at about 100 ft below NAVD 1988 is believed to be a washout caused by the action of the drill bit on the soft formation. The openings where the caliper log strongly indicated a fracture or bedding plane cavity were summed for the 418 ft of open hole and resulted in 14 ft of cavity space. The 14 ft of vertical cavity space over 418 ft of aquifer gives 3.3 ft of vertical cavity space per 100 ft of aquifer. Only fractures where the caliper tool opened abruptly and strongly were counted; if more questionable openings of the tool had been counted, then the total open space would have approximately tripled to 42 ft, or 10 ft of vertical cavity space per 100 ft of aquifer. Interestingly, the PCE contamination level in the bottom 100 ft of the Lafayette Park well (measured after being completed with the last 100 ft open to the aquifer) was similar to the level in an adjacent well completed in the upper 100 ft of the aquifer. The caliper log (fig. 9) is a composite of several geophysical logging surveys; the Lafayette Park well was never open over the specified length at one time. Because the water levels in these two adjacent wells move in tandem, the contamination likely extends from the top of the aquifer to the bottom, which indicates that the ground water is able to move throughout the vertical thickness of the aquifer in this area.

The combined recharge area for Wakulla Springs and Spring Creek Springs is shown in figures 6 and 10. The recharge areas were combined because there is no clear ground-water divide that separates these areas, which may be connected by caves. The most southerly mapped cave at Wakulla Springs is oriented southward toward Spring Creek Springs, and flow from this cave also is southward.

The period of time it takes water to move from initial recharge to discharge at a spring (or capture by a well) is influenced by two primary factors: (1) the time required to move through the Hawthorn clays, and (2) the time required to travel through the Upper Floridan aquifer to the spring (or well). Where the Hawthorn clays are thickest, the time period could be hundreds or maybe thousands of years; where the clays are thin, the time period could be tens or hundreds of years; and where the clay is absent, rainfall could move into the Upper Floridan aquifer and discharge within days or weeks. Even where the Hawthorn clay is present, rainfall sometimes enters the Upper Floridan aquifer quickly through sinkholes that bypass the clays.

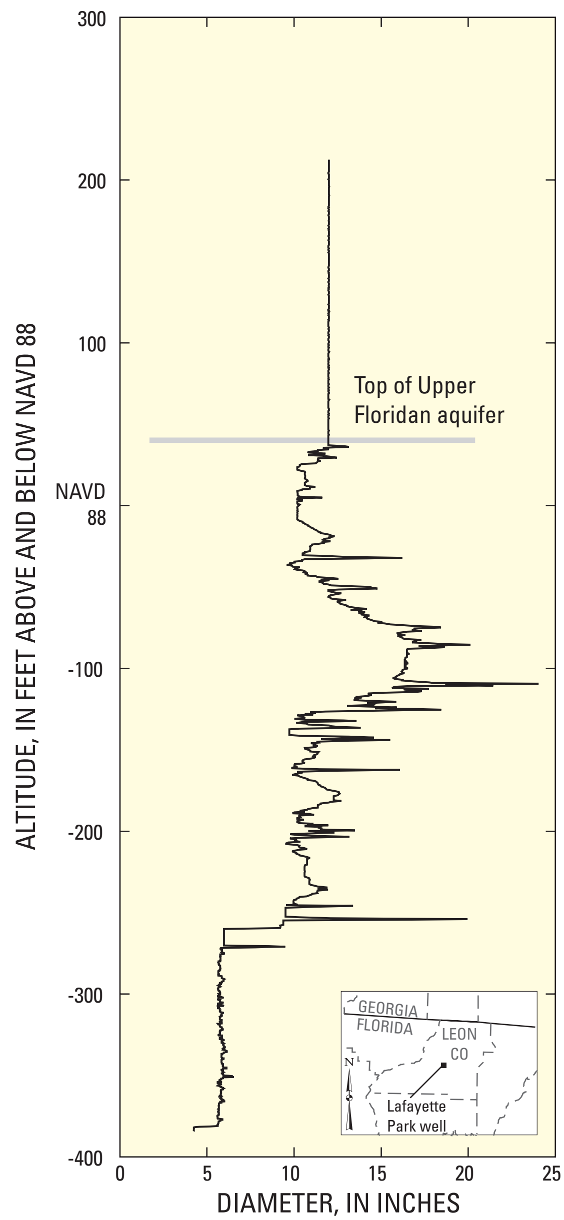

Figure 9. Frequency and size of voids in the 600-foot deep Lafayette Park well.

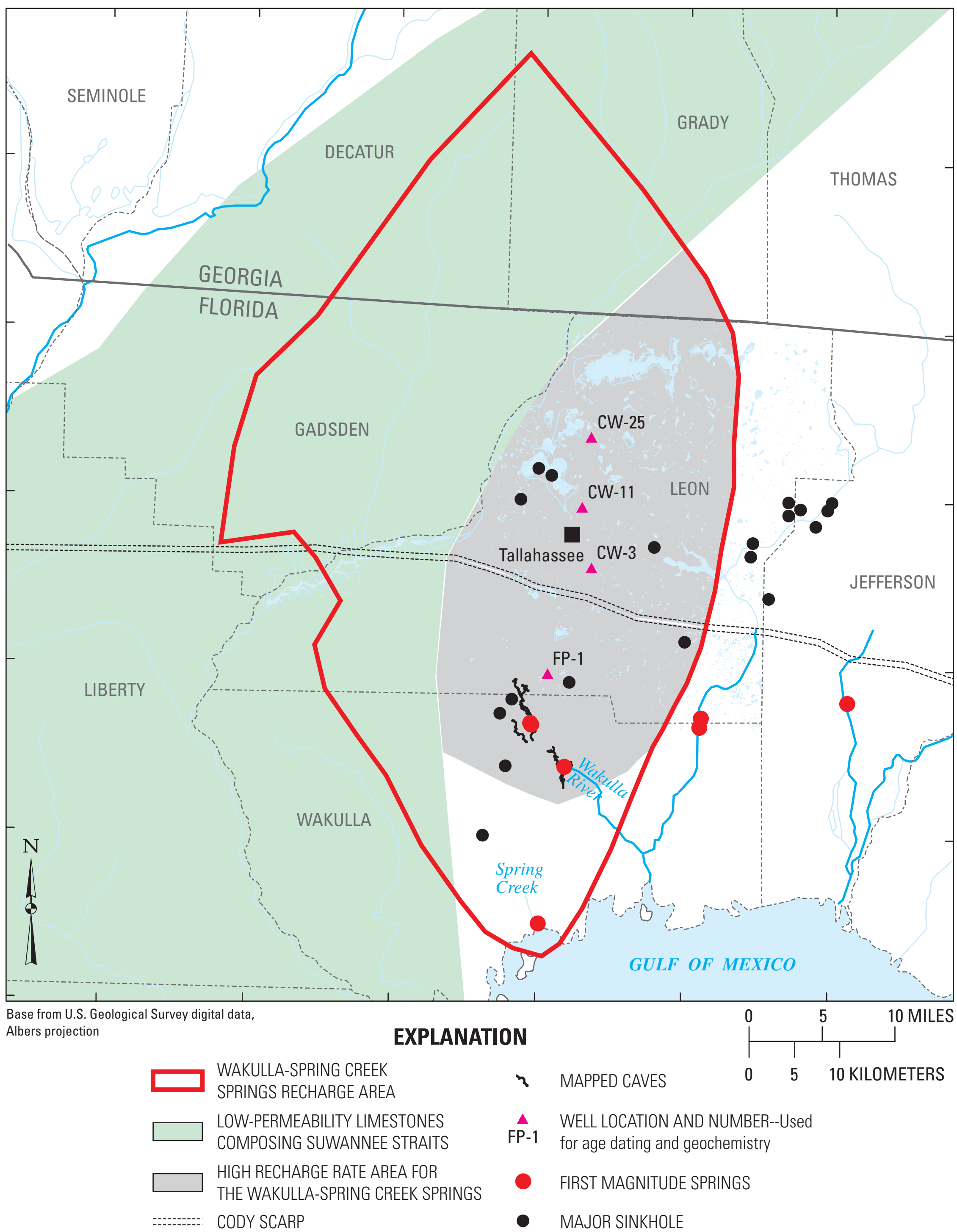

Figure 10. Location of ground-water samples collected for age dating within and near the Wakulla-Spring Creek Springs recharge area.

Ground-Water Chemistry and Age Dating

Ground-water samples were collected from four public-supply wells to determine ground-water chemistry and age dating in the study area. The first part of this section describes the methods that were used for chemical and isotope analyses; the second part presents results of the ground-water chemistry analysis.

Water Sample Collection and Analysis

Ground-water samples were collected from four public-supply wells. Pumping rates were about 2,600 gal/min for well CW-25, 1,320 gal/min for well CW-11, 1,435 gal/min for well CW-3, and 200 gal/min for well FP-1 (fig. 10). Specific conductance, pH, dissolved oxygen, and temperature were measured in the field using a multi-parameter probe inserted into a flow-through cell that was closed to the atmosphere. Field-sampling protocols for well sampling and methods for chemical and isotopic analyses are described by Katz and others (1997, 2004). Samples were analyzed for tritium (^3H), chlorofluorocarbons (CFCs), sulfur hexafluoride (SF_6), stable isotopes, dissolved gases, and major ions.

All of the wells sampled are located within the Wakulla-Spring Creek Springs recharge area. This recharge area can be divided into two separate areas based on the hydrology (fig. 10). The area shown in gray on figure 10 has relatively high recharge rates because the Hawthorn clays are relatively thin; recharge rates south of the Cody Scarp are especially high because the clays are thin or completely absent. In the western part of the recharge area (shown in green on figure 10), the clay is relatively thick and the Upper Floridan has a low permeability, resulting in much lower recharge rates. The northernmost three wells are north of the Cody Scarp, and thus, penetrate a substantial thickness of the Hawthorn clays, but these wells are completed in the Upper Floridan aquifer. Well FP-1 is south of the Cody Scarp where the water table is at or in the Upper Floridan aquifer and is about 10 ft below land surface.

Estimates of ground-water age and mean transit times were made by measuring the concentrations of certain chemicals in ground water and then comparing these concentrations to the historic release of the chemicals to the atmosphere (fig. 11). Anthropogenic activities, such as atmospheric testing of thermonuclear devices and industrial processes, have released ^3H, CFCs, and SF_6, into the atmosphere in low but measurable concentrations. These chemicals subsequently

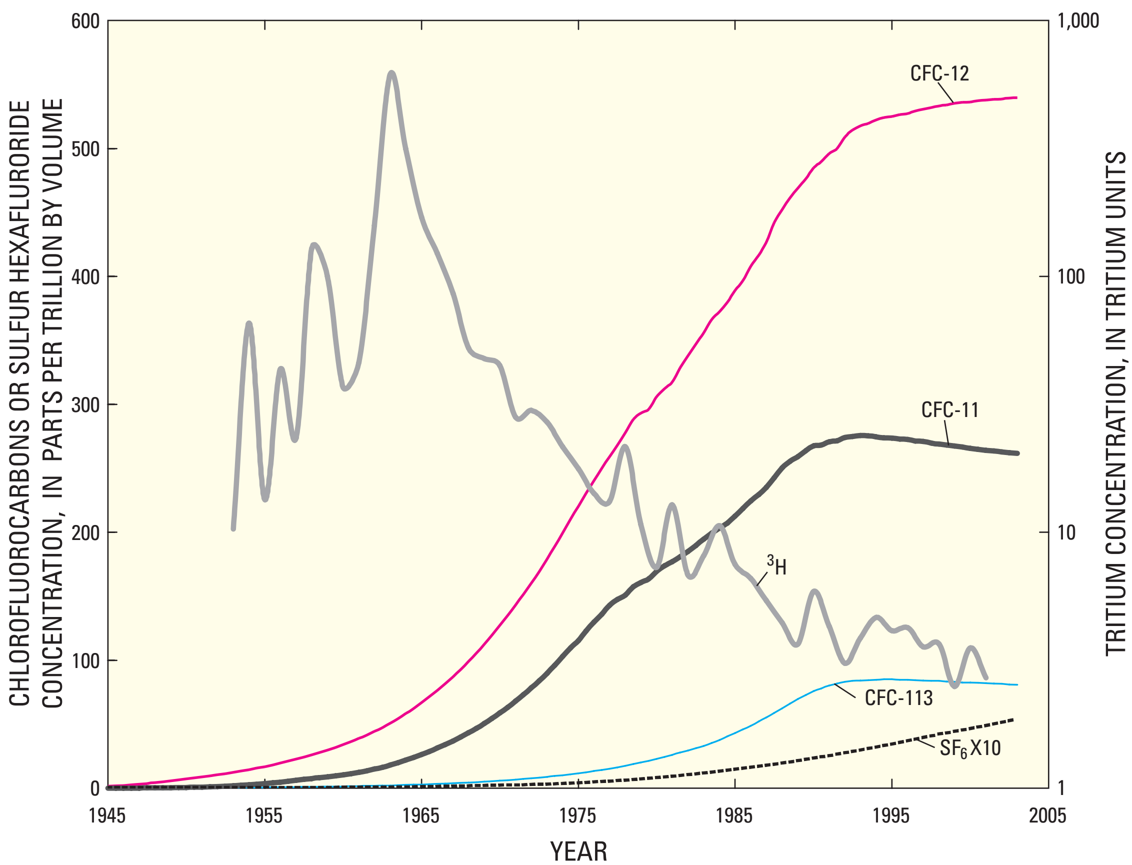

Figure 11. Atmospheric concentrations of tritium (^3H), chlorofluorocabons, and sulfur hexafluoride (SF_6) in rainfall. CFC-11 is trichlorofluoromethane; CFC-12 is dichlorodifluoromethane; and CFC-113 is trichlorotrifluoroethane.

dissolve into rainfall that infiltrates into the ground. Thus, the chemical or isotopic signature of the recharging water reflects atmospheric conditions at the time of recharge (Schlosser and others, 1988, 1989; Busenberg and Plummer, 1992, 2000).

Tritium and Tritium/Tritiogenic Helium-3 Dating Method

The age of ground water can be estimated by comparing measured tritium (^3H) concentrations in ground water with the long-term ^3H atmospheric input measured at the International Atomic Energy Agency precipitation monitoring station in Ocala, north-central Florida (Michel, 1989), as shown in figure 12. Atmospheric weapons testing, beginning in the early 1950s increased ^3H concentrations in rainfall in this area to a maximum of several hundred tritium units during the mid-1960s, followed by a nearly logarithmic decrease in concentrations to the present. The concentration of ^3H is reported in tritium units (TU), with 1 TU equal to 1 ^3H atom in 10^{18} hydrogen atoms with a known half-life of ^3H of 12.26 years. Combined measurements of ^3H and tritiogenic helium-3 ($^3He_{trit}$), the radioactive daughter product of tritium decay, define a relatively stable tracer of the initial ^3H input to ground water, which can be used to calculate the $^3H/^3He_{trit}$ age from a single water sample (Schlosser and others, 1988 1989; Solomon and Sudicky, 1991). The $^3H/^3He_{trit}$ ages generally are not affected by contamination, sorption, and microbial degradation processes that can alter CFC or SF_6 concentrations (Busenberg and Plummer, 2000); however, the distribution of ^3H and $^3He_{trit}$ can be affected by hydrodynamic dispersion and mixing of different age waters (Solomon and Sudicky, 1991; Reilly and others, 1994).

Water samples that were analyzed for $^3H/^3He_{trit}$, helium-4 (^4He), and neon (Ne) were collected in pinch-off copper tubes (about 0.39-in.-diameter, about 2.6-ft length, about 40-mL volume), while applying back pressure to the discharge from the sample tube to prevent formation of gas bubbles during sample collection. Samples were analyzed at the noble gas laboratory of Lamont-Doherty Earth Observatory of Columbia University using quantitative gas extraction followed by mass-spectrometric techniques (Schlosser and others, 1989).

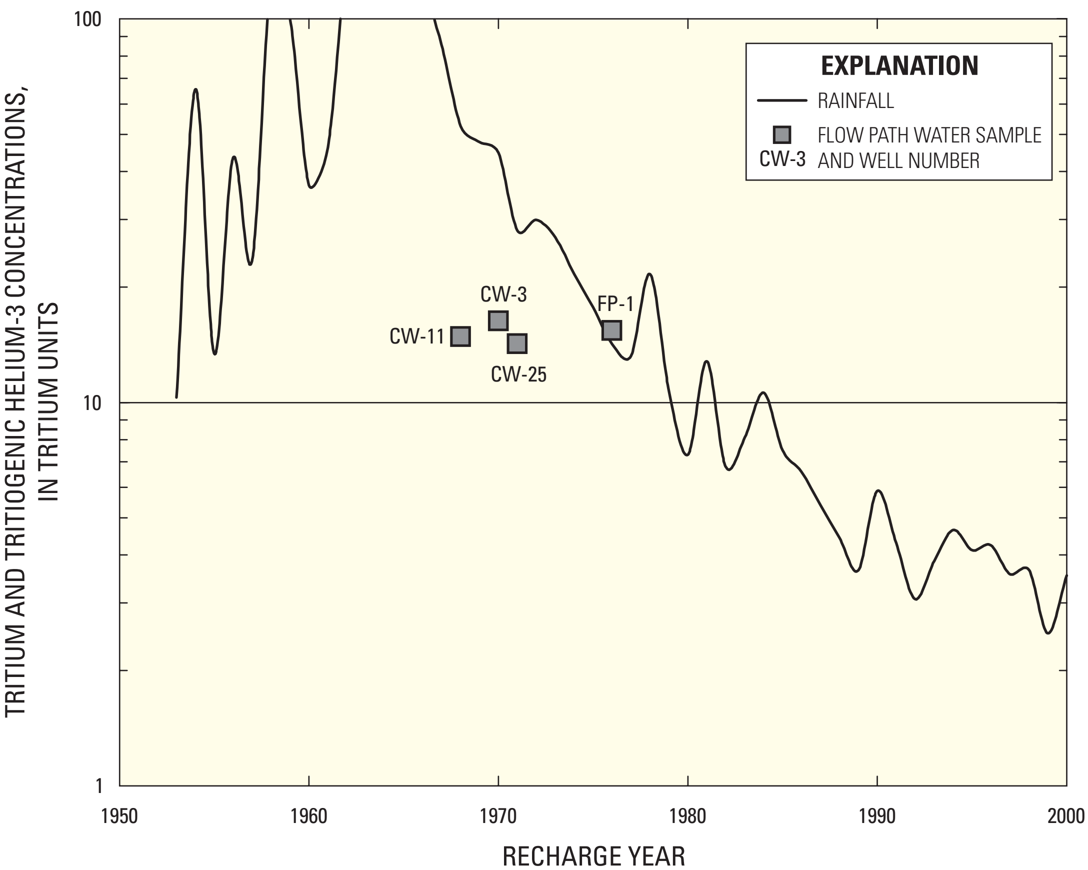

Figure 12. Comparison of measured tritium (^3H) and tritiogenic helium-3 ($^3He_{trit}$) concentrations in ground-water and spring-water samples and the tritium input history recorded at the International Atomic Energy Agency station in Ocala, Florida. CFC-11 is trichlorofluoromethane; CFC-12 is dichlorodifluoromethane; and CFC-113 is trichlorotrifluoroethane.

Chlorofluorocarbon and Sulfur Hexafluoride Dating Methods

Both chlorofluorocarbons (CFCs) and sulfur hexafluoride (SF_6) are stable in the hydrosphere, which has led to their effective use in age dating ground water recharged during the past 50 years (Plummer and Busenberg, 1999; Busenberg and Plummer, 2000). If the CFC and SF_6 concentrations in ground water have not been altered by biological or geochemical processes, and are of atmospheric source, apparent ages can be determined. Apparent ages for CFCs and SF_6 are estimated based on the equilibrium partitioning between recharging ground water and the partial pressures of trichlorofluoromethane (CCl_3F) as CFC-11, dichlorodifluoromethane (CCl_2F_2) as CFC-12, trichlorotrifluoroethane ($C_2Cl_3F_3$) as CFC-113, and SF_6 in the troposphere or soil atmosphere (fig. 13). Concentrations of CFCs and SF_6 in ground water are a function of the atmospheric partial pressures and the temperature at the base of the unsaturated zone during recharge. The recharge temperature and the quantity of dissolved excess air are determined from gas-chromatography analyses of nitrogen (N_2) and argon (Ar) in the headspace of water samples collected in the field (Busenberg and others, 1993). An apparent age of the sampled water is determined from a comparison of the partial pressure of each CFC compound and SF_6 in the sample, calculated from their measured concentrations using solubility data for each compound, with the record of atmospheric partial pressures over North America at different times. Input functions for CFCs and SF_6 were obtained from their atmospheric input curves and assumed a ratio of summer-to-winter infiltration coefficient of 1.0. Concentrations of the three CFC compounds and SF_6 ideally provide four independent ages that can be used as a quality-assurance check on the sampling and analytical methods and to evaluate mixing processes. Analytical procedures for CFCs and SF_6 are described by Busenberg and Plummer (1992; 2000).

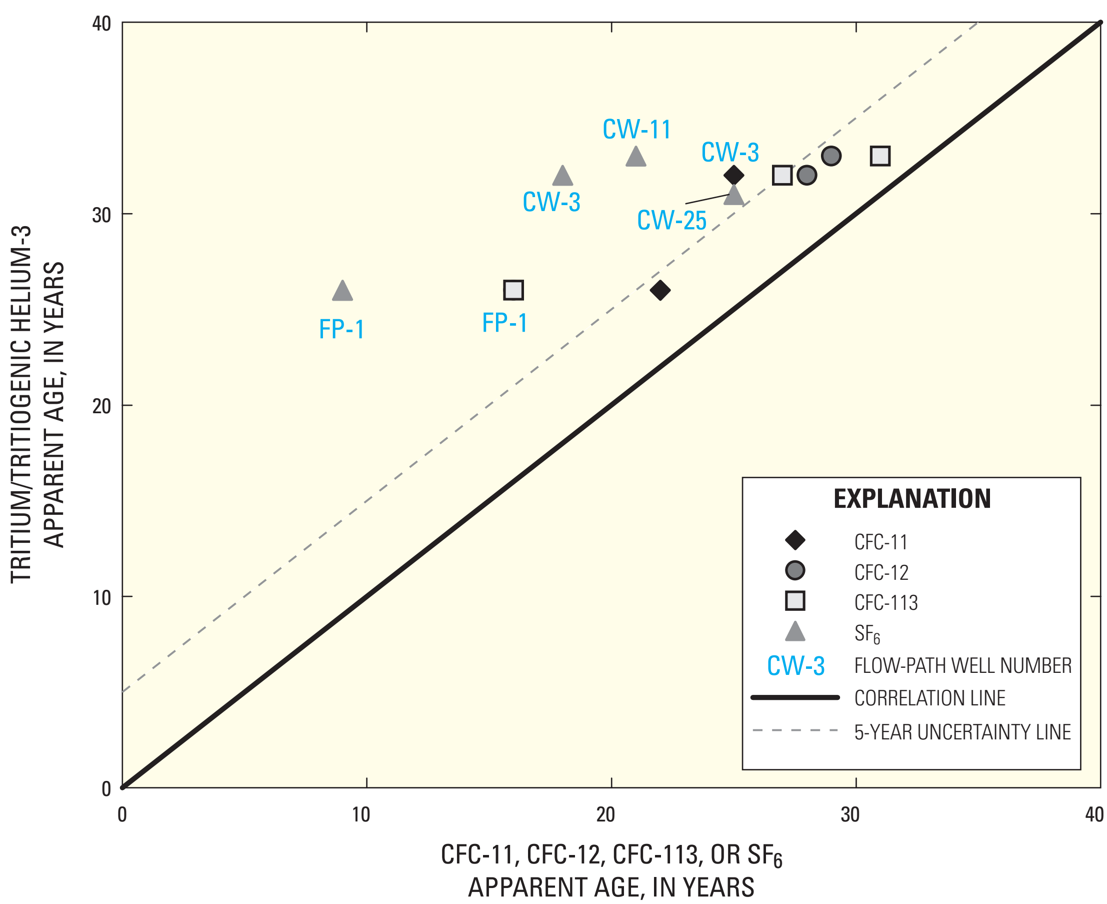

Figure 13. Plot showing comparison of apparent ages for different tracers of water from flow-path wells. Dashed line represents the +5-year uncertainty line relative to the 1:1 correlation line between apparent ages from tritium/tritiogenic helium-3 ($^3He_{trit}$) and from chlorofluorocarbon (CFC) and sulfur hexafluoride (SF_6) methods. CFC-11 is trichlorofluoromethane; CFC-12 is dichlorodifluoromethane; and CFC-113 is trichlorotrifluoroethane.

Chemistry Analysis

Water samples from wells CW-3, CW-11, CW-25, and FP-1 are a calcium bicarbonate type with low dissolved solids concentrations (92-181 mg/L) and are oxic (2.9-4.8 mg oxygen/L). Differences in ground-water chemistry (table 1) are related to confinement of the Upper Floridan aquifer and physiography. For example, concentrations of magnesium, silica, and fluoride were substantially higher in water from wells CW-25, CW-11, CW-3 (completed in the part of the Upper Floridan aquifer that is overlain by the Hawthorn clays than in water from well FP-1 (where the Hawthorn is thin or absent). The Hawthorn clays contain magnesium-rich clay minerals and phosphatic deposits (Scott, 1988). Nitrate nitrogen concentrations increased from 0.22 mg/L in water from the northernmost well (CW-25) to 0.80 mg/L in water from the southernmost well (FP-1). Nitrate nitrogen concentrations in ground water generally exceed background concentrations (0.05 mg/L) in the wells that are oxic in the Upper Floridan aquifer (Katz, 1992; Maddox and others, 1992). Waters were saturated with respect to calcite, but generally were undersaturated with respect to dolomite (table 1).

Stable Isotopes

Values of delta deuterium (δ^2H) and delta oxygen-18 ($\delta^{18}O$) in water samples from wells CW-3, CW-11, CW-25, and FP-1 plot along the global meteoric water line (Craig, 1961), indicating that recharge to the aquifer from rainfall is not affected by evaporation processes. The delta carbon-13 values of dissolved inorganic carbon are -12 ±1.1 per mil, which indicates that dissolved inorganic carbon in these waters originates from two sources in nearly equal amounts: (1) carbon dioxide (CO_2) respired by microorganisms from the oxidation of organic carbon in the unsaturated zone (Deines, 1980); and (2) dissolution of calcite and dolomite that compose the aquifer matrix.

Dissolved Gases

The concentration of dissolved nitrogen gas (N_2) and argon (Ar) in water from wells CW-3, CW-11, CW-25, and FP-1 are consistent with atmospheric equilibration during ground-water recharge, with minor amounts of excess air (less than 3.2 cm^3 standard temperature and pressure per liter) added during recharge or as a result of sampling methods.

Table 1. Physical characteristics, chemical constituents, saturation index (with respect to calcite and dolomite), and stable isotopes for selected public-supply wells.

[Well and casing depths, in feet below land surface. Abbreviations of charactreristics and constituents (concentrations in milligrams per liter, except where noted): T, temperature degrees Celsius; SC, in microsiemens per centimeter; pH, in units; O_2, dissolved oxygen; Ca, calcium; Mg, magnesium; Na, sodium; K, potassium; Cl, chloride; SO_4; sulfate; F, fluoride; HCO_3, bicarbonate; SiO_2, silica; NH_3N, nitrite plus nitrate nitrogen; Org-N, organic nitrogen; NO_3-N, nitrate nitrogen; o-PO_4-P, orthophosphate; DOC, dissolved organic carbon; DS, dissolved oslids; Cal SI, calcite saturation index; Dol SI, dolomite saturation index; δ^2H, delta deuterium; per mil; $\delta^{18}O$, delta oxygen-18, per mil; $\delta^{13}C$, delta carbon-13, per mil; log PCO_2, log partial pressure of carbon dioxide]

Well number	Well depth	Casing depth	Sample date	T	SC	pH	O_2	Ca	Mg	Na	K	Cl	SO_4	F
CW-25	450	305	12/12/02	20.4	300	7.64	2.9	44	14	2.5	0.3	4.5	6.9	0.2
CW-11	454	274	12/12/02	20.6	315	7.99	4.8	44	14	2.7	0.4	4.8	6.5	0.2
CW-3	380	185	12/12/02	21.0	284	7.68	3.8	44	11	3.0	0.4	5.5	3.2	0.2
FP-1	200	112	12/13/02	21.2	163	8.10	4.6	27	3	2.2	0.2	3.7	1.3	<0.1

Well number	HCO_3	SiO_2	NH3-N	Org-N	NO_3-N	o-PO_4-P	DOC	DS	Cal SI	Dol SI	δ^2H	$\delta^{18}O$	$\delta^{13}C$	log PCO_2
CW-25	185	13	<0.01	0.2	0.22	0.03	0.2	178	0.06	-0.09	-16.5	-3.4	-13.1	-2.41
CW-11	190	14	<0.01	<0.20	0.21	0.02	0.3	181	0.42	0.63	-12.7	-3.0	-12.4	-2.75
CW-3	176	14	<0.01	<0.20	0.51	0.03	0.2	170	0.09	-0.12	-15.8	-3.1	-12.8	-2.47
FP-1	91	5.8	<0.01	<0.20	0.80	<0.01	0.2	92	0.06	-0.54	-18.4	-3.7	-12.3	-3.17

Based on N_2 and Ar data, the calculated recharge temperature is 18 ±1.5 °C (assuming a recharge elevation of 200 ft for wells CW-25, CW-11, and CW-3, a recharge elevation of 80 ft for well FP-1, and 100-percent humidity at the water table). This calculated recharge temperature is similar to the mean annual air temperature (19 °C) recorded at a nearby National Oceanic and Atmospheric Administration (NOAA) weather station during 1971-2003.

Ground-Water Ages

Apparent ages of water samples from wells CW-3, CW-11, CW-25, and FP-1 are based on the assumption of piston flow. Using data for the three CFC compounds (CFC-11, CFC-12, and CFC-113), apparent ages ranged from 7 years at well FP-1 to 31 years at CW-11 (table 2). Water samples from three wells had concentrations of at least one CFC compound that were higher than those possible for equilibrium with maximum atmospheric values and are termed “contaminated.” All three CFC compounds were highly contaminated in water from wellCW-25. The CFC contamination in these waters likely originates from a local nonatmospheric source for elevated CFC concentrations (such as the improper waste disposal of CFC refrigerants). Apparent ages from CFC-11, CFC-12, CFC-113, and the CFC-113/CFC-12 ratio generally were concordant (±2 years), based on assumptions of atmospheric equilibrium and the piston-flow assumption (table 2).

The SF_6 apparent ages (corrected for excess air) of water samples from wells CW-3,CW-11, CW-25, and FP-1 tended to be about 5 to 10 years younger than those from the CFCs (table 3). This discrepancy could be a result of the following scenarios: (1) degradation of CFC-11, CFC-12, and CFC-113; (2) SF_6 concentrations are affected by nonatmospheric sources of contamination; and (3) mixing of waters of varying ages. Because the CFC apparent ages are concordant, it is unlikely that all three compounds would have degraded at the same rate to produce similar apparent ages. Excess SF_6 concentrations in air near urban areas have been observed (Ho and Schlosser, 2000); however, contamination of urban ground water with SF_6 is less likely to occur than with CFCs because SF_6 is not present in any commonly used household product (Busenberg and Plummer, 2000). Concentrations of SF_6 and CFC in the ground-water samples were adjusted for excess air, which could introduce more uncertainty in the SF_6 age estimate as

Table 2. Concentrations of chlorofluorocarbons (CFC-11, CFC-12, and CFC-113) in water samples from wells along the flow path and piston-flow model apparent ages.

[°C, degrees Celsius; pptv, parts per trillion by volume, pg/kg, picograms per kilogram; NAVD 88, North American Vertical Datum of 1988; NPC, CFC concentrations in water samples are higher than values in equilibrium with peak atmospheric concentrations; NP, age calculation not possible due to likely contamination]

Well number	Sample date	Recharge temperature (°C)	Recharge elevation (feet relative to NAVD 88)	Calculated atmospheric mixing ratio (pptv)			Concentration in solution (pg/kg)			Piston-flow model recharge year (excess-air corrected)				Apparent age (years)
				CFC-11	CFC-12	CFC-113	CFC-11	CFC-12	CFC-113	CFC-11	CFC-12	CFC-113	CFC-113/CFC-12	
CW-25	12/12/02	16.3	200	7,757	10,414	1,374	14,475	4,642	1,035	NPC	NPC	NPC	NP	NP
		16.3	200	7,614	9,500	1,321	14,207	4,235	995	NPC	NPC	NPC	NP	NP
		16.3	200	7,760	10,144	1,359	14,480	4,522	1,024	NPC	NPC	NPC	NP	NP
CW-11	12/12/02	18.4	200	455	189	5.8	840	83	4.4	NPC	1973	1970	NP	31
		18.4	200	453	186	7.4	838	82	5.5	NPC	1973	1972	NP	30
		18.4	200	449	187	6.3	831	83	4.7	NPC	1973	1971	NP	30
CW-3	12/12/02	18.2	200	143	203	11.5	292	98	9.6	1977	1974	1975	1976	27
		18.2	200	143	208	12.7	292	101	10.6	1977	1974	1976	1978	27
		18.2	200	511	582	85.9	1,046	282	71.6	NPC	NPC	1995	NP	7
FP-1	12/13/02	19.6	80	216	821	74.0	380	347	52	1985	NPC	1990	NP	14
		19.6	80	202	852	71.7	354	360	50	1984	NPC	1989	NP	15
		19.6	80	170	410	50.9	299	173	36	1980	1986	1986	1986	17

Table 3. Concentrations of sulfur hexafluoride (SF_6) in water samples from wells along the flow path and piston-flow model apparent ages.

[°C, degrees Celsius, cm^3/STP/L, cubic centimer per standard temperature and pressure per liter; pptv, parts per trillion by volume]

Well number	Sample date	Field temperature, (°C)	Recharge temperature, (°C)	Recharge elevation (feet relative to NAVD 88)	Excess air (cm^3/STP/L)	SF_6, (pptv)	Model SF_6 recharge date	Model SF_6 apparent age (years)
CW-25	12/12/02	20.4	16.3	200	3.2	0.55	1977	25
CW-11	12/12/02	20.6	18.4	200	2.9	0.95	1982	20
CW-11	12/12/02	20.6	18.4	200	2.9	0.87	1980	22
CW-3	12/12/02	21.0	18.2	200	2.3	1.45	1985	17
CW-3	12/12/02	21.0	18.2	200	2.3	1.28	1984	18
FP-1	12/13/02	21.2	19.6	80	0.9	3.17	1994	8
FP-1	12/13/02	21.2	19.6	80	0.9	3.01	1993	9

Table 4. Summary of tritium/tritiogenic helium-3 ($^3H/^3He_{trit}$) method data for water samples collected from wells along the flow path and piston-flow model apparent ages.

[$\delta\ ^3He$, delta helium-3; ^4He, helium-4; He, helium; $^3H/^3He_{trit,}$ tritium/tritiogenic helium-3; TU, tritium units; cc/STP/g, cubic centimeters of gas at standard temperature and pressure per gram of water]

Well number	Sample date	Tritium (TU)	Tritium, error (TU)	δ^3He, in percent	^4He (ccSTP/g)	He ccSTP/g	Percent of ^4He terrigenic	$^3H + ^3He_{trit}$ (TU)	$^3H/^3He_{trit}$ apparent age (years)	$^3H/^3He_{trit}$ apparent age error (years)
CW-25	12/12/02	2.47	0.23	22.86	6.62×10^{-8}	2.42×10^{-7}	48	14.2	31.0	±1.4
CW-11	12/12/02	2.41	0.24	19.25	6.99×10^{-7}	2.44×10^{-7}	56	14.8	33.0	±1.5
CW-3	12/12/02	2.70	0.07	10.27	1.18×10^{-7}	4.01×10^{-7}	164	16.3	32.0	±0.7
FP-1	12/13/02	3.60	0.13	31.42	5.50×10^{-8}	2.09×10^{-7}	23	15.4	26.0	±0.6

a result of the lower solubility of SF_6 than CFCs. Mixing of waters with different ages may account for differences in ages between SF_6 and CFCs and is discussed below.

The apparent ages of water samples from wells CW-3, CW-11, CW-25, and FP-1 based on the $^3H/^3He_{trit}$ method ranged from 26 years at well FP-1 to 33 years at well CW-11 (table 4). Apparent ages of $^3H/^3He_{trit}$ are slightly older (2-5 years) than those based on CFCs for wells CW-11 and CW-3, but are about 10 years older than CFC apparent ages for water from well FP-1. The apparent age (from $^3H/^3He_{trit}$) of 26 years for water from well FP-1 in this study is somewhat higher than the apparent age of 17 years determined from water samples collected in 1997 (Katz and others, 2004), which is more consistent with CFC apparent ages in the present study. Water from all four wells had relatively high amounts of excess ^4He (greater than 20 percent), which may indicate a relatively deeper source of some portion of the water from the well. Excess ^4He is produced by the radioactive decay of uranium and thorium radionuclides, and ^4He likely diffuses from aquifer solids where it has been stored over geologic time periods (Solomon and others, 1996). An additional component of radiogenic ^3He might be included in the estimate of $^3He_{trit}$ calculated using the standard radiogenic $^3He/^4He$ ratio of 2×10^{-8}, which would cause the $^3H/^3He$ apparent age to be older than CFC or SF_6 apparent ages. The average $^3He/^4He$ crustal ratio (2×10^{-8}) is used in the age calculation; however, higher ratios have been measured in many geologic materials, including the Eocene limestone that composes the Upper Floridan aquifer (Happell and others, 2006).

If $^3H/^3He_{trit}$ apparent ages have been substantially influenced by mixing of post-1960 recharge waters with old (pre-1950 recharge) waters, one would expect that measured $^3H + ^3He_{trit}$ concentrations in water from the wells CW-3, CW-11, CW-25, and FP-1 would deviate substantially from the reconstructed original ^3H content (historical record of ^3H in rainfall is assumed to represent the ^3H concentrations at the time of recharge). The ^3H record from the International Atomic Energy Agency network station in Ocala, Florida, was used for this comparison, with the assumption that the local ^3H input history for the Tallahassee area is closely approximated by this record (fig. 12). Data are plotted for each well site relative to the input history by assuming that the time of infiltration near each well site is calculated at the sampling date minus the $^3H/^3He_{trit}$ apparent age. Corresponding to these points on the time (x) axis, the “initial tritium” represents the sum of the measured ^3H and $^3He_{trit}$ concentrations (y-axis). The $^3H + ^3He_{trit}$ data for the water sample from well FP-1 plot on the rainfall input curve (fig. 12); however, data for the other three wells (CW-25, CW-11, and CW-3) plot slightly below the input curve, indicating that mixing of waters of varying ages is possible.

Although uncertainties and limitations are associated with each dating method, all three dating methods consistently indicate that the apparent age of ground water decreases from the northernmost well CW-25 to the southernmost well FP-1 (fig. 13). Median values for apparent age calculated for each well from data for all five tracers (noncontaminated samples of CFC-11, CFC-12, CFC-113, SF_6, and $^3H/^3He$) and the CFC-113/CFC-12 ratio decrease from 30 to 16 years. This southward trend of decreasing ages is consistent with hydrologic and chemical information. Increasing amounts of recharge occur as ground water moves from north to south, especially south of the Cody Scarp (Davis, 1996). The older waters have higher concentrations of dissolved solids, major ions, and silica (table 1), all of which are consistent with ground water with longer residence times.

Ground-Water Flow Modeling

Ground-water flow in the Upper Floridan aquifer was simulated in a previous study (Davis, 1996); the study being described in this report used a modified version of that model. The original model was constructed using MODFLOW-88 (McDonald and Harbaugh, 1988), and the present model was constructed using MODFLOW-2000 (Harbaugh and others, 2000). Some structural changes were required to adapt the model to MODFLOW-2000 (Harbaugh and others, 2000), and additional modifications were made to incorporate recent advances in the understanding of hydrology within the study area. To improve the resolution of the model, the finite-difference grid was refined; the updated model has 241 rows and 265 columns (fig. 14). The largest cells are 10,290 × 10,290 ft; the smallest cells are 400 × 400 ft. As a result of regridding, each City well is within its own small model cell.

Conversion of Original MODFLOW Model

In the original model, layer 1 consisted entirely of constant head cells. The water level in these cells represented the water table, and a low vertical conductance between layers 1 and 2 represented the Hawthorn clays. In the current model, a thin layer 1 represents the water table and layer 2 represents the Hawthorn clays. An explicit representation of this unit allows ground water to be tracked through the Hawthorn clay and back to (or from) the water-table aquifer. This additional layer results in the model being converted from a 3-layer model to a 4-layer model (fig. 15), with layers 3 and 4 in the current model equivalent to layers 2 and 3 in the original model. The current model is steady state, as was the case the original model.

Layer 3 in the current model represents the upper 200 ft of the Upper Floridan aquifer, and layer 4 extends from layer 3 to the bottom of the aquifer. The thickness of layer 4 is variable because the aquifer thickens from north to south. For water-resources management purposes, the Upper Floridan aquifer has been simulated with two layers even though the aquifer acts as a single water-bearing unit within the study area. The sole reason for dividing the aquifer into two layers is to better represent the location of water-supply wells within the model domain. Layer 3 is the most extensive layer and defines the maximum lateral extent of the model. In the northwestern part of the study area, the Upper Floridan aquifer thins to less than 200 ft and the aquifer is represented solely by layer 3. The Upper Floridan aquifer is bounded below by low-permeability sediments, represented in the model as a no-flow boundary. A more detailed discussion of the model and model calibration is presented in a report by Davis (1996).

The most substantial change from the original model to the current model is in how the hydraulic conductivity of the Upper Floridan aquifer is represented. Hydraulic conductivities in the original model were defined as cell-by-cell input values. Hydraulic conductivities in the current model are defined as zones within the model domain; cells within each zone are assigned a common hydraulic conductivity parameter value (fig. 16).

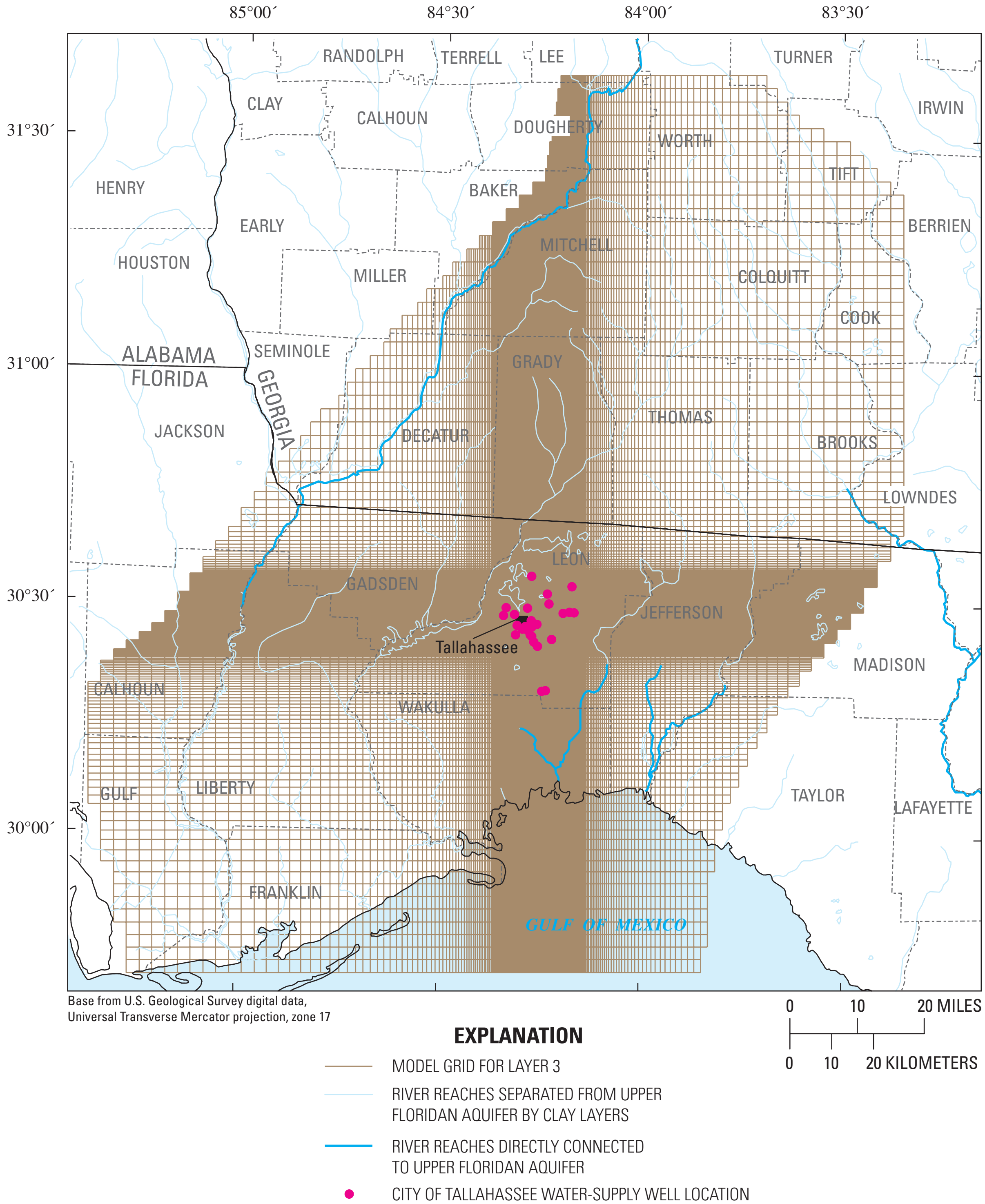

Figure 14. Location of finite-difference grid.

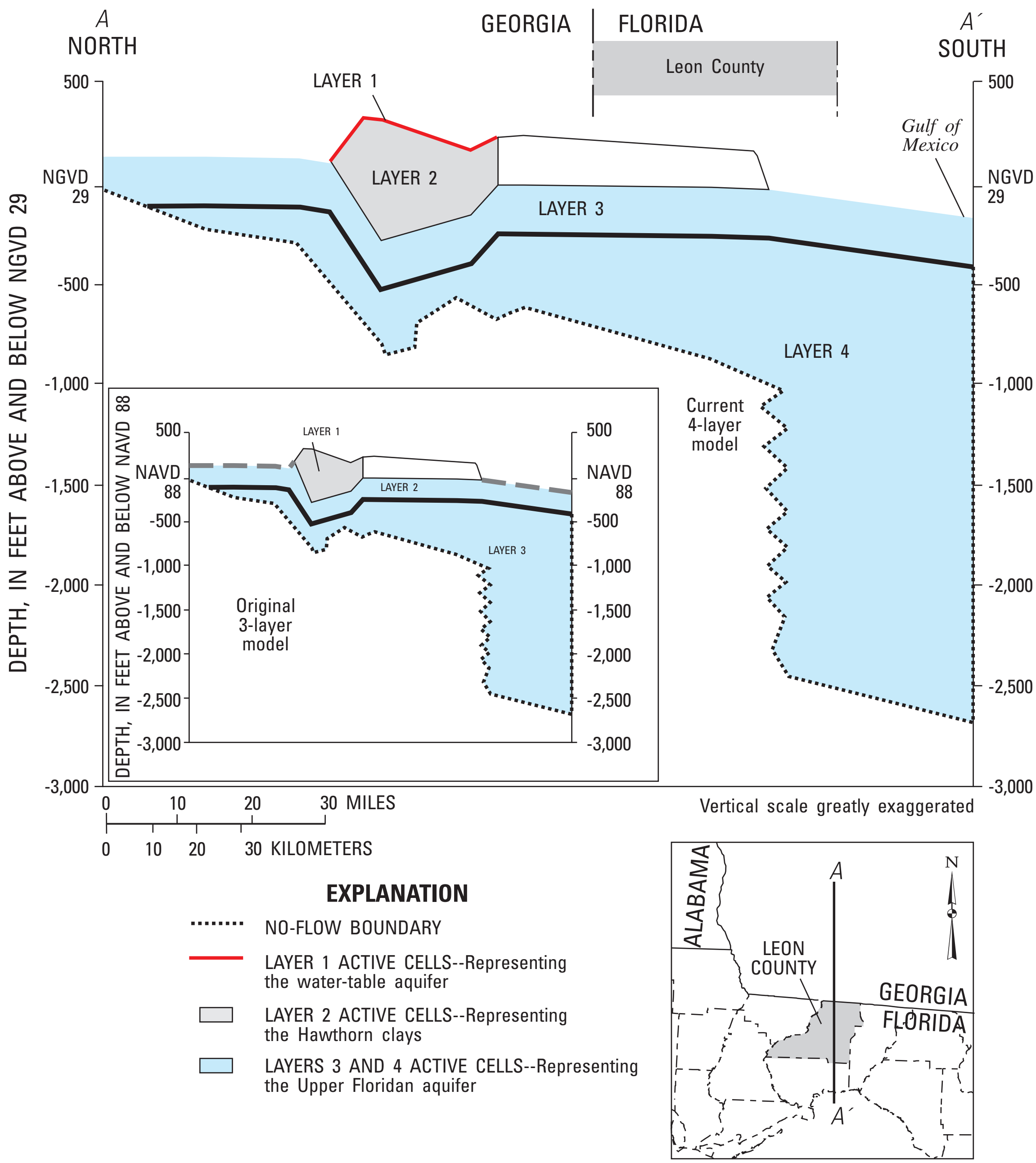

Figure 15. Generalized hydrologic section A-A´ showing the original and current model layers.

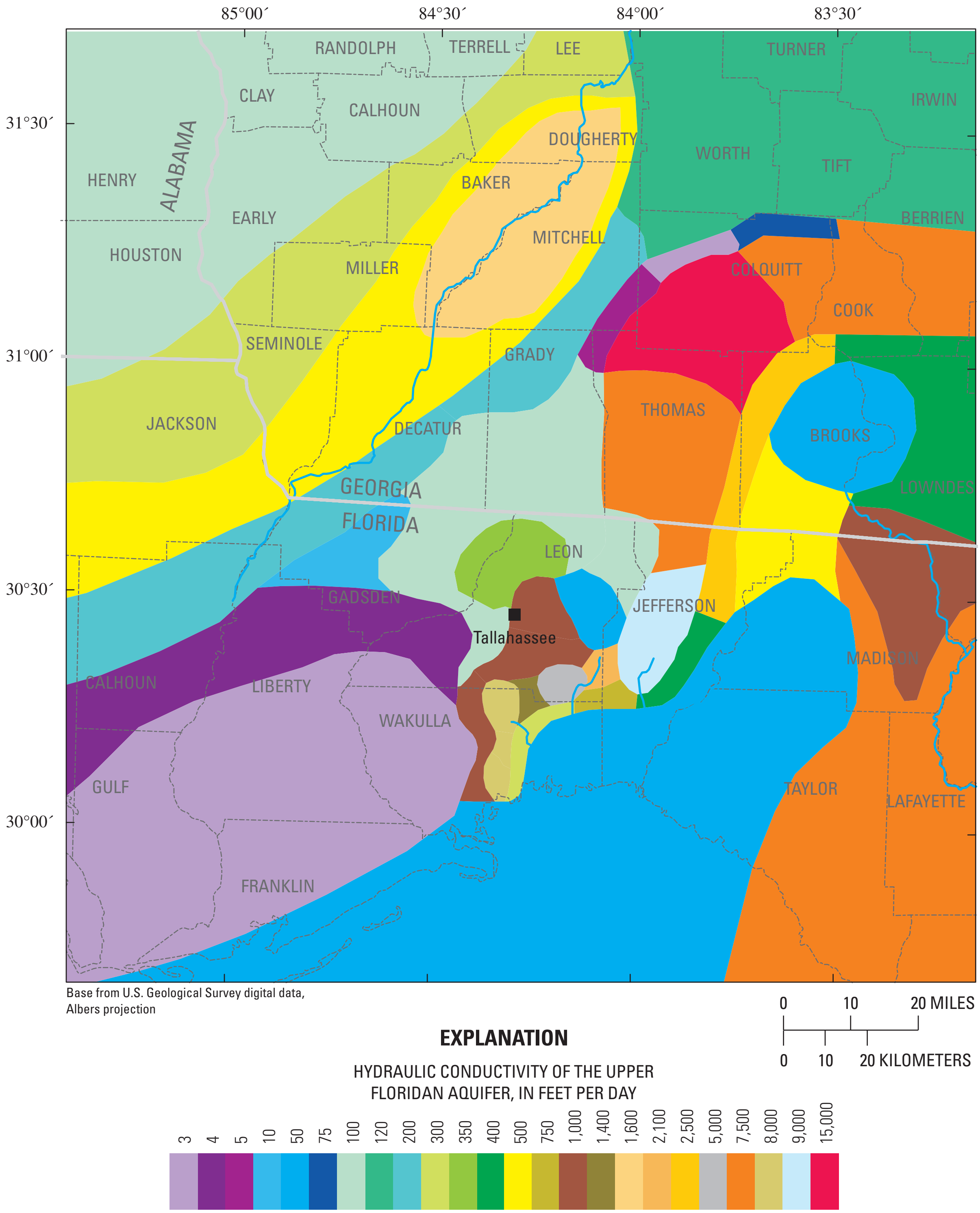

Figure 16. Simulated hydraulic conductivities of the Upper Floridan aquifer in north-central Florida and southwestern Georgia.

Model Recalibration

There were 191 head measurements and 6 stream discharge measurements used for model calibration. After calibration, 183 simulated heads were within 10 ft of the 191 measured values (8 of the simulated heads exceeded measured values by more than 10 ft), and 112 of these values were within 5 ft (fig. 17). Simulated and measured river discharge gains are listed in table 5. All simulated river gains were within less than 7 percent of the measured values (table 5). The simulated potentiometric surface of the Upper Floridan aquifer shown in figure 18 represents steady-state conditions. The current model is essentially the same as the original model, so sensitivity analysis was not rerun and the reader is referred to a report by Davis (1996) for discussions regarding model sensitivity.

Table 5. Comparison of measured and simulated net-river gains.

[Measured net-river gains, cubic feet per second, taken in November 1991]

River	Measured net gain	Simulated net gain	Difference (percent)
Aucilla	61	64	4.9
Wacissa	319	337	5.6
St. Marks	602	611	1.5
Flint	490	516	5.3
Wakulla	350	328	-6.3
Spring Creek	307	316	2.9

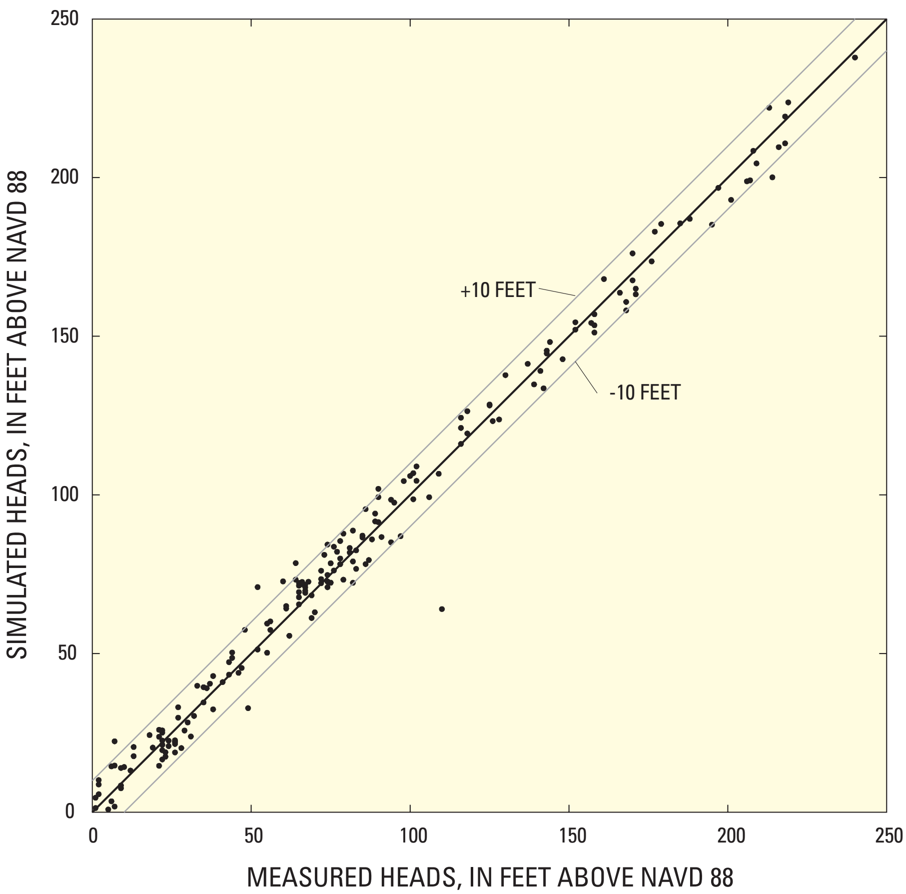

Figure 17. Comparison of simulated and measured heads.

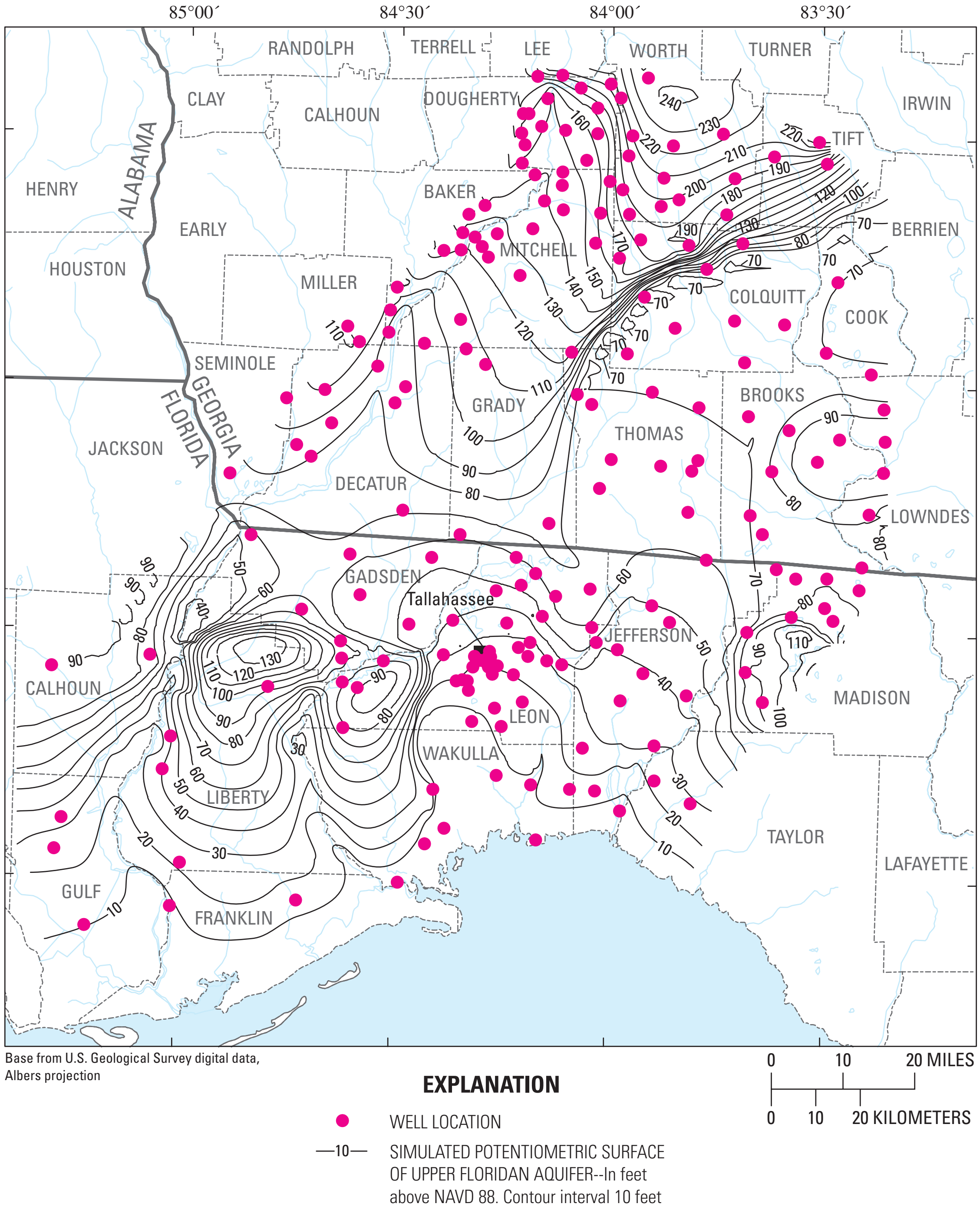

Figure 18. Simulated potentiometric-surface of the Upper Floridan aquifer.

Simulated and Measured Drawdowns for an Aquifer Test

To determine if the model accurately represents hydraulic properties of the Upper Floridan aquifer near well CW-2, the model was modified to simulate an aquifer test conducted in downtown Tallahassee in 1992. During the test, this well was pumped at about 1,400 gal/min, and drawdown was measured in five adjacent monitoring wells (fig. 19). To accurately simulate the aquifer test, the model grid was modified so that the model cell containing the pumped well was 1 × 1 ft, which is approximately the size of the borehole, and model cell dimensions slowly increased by a multiplier of 1.1 away from the well. Simulated and measured drawdowns were similar (fig. 19), indicating that the model represents the hydraulic properties reasonably well in the vicinity of well CW-2.

Ground-Water Age Dating and Effective Porosity Determination

The ground-water age data discussed earlier were used in combination with the flow model to determine effective porosities for the Upper Floridan aquifer and Hawthorn clays. For each of four wells in which age-dating samples were collected, the model was run 20 times and the effective porosity was systematically changed in both the Hawthorn clays and the Upper Floridan aquifer. Simulated effective porosities in the Hawthorn clays ranged from 12.5 to 35 percent and simulated effective porosities in the Upper Floridan aquifer ranged from 0.1 to 25 percent. The simulated traveltimes for each combination of effective porosities for each well were determined using the MODPATH particle-tracking program (Pollock, 1989). Using this program, particles were assigned to the cells containing pumping wells and were tracked backward in time to the point of recharge. Reversing the particle pathlines from recharge areas to the wells reveals that particles within the low-permeability Hawthorn clays move vertically downward from the water table. Once into the Upper Floridan aquifer, the particles follow a horizontal path with a slightly downward gradient to the pumping well. The effective porosities used and the simulated traveltimes (ground-water ages) are presented in table 6. Four simulations were run in which only the traveltime in the Upper Floridan aquifer was considered, and the ground-water age was simulated, assuming that all recharge occurred through sinkholes and bypassed the Hawthorn clays. The helium-derived age dates were used for this comparison because $^3H/^3He_{trit}$ ages generally are not affected by contamination, sorption, and microbial degradation processes that can alter CFC or SF_6 concentrations (Busenberg and Plummer, 2000).

Eight combinations of effective porosities resulted in total traveltimes that fell within 3 years of the calculated times (given in bold on table 6). The effective porosities for the Upper Floridan aquifer that resulted in matches were averaged to produce an effective porosity of 7 percent; the effective porosities for the Hawthorn clays that resulted in a match were averaged to produce an effective porosity of 22 percent.

Because ground-water flow in the Hawthorn clays is vertical, particle traveltime can be contoured. The traveltime through the clay layer in the Tallahassee area assumes an effective porosity of 22 percent (fig. 20). Traveltimes ranged from less than 10 years in low areas, where the clays are thinnest, to about 40 years in areas where the clay is thickest. In areas where sinkholes are present, water can bypass the clay and directly recharge the Upper Floridan aquifer.

The contaminant PCE, derived from commercial use, was disposed of at land surface from the 1930s until the 1960s within the City. This contaminant was first detected in City water-supply wells in the late 1980s, indicating that it may have taken 20 to 50 years for PCE to reach these wells; PCE sorbs onto organic matter in the aquifer and would be expected to move slower than the average ground-water velocity.

Delineation of Contributing Areas for City of Tallahassee Public-Supply Wells

Contributing areas were determined for 26 wells in Tallahassee (table 7). As previously discussed, the Upper Floridan aquifer is composed of limestone with secondary porosity development as a result of dissolution. The exact distribution of permeability variations beneath the City cannot be precisely determined. The contributing area for a well is dependent on the permeability distribution, so it is difficult to delineate a single deterministic contributing area for each well. In such cases, stochastic techniques can be used to characterize potential contributing areas.

Overview of Contributing-Area Delineation

To delineate each contributing area, the model was run 100 times and the results were analyzed statistically. For each of the 100 runs, a different hydraulic conductivity (for each of the zones shown in fig. 16) was assigned to the Upper Floridan aquifer. The distribution of hydraulic conductivities within the Upper Floridan aquifer was assumed to be a lognormal distribution. The mean of the distribution was equal to the calibrated hydraulic conductivity value. Upper and lower limits were placed on the range of hydraulic conductivities to keep them within a reasonable range. The limits were set at one order of magnitude above and below the calibrated value. Beneath downtown Tallahassee, for example, the calibrated value for the hydraulic conductivity was 1,000 ft/d; therefore, the upper limit was set at 10,000 ft/d and the lower limit was set at 100 ft/d. All of the wells were pumping during each simulation.

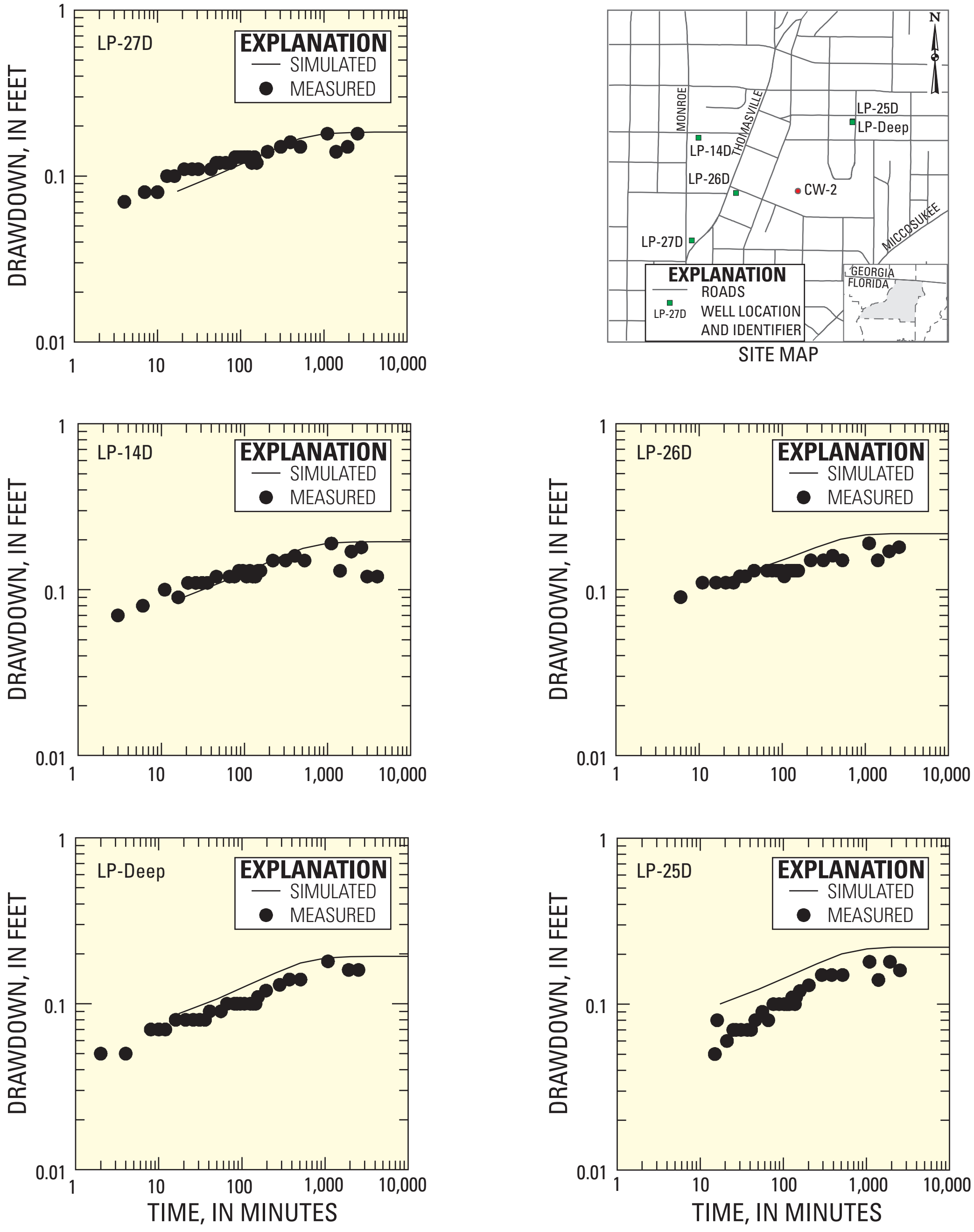

Figure 19. Measured and simulated aquifer-test data for five monitoring wells adjacent to well CW-2 in Tallahassee.

Table 6. Simulated effective porosities of the Hawthorn clays and Upper Floridan aquifer and simulated traveltimes using helium-derived age dates and calculated for ground-water ages.

[Values in bold indicate that effective porosities resulted in total traveltimes that fell within 3 years of the calculated time. na, Hawthorn clay layer assumed to be absent; $^3H/^3He_{trit}$, tritium/tritiogenic helium-3; ND, no data]

Effective porosity (percent)		Siumulated age of ground water (years)			
Hawthorn clays	Upper Floridan aquifer	Well CW-25	Well CW-11	Well CW-3	Well FP-1
NA	0.1	0.5	0.6	0.4	0.1
NA	1.0	4.6	5.5	4.0	1.3
NA	5.0	17.9	13.4	15.6	6.6
NA	25.0	23.5	25.8	27.3	21.3
12.5	0.1	8.2	16.4	19.9	7.7
12.5	1.0	11.3	15.4	23.5	8.9
12.5	2.5	16.6	19.1	**29.4**	10.9
12.5	5.0	22.8	25.8	36.7	14.2
12.5	10.0	**28.7**	**33.0**	45.6	20.8
12.5	25.0	**32.6**	39.7	44.8	22.3
25	0.1	14.9	25.1	**35.0**	9.2
25	1.0	18.3	27.5	38.9	9.4
25	2.5	23.2	**31.5**	44.6	9.7
25	5.0	**29.0**	36.8	48.8	10.6
25	10.0	**29.2**	44.0	44.0	11.5
25	25.0	39.5	50.9	58.2	20.2
35	0.1	20.3	**33.8**	39.4	5.6
35	1.0	22.9	36.7	44.3	5.1
35	5.0	**32.0**	42.3	51.3	5.2
35	25.0	38.7	ND	ND	20.2
$^3H/^3He_{trit}$ apparent ages (calculated)		31.0	33.0	32.0	26.0

For each individual model run, particles were started in all model cells and tracked forward in time; the starting point of each particle captured by a pumping well was recorded. The particles moved in a direction defined by the model simulation. After the 100 runs were completed, the data were analyzed to determine the contributing area of each well using the following method: each particle's starting location was noted, and if, for example, in one-half the model runs a particle from a certain location was captured by a well, then that starting location was assigned a 50-percent probability of capture by that well; this type of probability was calculated for each particle. The probabilities for each starting location were then contoured to give a probabilistic contributing area for each well. As an example, the probabilistic contributing area to well CW-1 is shown in figure 21. Within the red contour area, the probability of ground water in the Upper Floridan aquifer being captured by the well exceeds 80 percent; within the orange contour area, the probability exceeds 60 percent; within the pale-green contour, the probability exceeds 40 percent; within the dark-green contour, the probability exceeds 20 percent; and within the blue contour, the probability exceeds 10 percent.

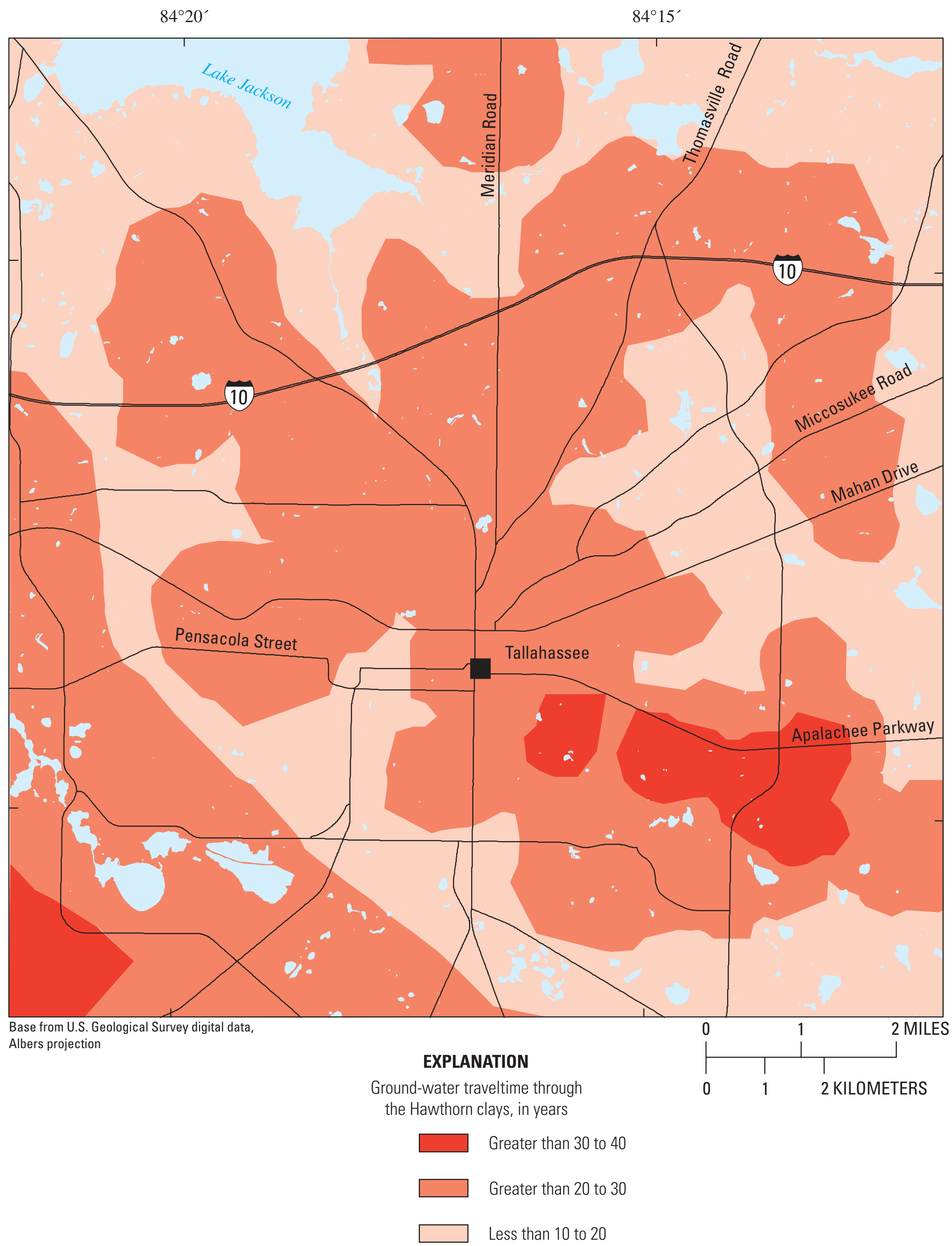

Figure 20. Computed traveltime through the Hawthorn clays in the Tallahassee area.

Table 7. Characteristics of City of Tallahassee public-supply wells for which contributing areas were delineated.

[Well depths are in feet below land surface; altitude and open-hole intervals are in feet relative to the North American Vertical Datum of 1988]

Well no.[1]	Altitude of top of casing (feet)	Depth of well (feet)	Top of open-hole interval (feet)	Bottom of open-hole interval (feet)	Well diameter (inches)	Length of open hole (feet)	Pumping rate (gallons per minute)
CW-1	125	350	-52	-225	20	177	1,189
CW-2	188	415	-26	-228	20	202	1,374
CW-3	135	380	-50	-245	18	185	1,435
CW-4	193	427	-45	-234	18	238	1,463
CW-5	142	390	-80	-248	18	222	1,226
CW-6	138	294	-13	-157	20	144	1,409
CW-7	163	364	-8	-202	20	194	1,154
CW-8	187	466	-36	-279	20	223	1,316
CW-9	140	347	-47	-207	20	187	1,330
CW-10	192	442	-50	-250	20	242	1,246
CW-11	230	454	-44	-224	20	274	1,320
CW-12	125	365	-67	-240	24	192	3,150
CW-13	157	370	-62	-213	24	219	2,402
CW-15	116	315	0	-199	24	116	2,040
CW-16	181	332	-74	-151	24	255	3,592
CW-17	210	483	-104	-273	20	314	2,304
CW-18	185	388	-82	-203	16	267	1,890
CW-19	170	428	-120	-258	8	290	427
CW-20	145	245	-6	-100	12	151	902
CW-21	110	270	-70	-160	24	180	1,498
CW-22	105	190	4	-85	8	101	422
CW-23	120	410	-130	-290	24	250	2,595
CW-25	230	450	-75	-220	24	305	2,600
CW-26	140	405	-167	-265	24	307	2,573
CW-27	158	316	8	-158	24	150	2,139
CW-29	158	405	-92	-247	24	250	3,070

[1]Wells CW-14, CW-24, and CW-28 are no longer in service.

Delineated Contributing Areas for All Wells

The probabilistic contributing areas were determined for all 26 wells. The relative sizes of each contributing area can be compared between plots as shown in figures 21 to 44, because all the figures are displaced at the same scale. In instances where wells are close together, such as wells CW-1 (fig. 21) and CW-3 (fig. 23), the contributing areas are more complicated because they are influenced by nearby wells. A more extreme example of this influence is shown in figure 22, where the contributing area of well CW-2 shows the effect of pumping by wells CW-4 and CW-8. Although deterministic contributing areas do not overlap under steady-state conditions, probabilistic contributing areas may overlap because boundaries can change in response to differences in hydraulic conductivities.

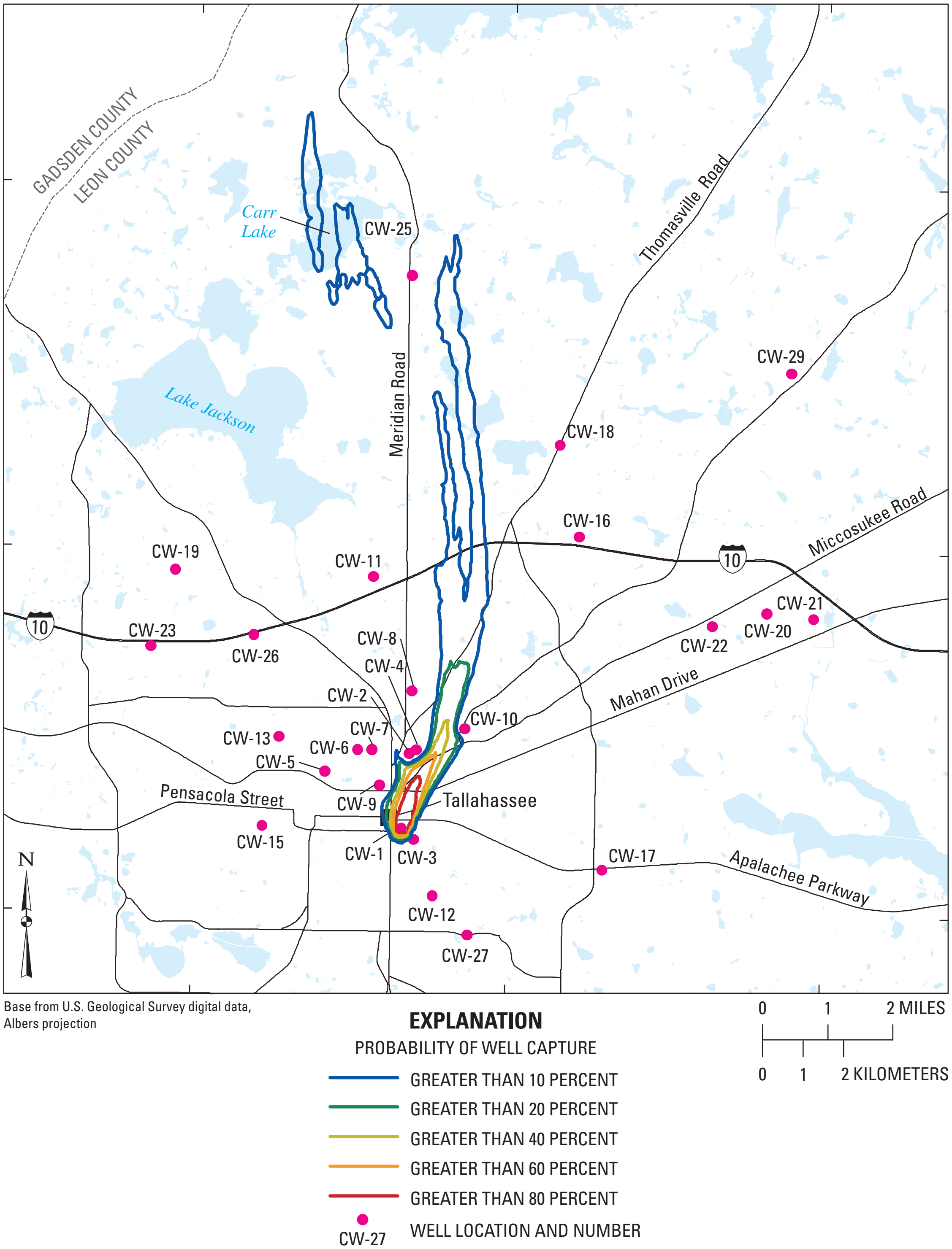

Figure 21. Probabilistic contributing area for City of Tallahassee well CW-1.

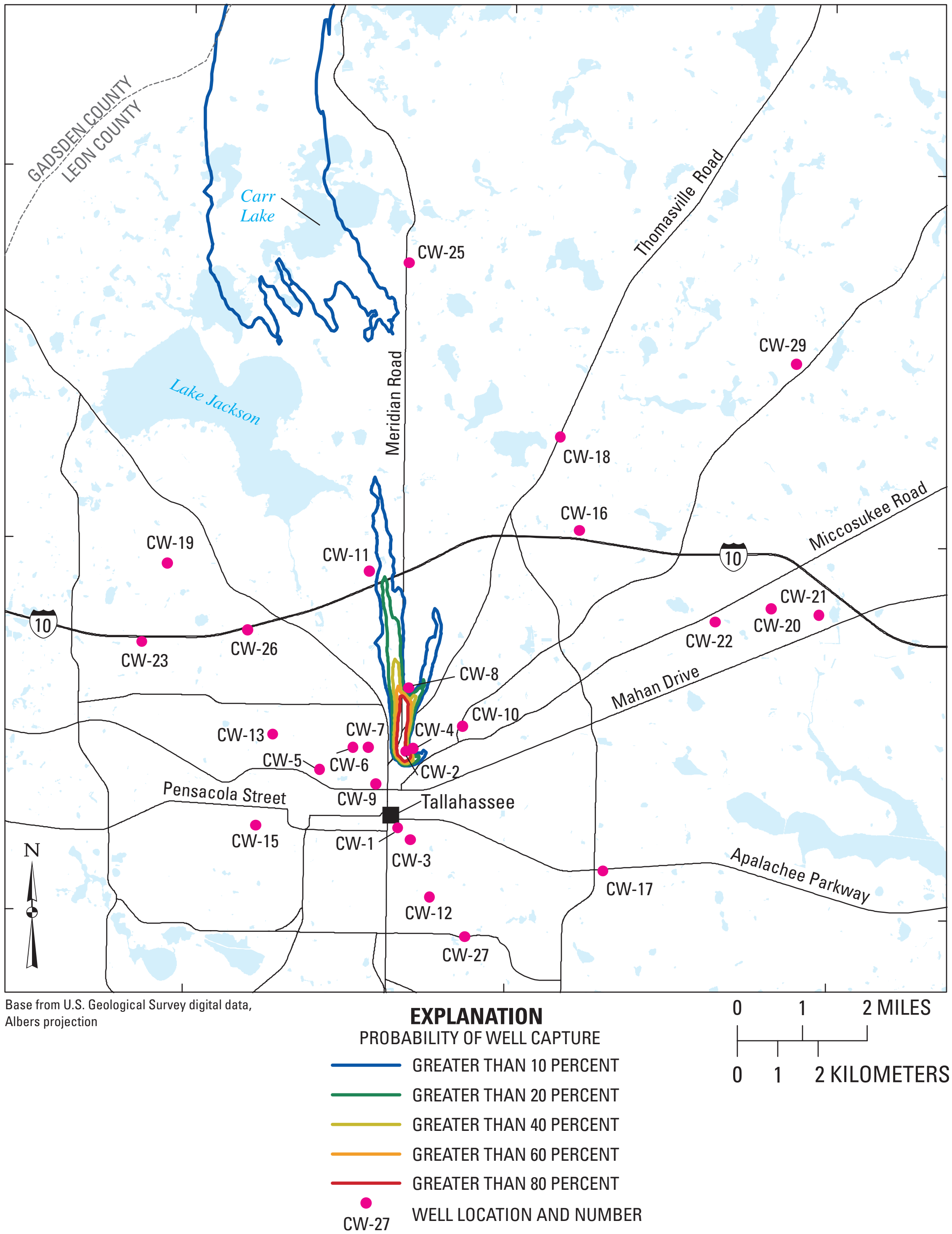

Figure 22. Probabilistic contributing area for City of Tallahassee well CW-2.

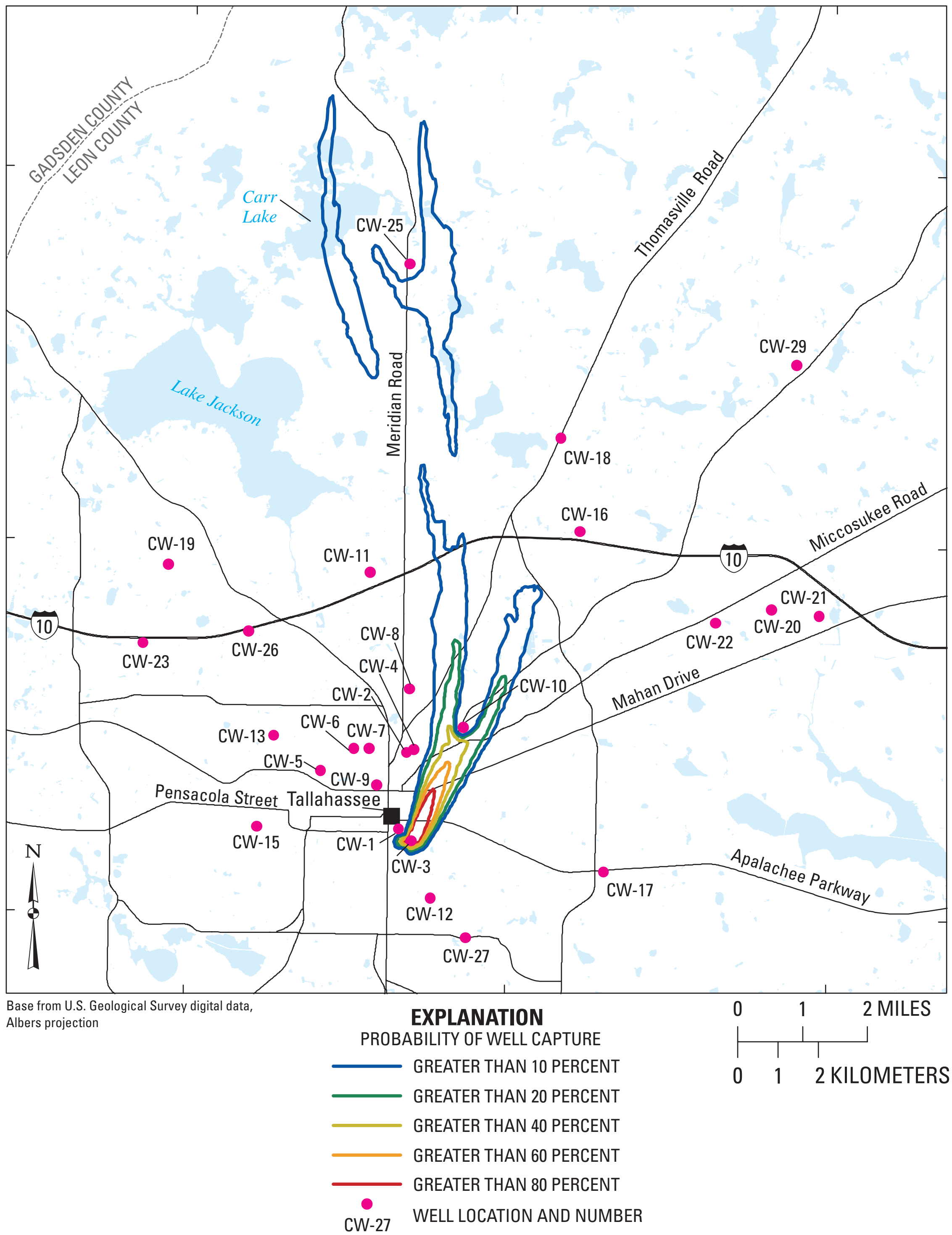

Figure 23. Probabilistic contributing area for City of Tallahassee well CW-3.

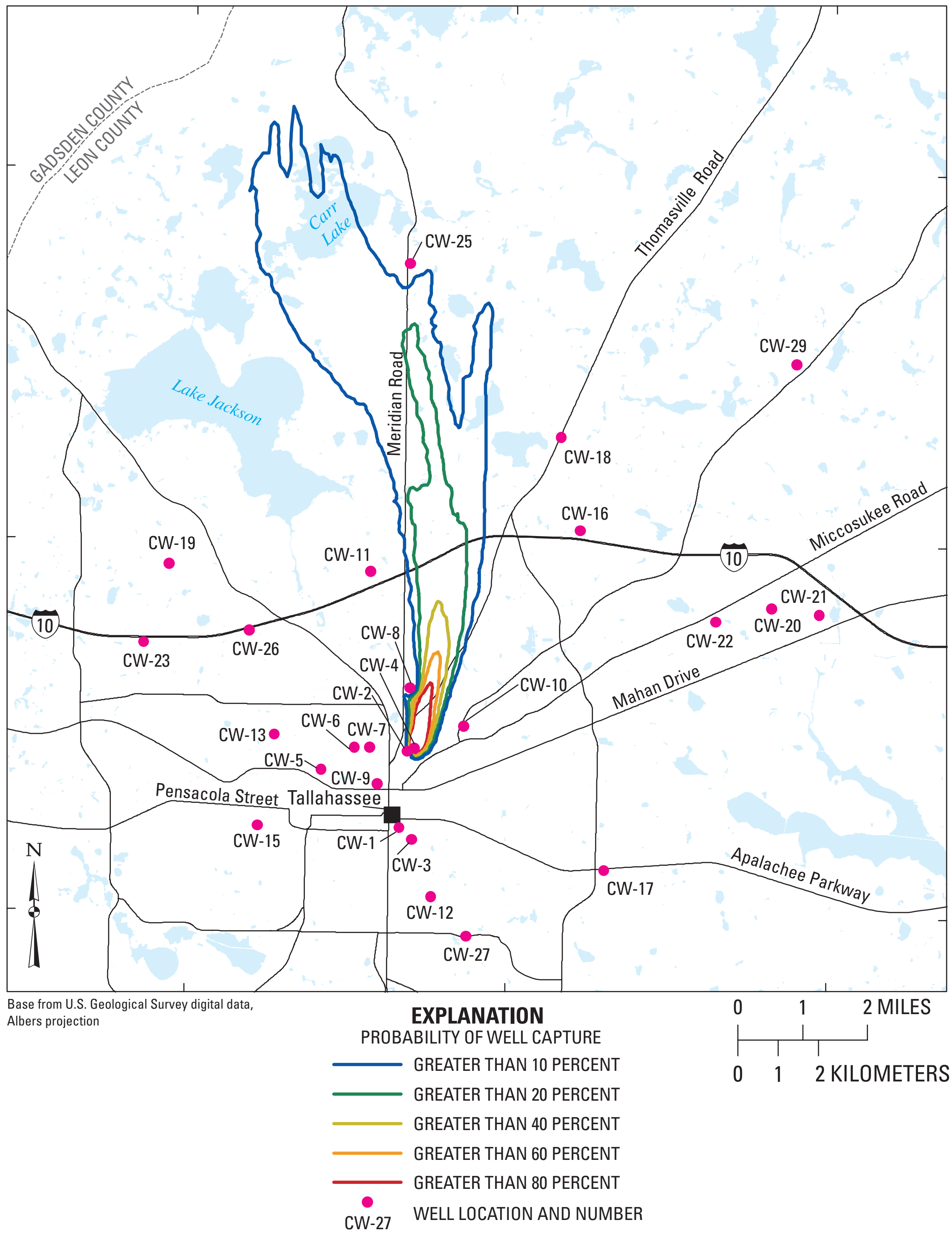

Figure 24. Probabilistic contributing area for City of Tallahassee well CW-4.

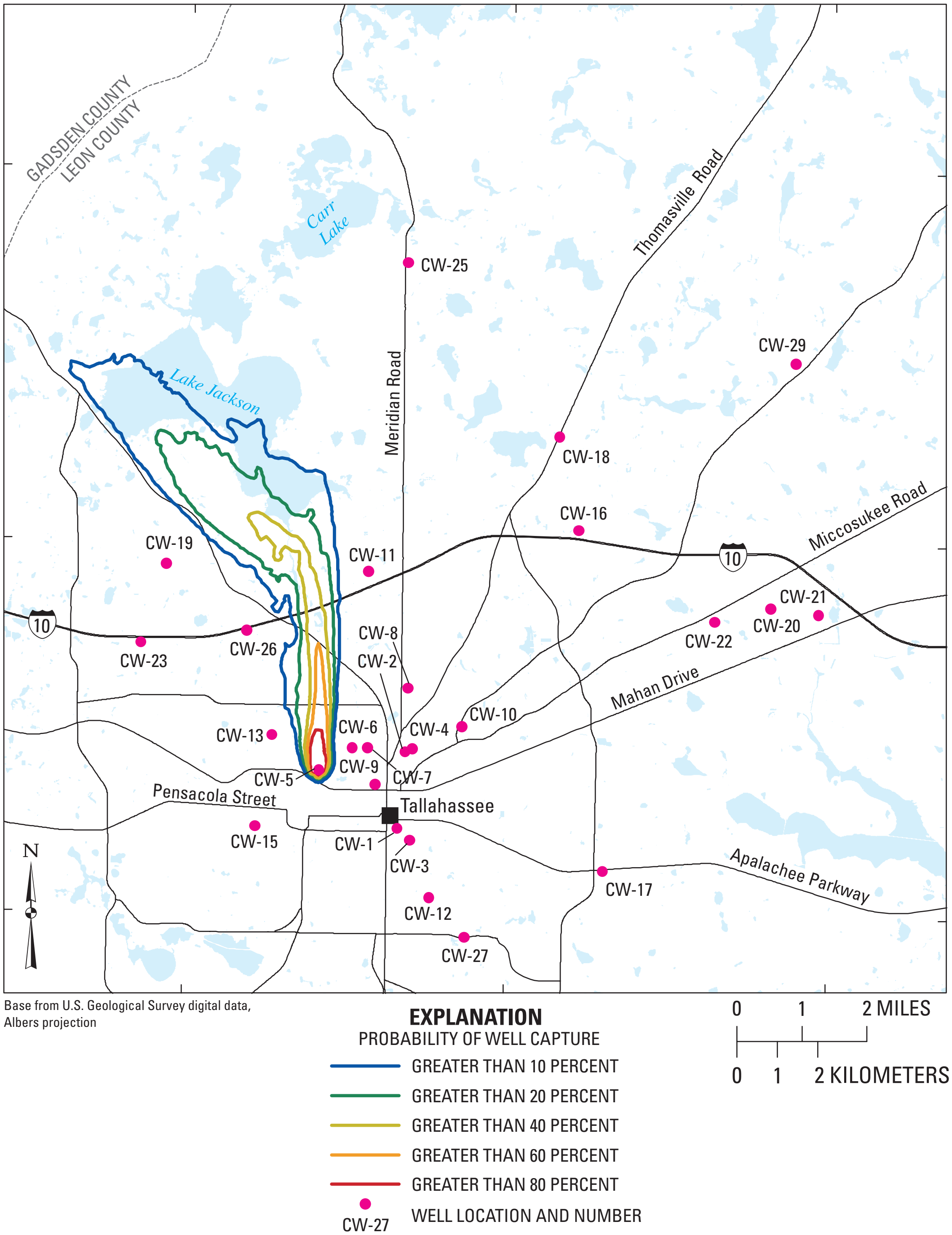

Figure 25. Probabilistic contributing area for City of Tallahassee well CW-5.

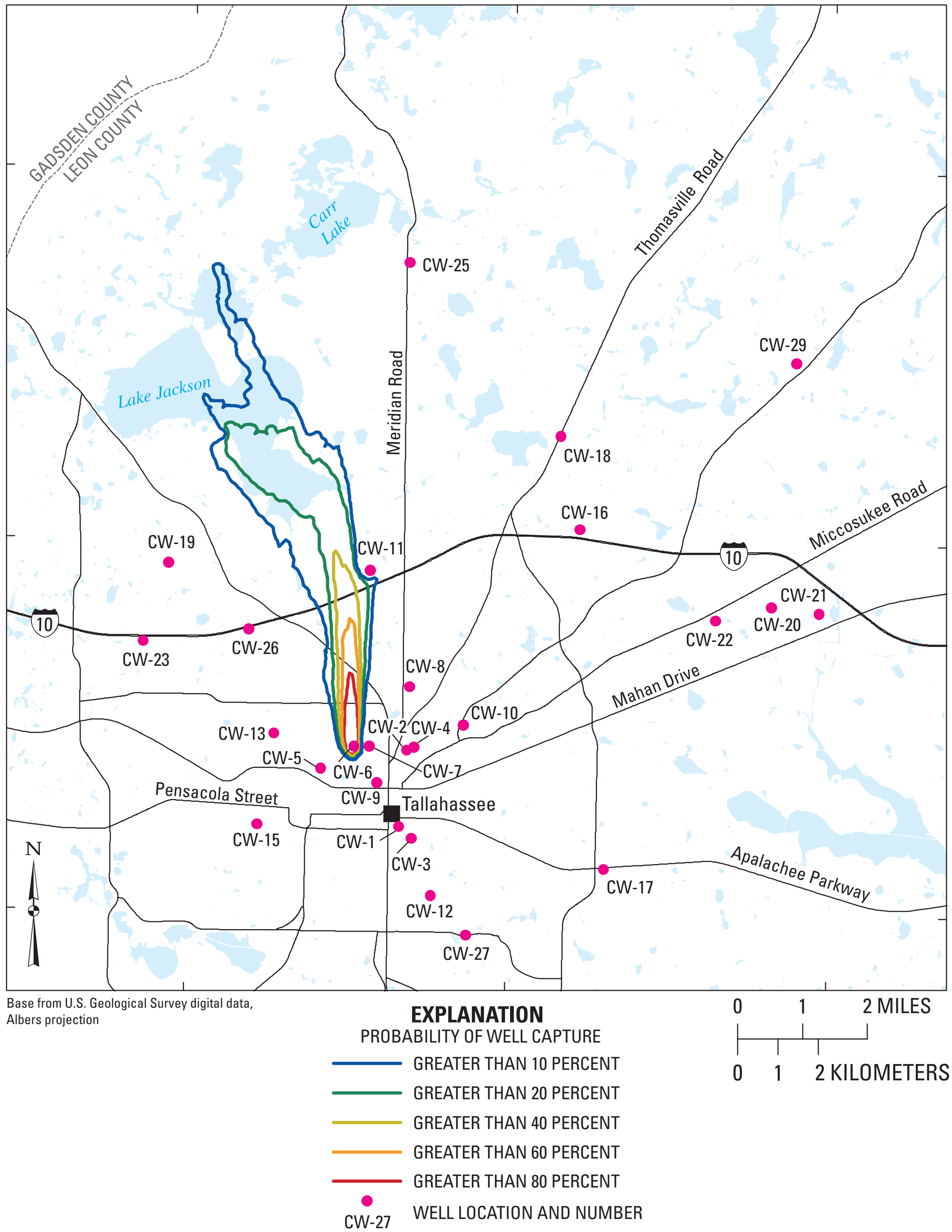

Figure 26. Probabilistic contributing area for City of Tallahassee well CW-6.

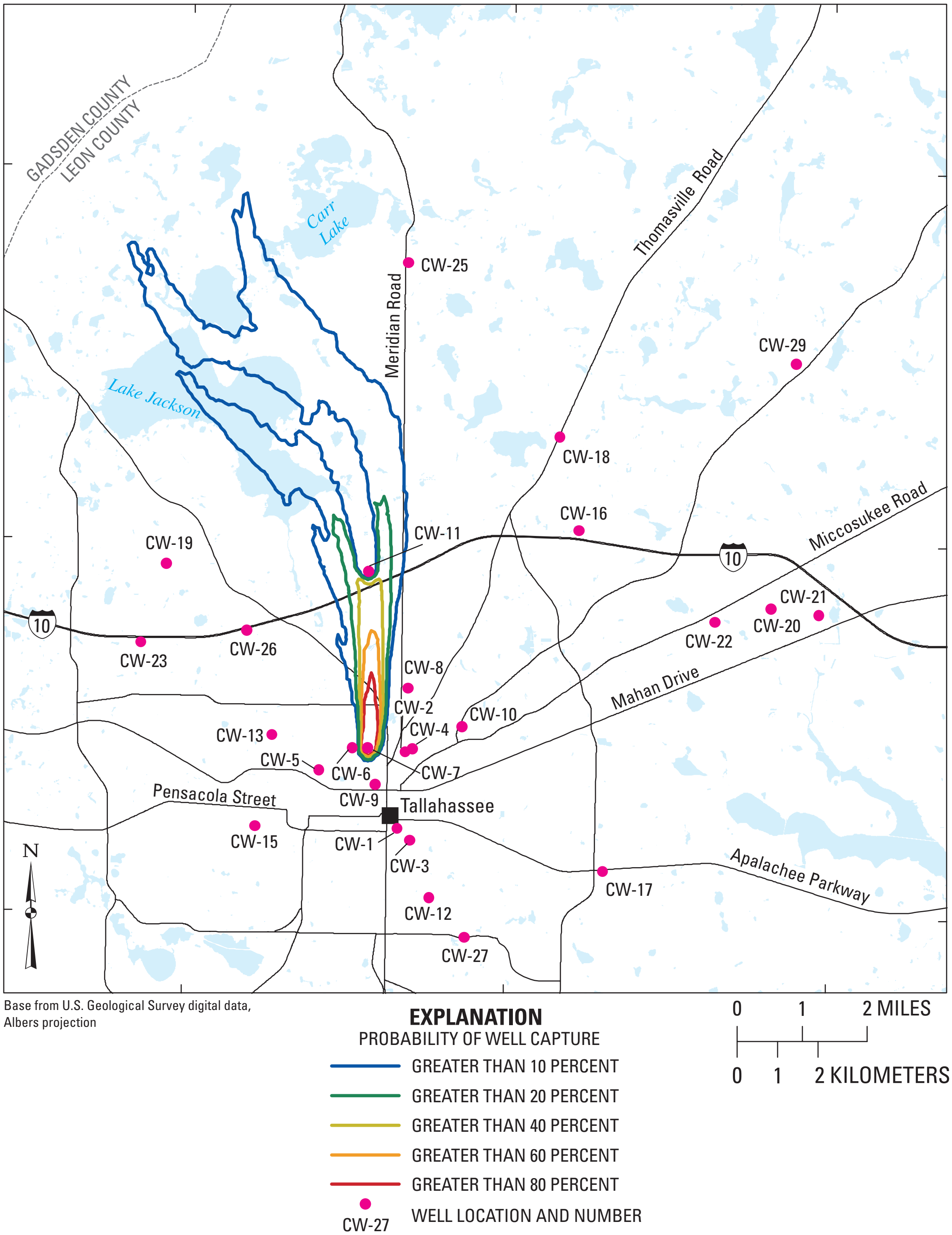

Figure 27. Probabilistic contributing area for City of Tallahassee well CW-7.

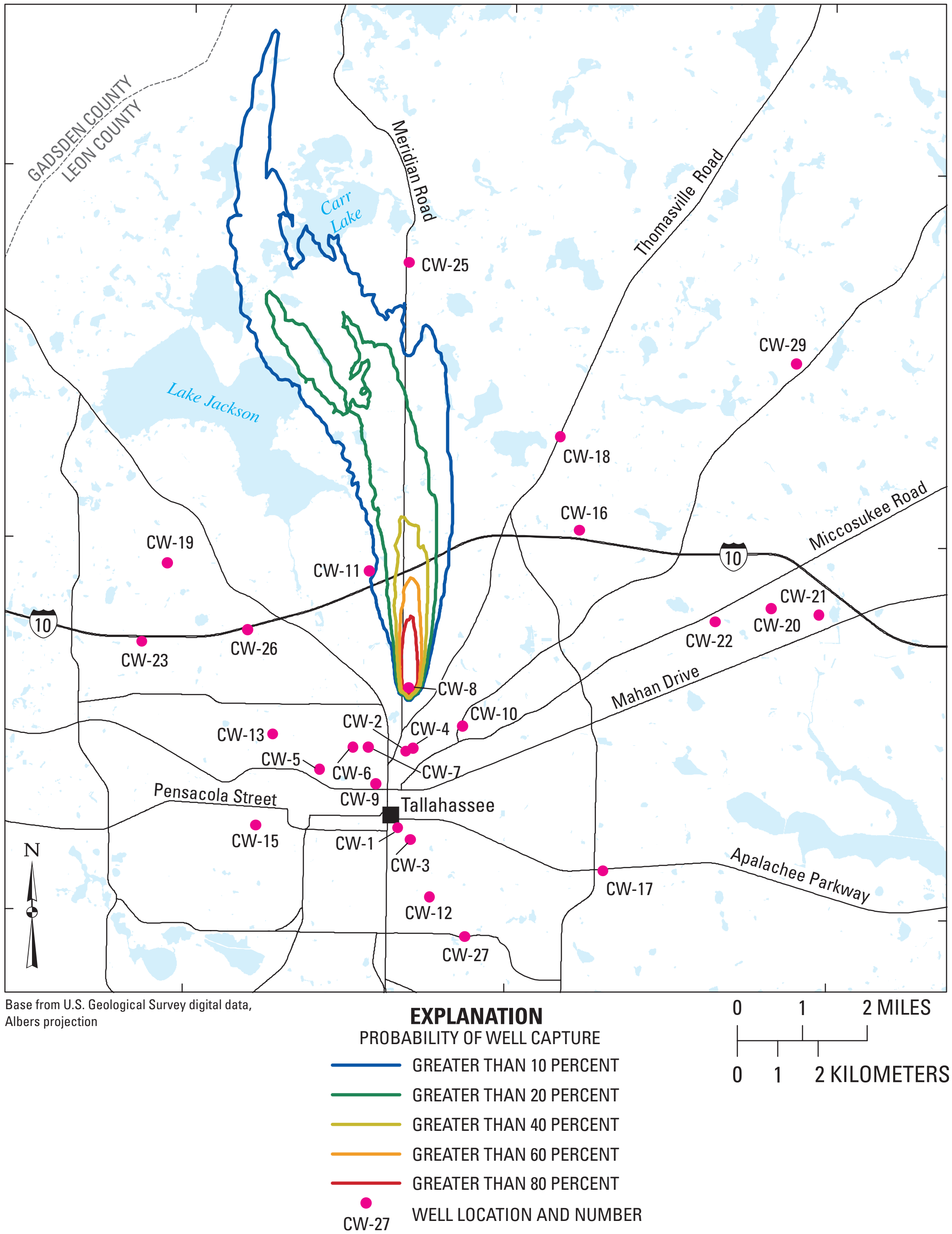

Figure 28. Probabilistic contributing area for City of Tallahassee well CW-8.

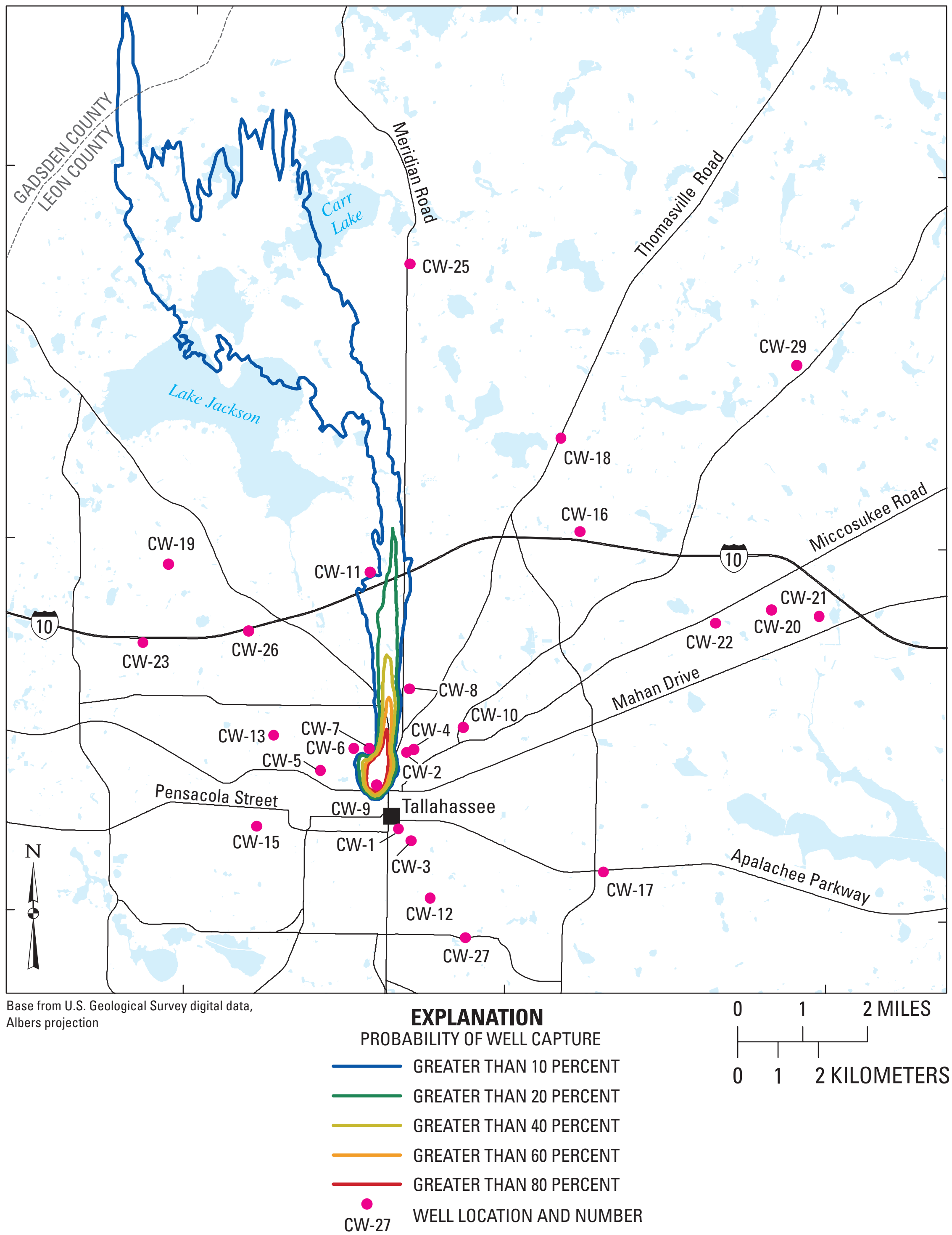

Figure 29. Probabilistic contributing area for City of Tallahassee well CW-9.

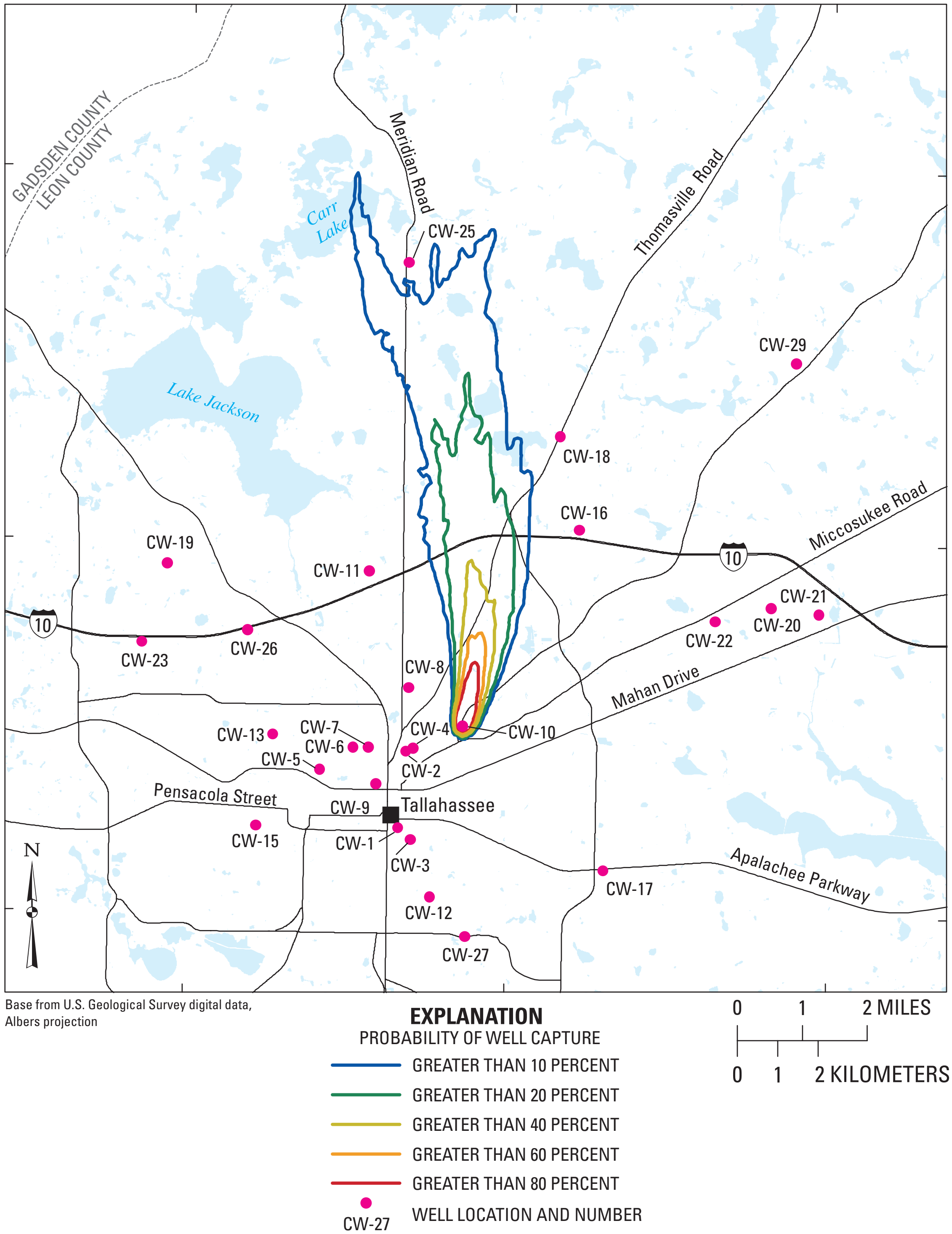

Figure 30. Probabilistic contributing area for City of Tallahassee well CW-10.

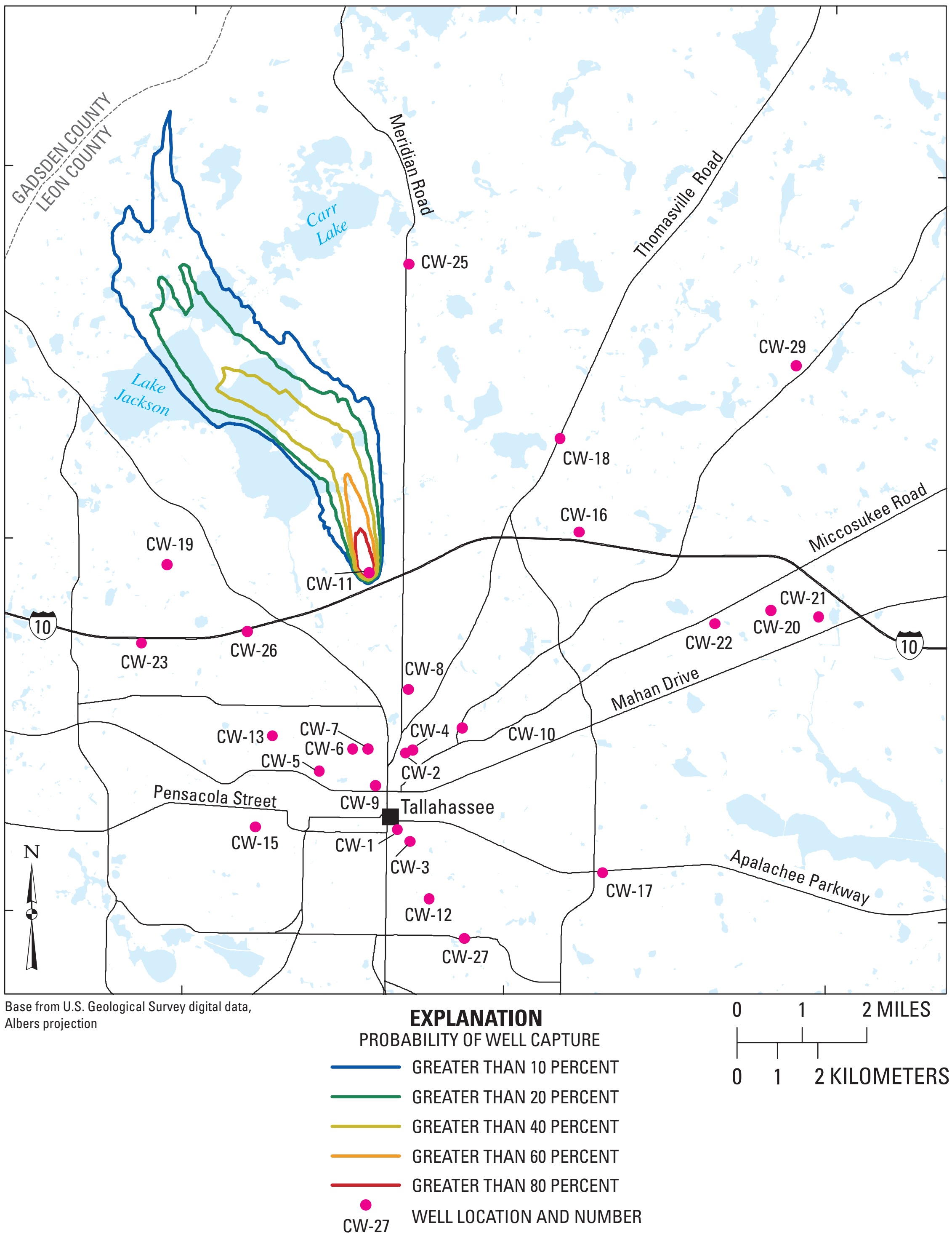

Figure 31. Probabilistic contributing area for City of Tallahassee well CW-11.

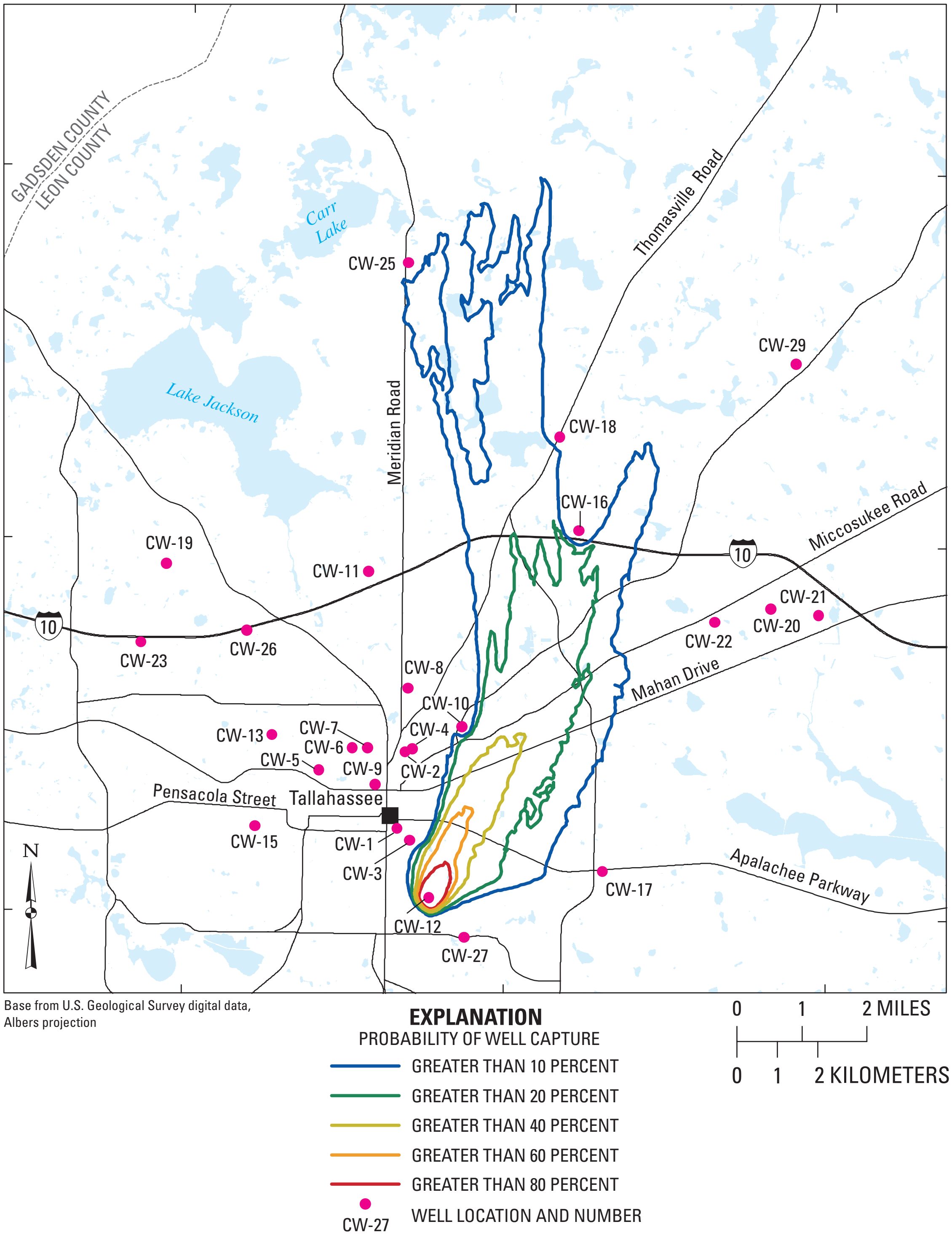

Figure 32. Probabilistic contributing area for City of Tallahassee well CW-12.

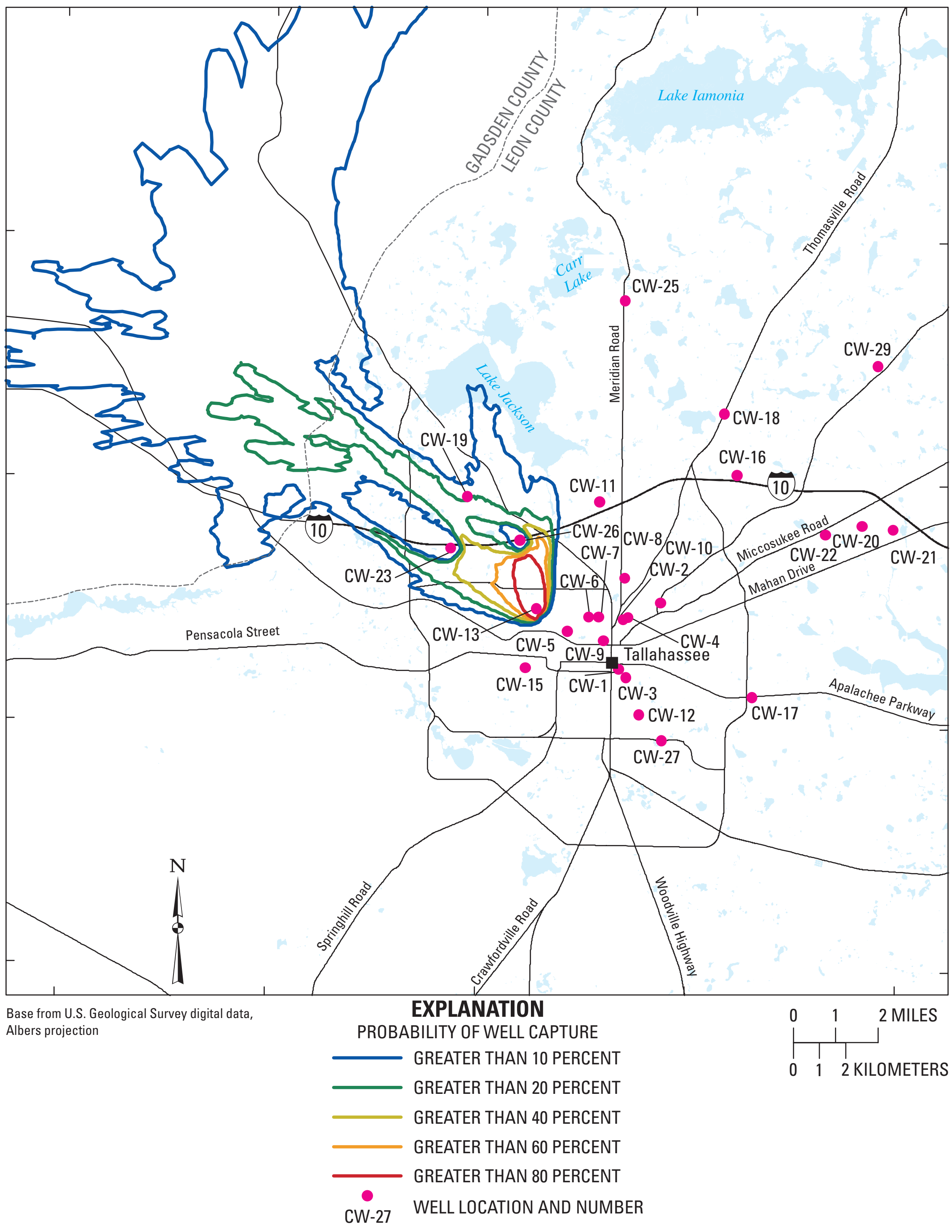

Figure 33. Probabilistic contributing area for City of Tallahassee well CW-13.

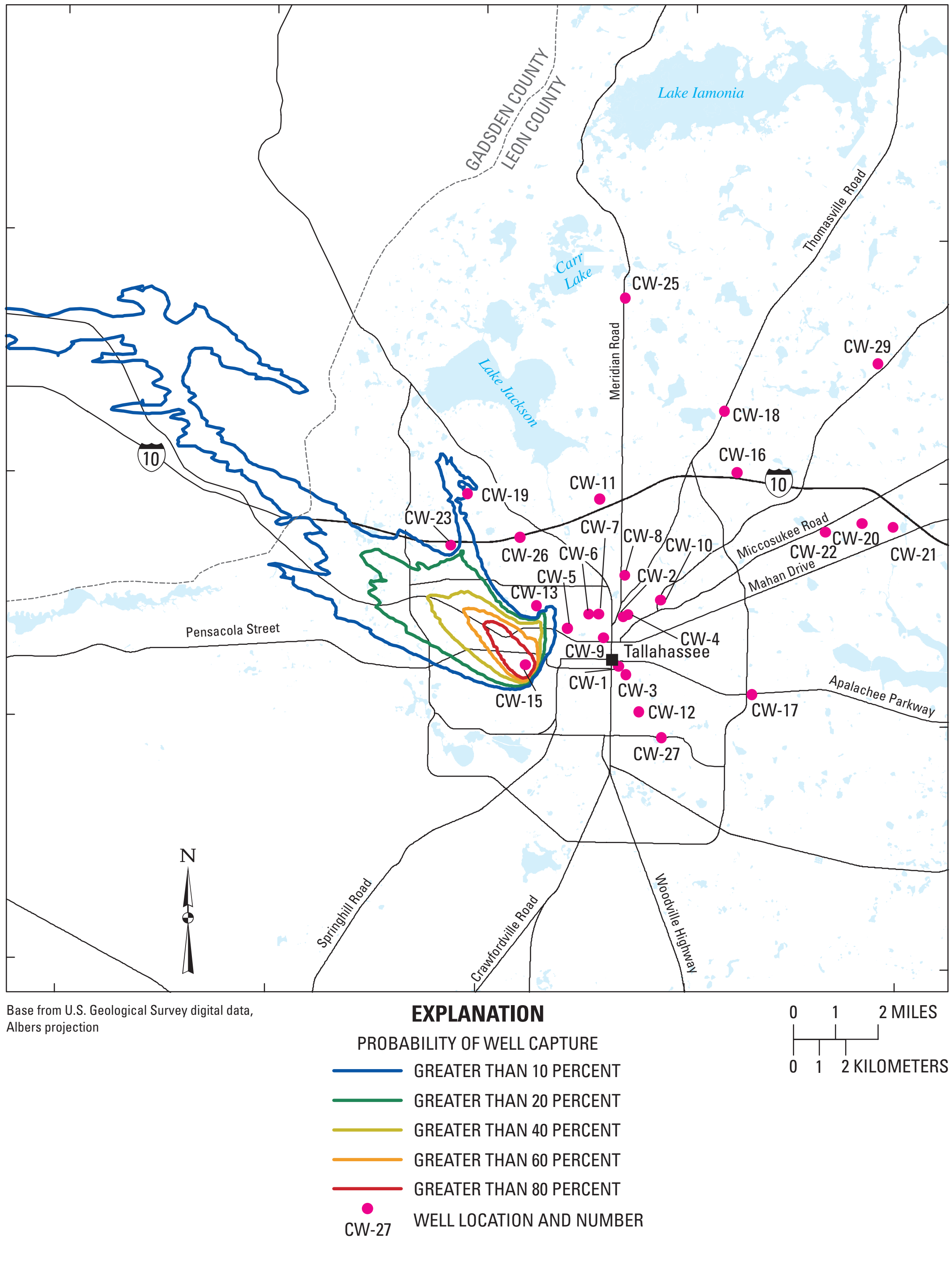

Figure 34. Probabilistic contributing area for City of Tallahassee well CW-15.

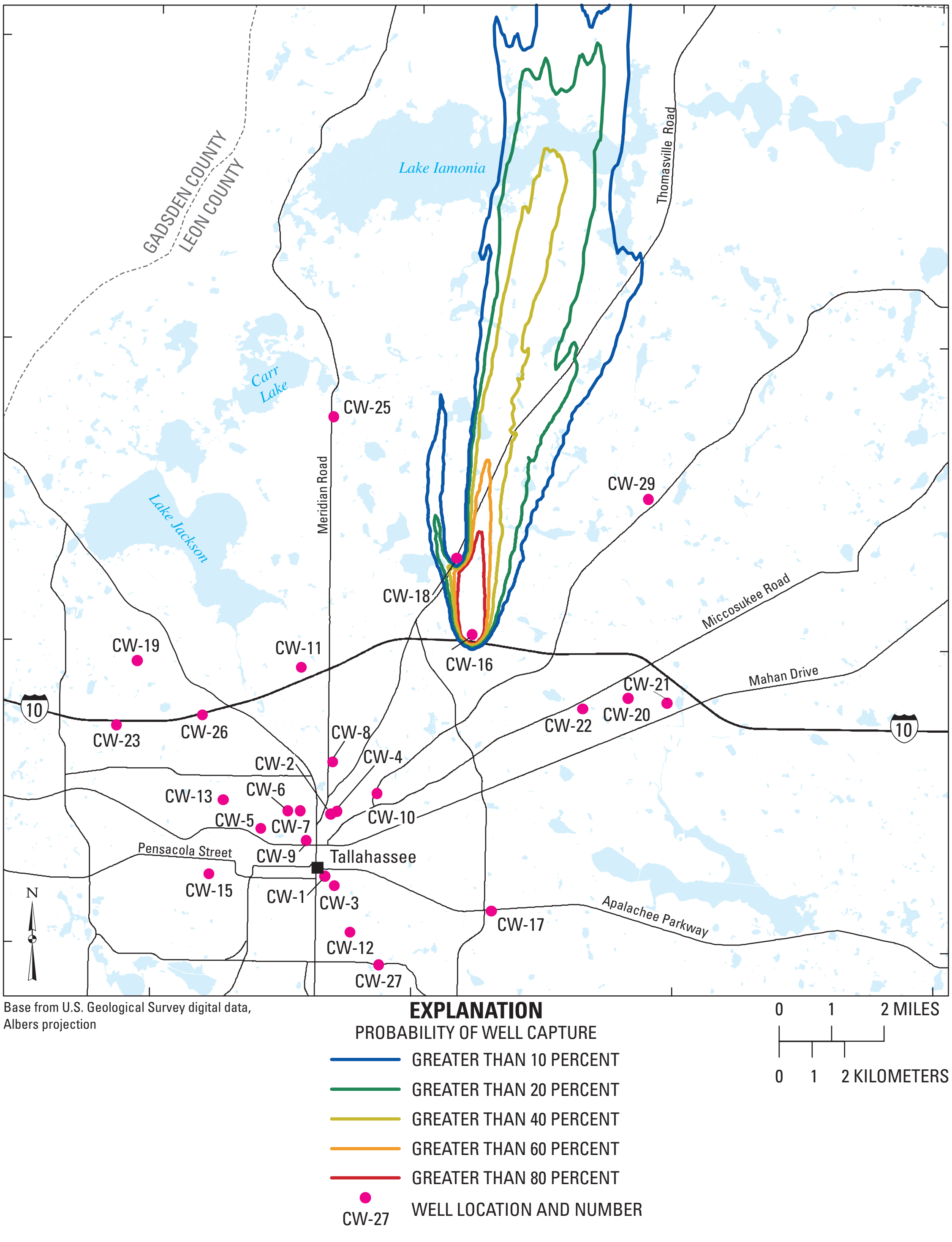

Figure 35. Probabilistic contributing area for City of Tallahassee well CW-16.

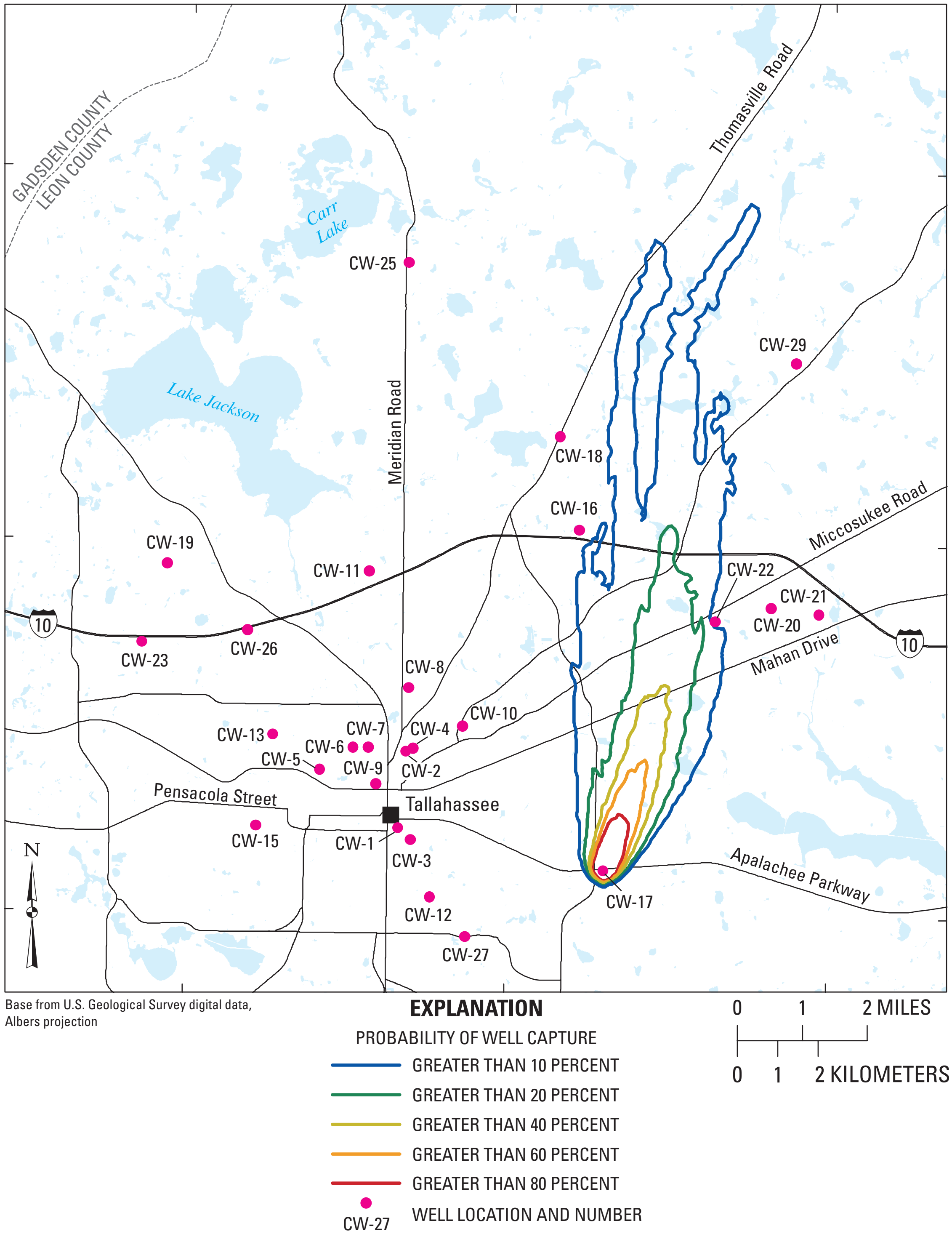

Figure 36. Probabilistic contributing area for City of Tallahassee well CW-17.

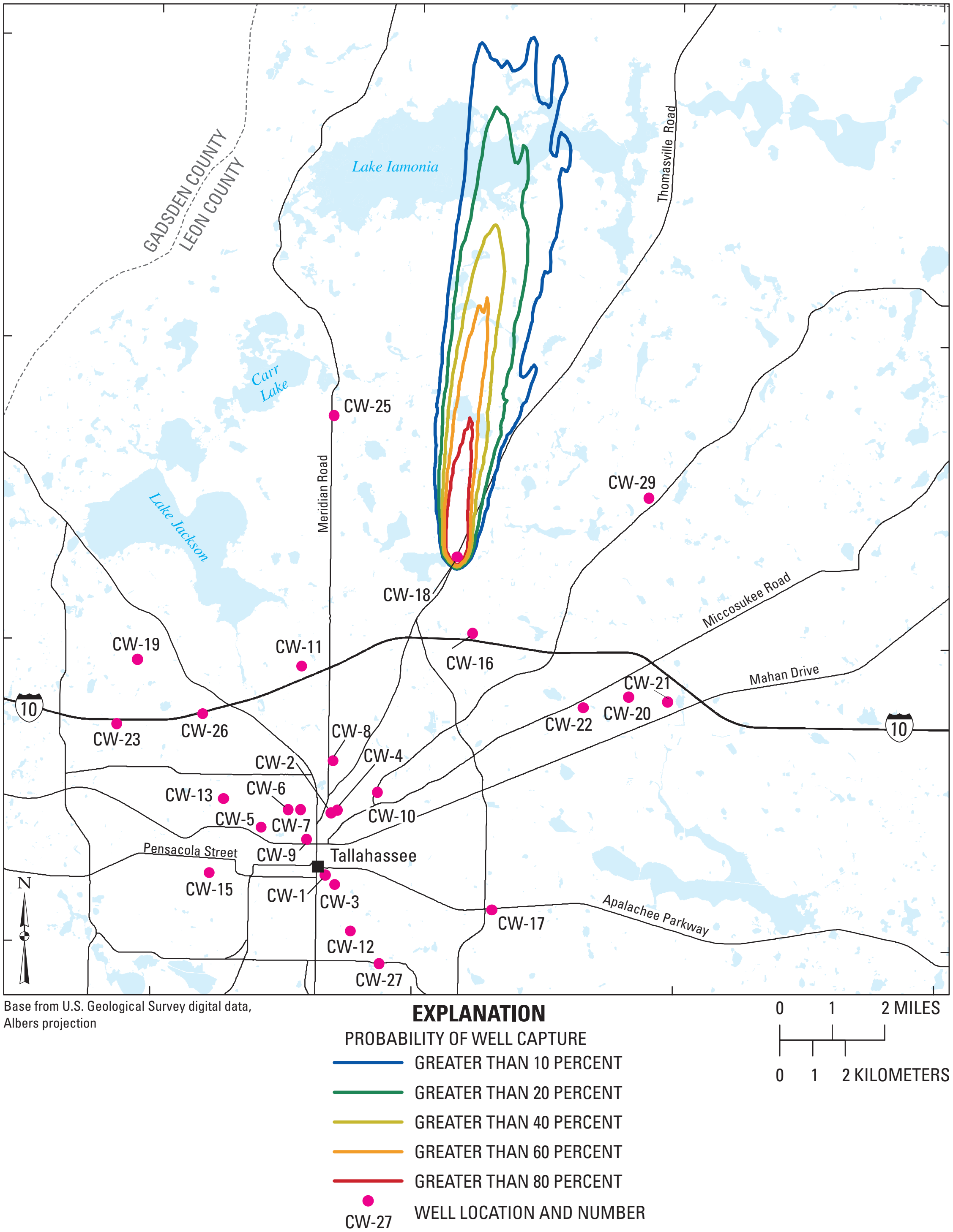

Figure 37. Probabilistic contributing area for City of Tallahassee well CW-18.

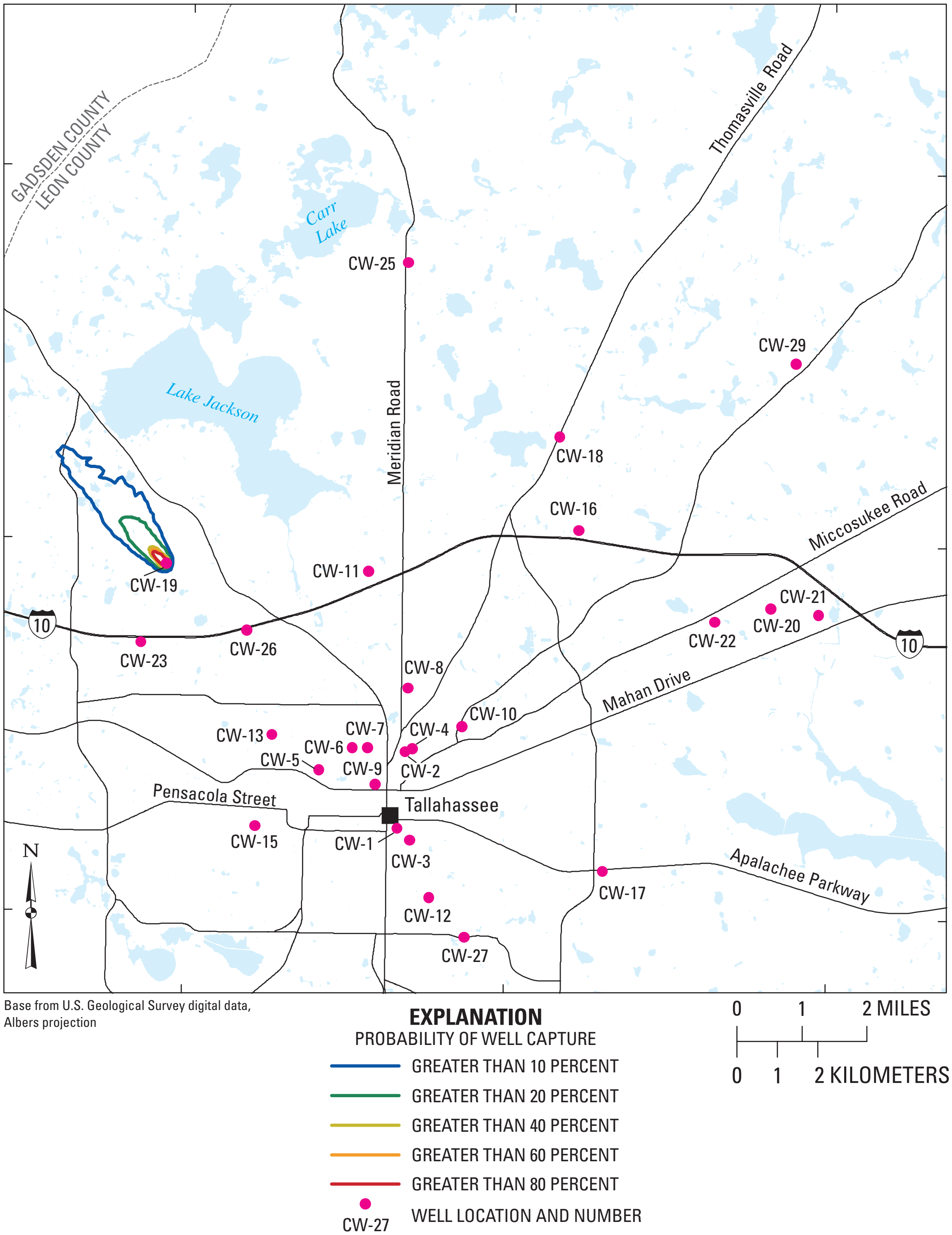

Figure 38. Probabilistic contributing area for City of Tallahassee well CW-19.

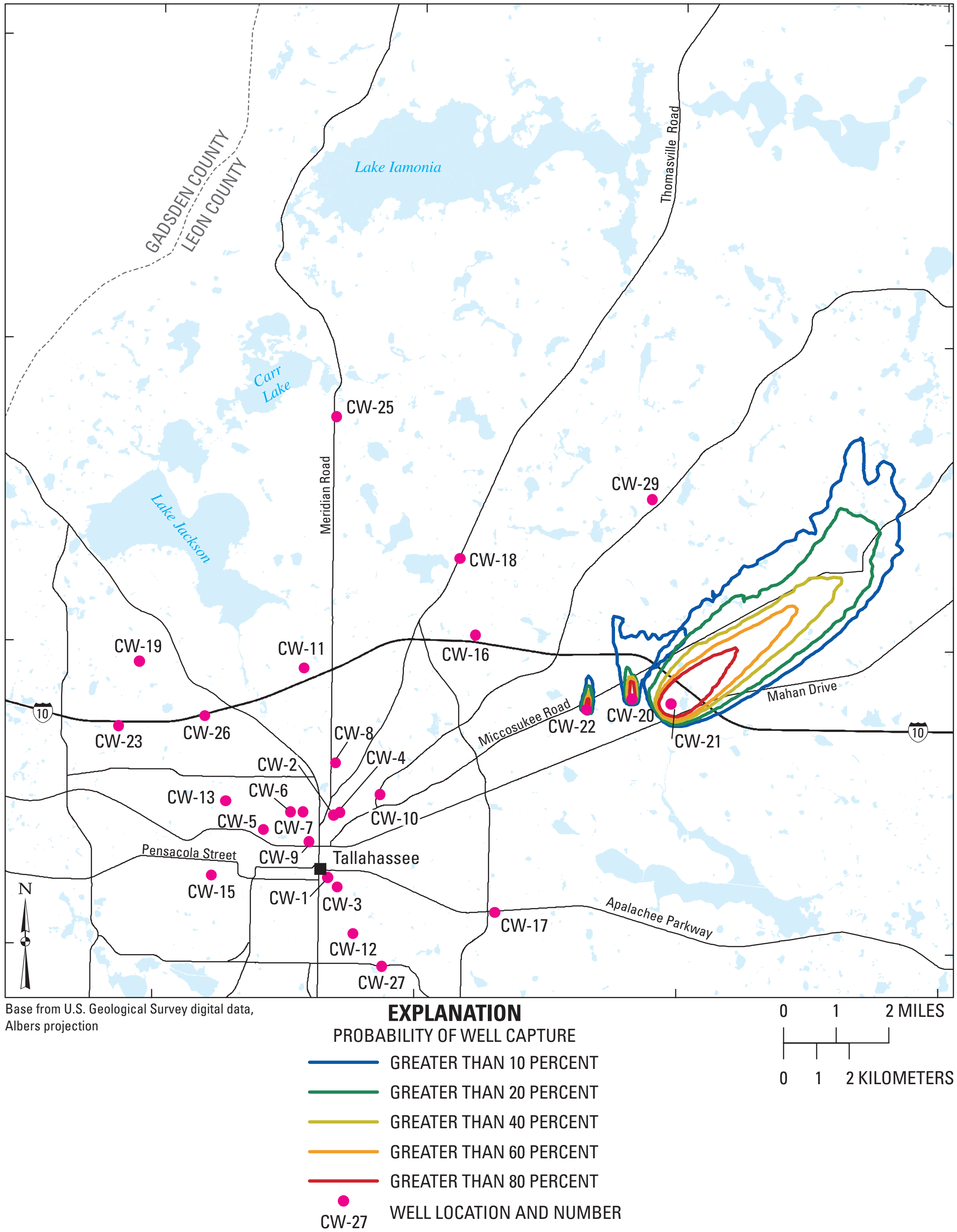

Figure 39. Probabilistic contributing area for City of Tallahassee wells CW-20, CW-21, and CW-22.

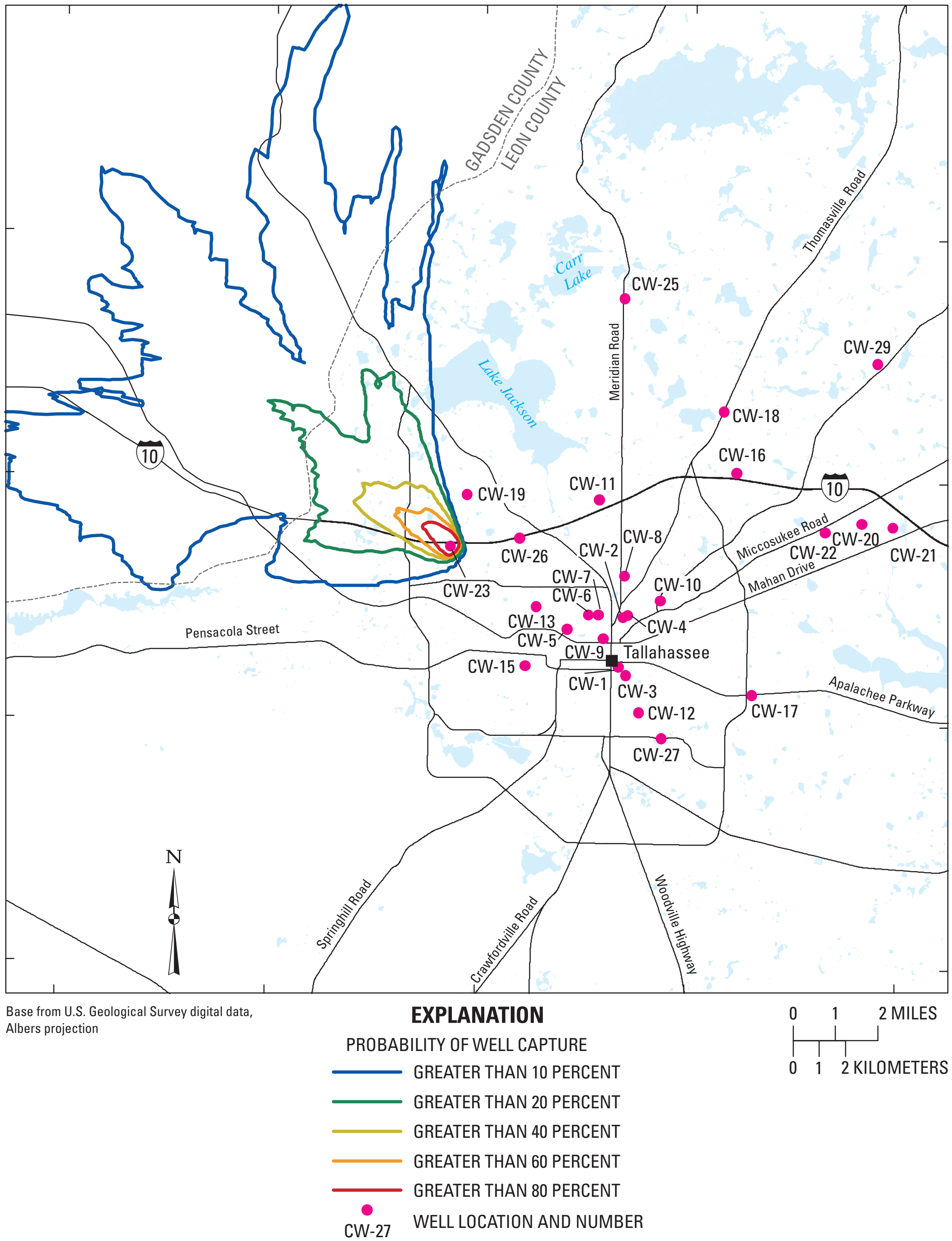

Figure 40. Probabilistic contributing area for City of Tallahassee well CW-23.

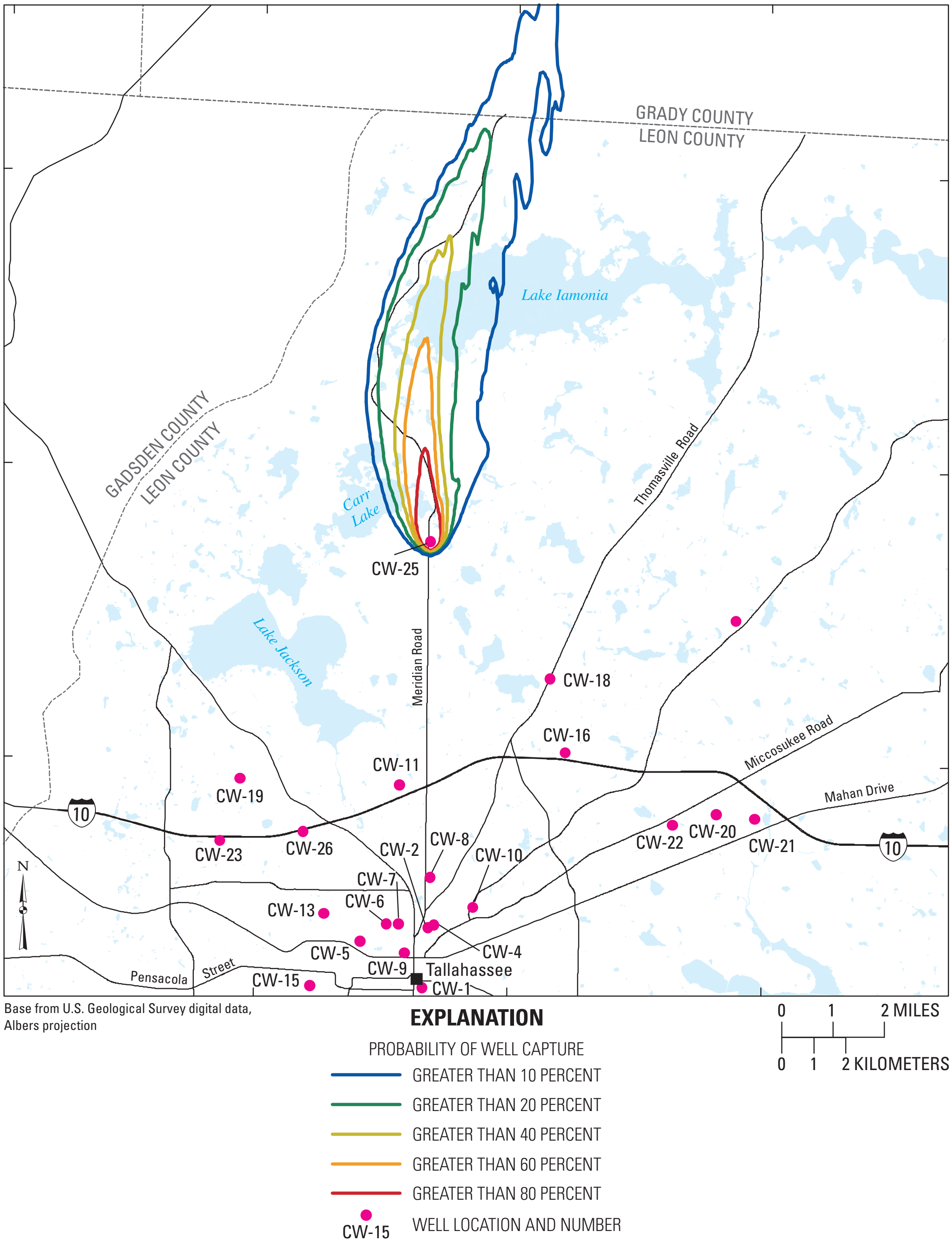

Figure 41. Probabilistic contributing area for City of Tallahassee well CW 25.

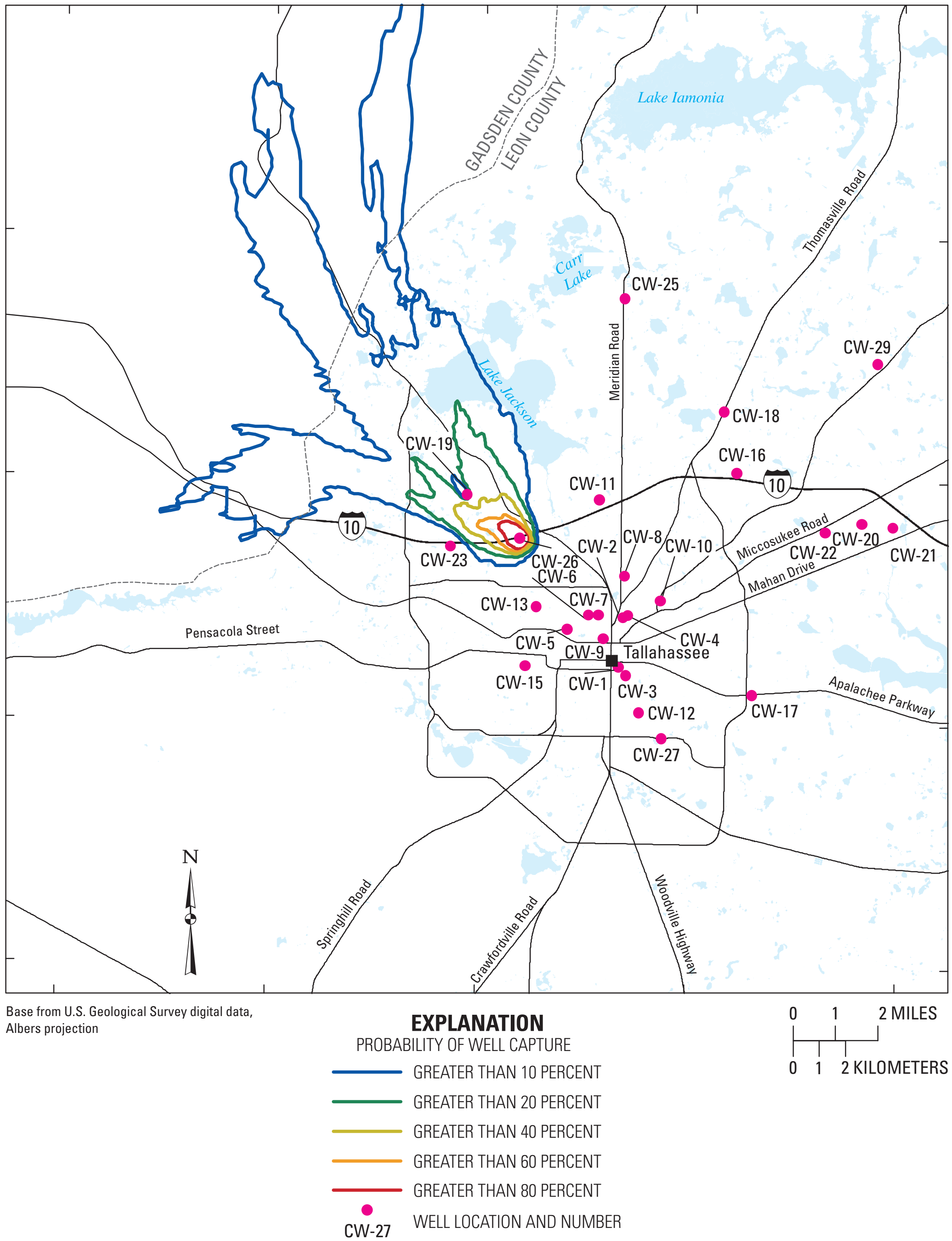

Figure 42. Probabilistic contributing area for City of Tallahassee well CW-26.

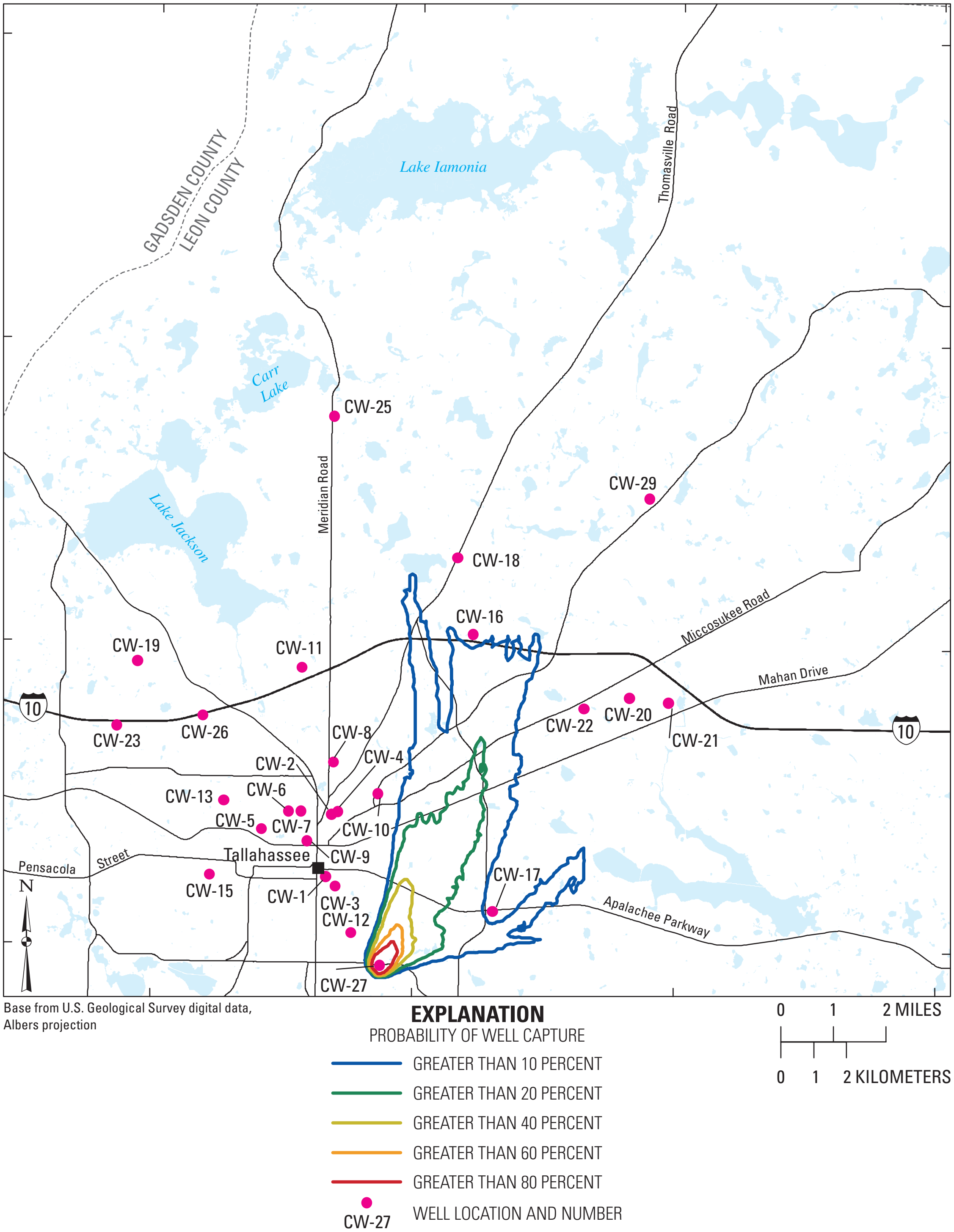

Figure 43. Probabilistic contributing area for City of Tallahassee well CW-27.

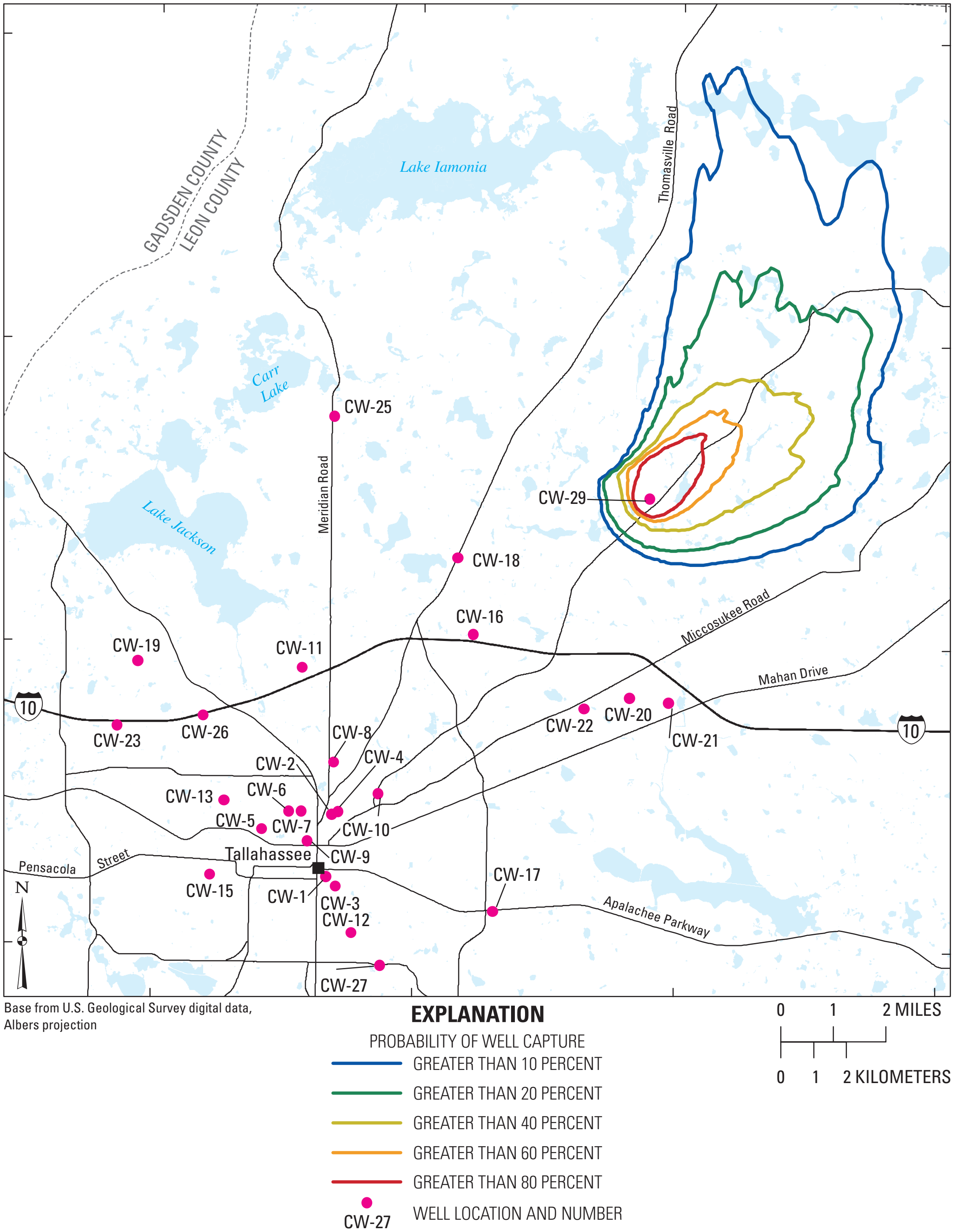

Figure 44. Probabilistic contributing area for City of Tallahassee well CW-29.

Time-Dependent Capture Zones for Representative Wells

The 5-year time-dependent capture zones (TDCZs) were delineated for four representative wells. To determine a TDCZ, (as previously discussed), an assumption about effective porosity must be made and included in the model simulation. Results of the age dating and analysis indicated that a 7-percent porosity represented the best average value for the Upper Floridan aquifer. The effective porosity, however, could vary widely in the local areas around an individual well. For this reason, a series of effective porosities (0.1, 1, and 7 percent) were used to delineate a 5-year TDCZ for wells CW-1, CW-25, CW-26, and CW-27.

The probabilistic contributing area and 5-year TDCZs for effective porosities 0.1, 1, and 7 percent were determined for well CW-1 (fig. 45). The capture zones with high probabilities of capture (greater than 40, 60, and 80 percent) are similar for all simulations, although the TDCZs delineated using a 7-percent porosity are slightly smaller than the other porosity values. The capture zones with low probabilities of capture (greater than 10 and 20 percent) showed a large range of variability. The TDCZ for 0.1-percent effective porosity is identical to the probabilistic contributing area, indicating that ground water in the Upper Floridan aquifer is completely captured within the 5-year period for this porosity. A value of 0.1 percent, however, is a very low (and probably unrealistically low) porosity and would represent only 0.1 ft of vertical open space per 100 vertical ft of aquifer. As previously discussed, the Lafayette deep well conservatively has 3.3 ft of vertical open space per 100 ft of aquifer. The 5-year TDCZs for a 1-percent effective porosity are substantially smaller (for the greater than 10- and 20-percent probabilities) than for the 0.1-percent value. The 1-percent effective porosity would represent 1 ft of vertical open space per 100 vertical ft of aquifer. The 7-percent porosity has relatively small overall 5-year TDCZs. The 7-percent effective porosity would represent 7 vertical ft of open space per 100 vertical ft of aquifer. The 5-year TDCZs and contributing area for wells CW-25, CW-26, and CW-27 are shown in figures 46, 47, and 48, respectively; each showed trends similar to well CW-1.

Contributing Areas for All Wells

The contributing areas were determined for all 26 wells for a capture probability of greater than 10 percent (fig. 49). As evidenced, almost all areas in northern Leon County could potentially provide water to a well within Tallahassee.

Effect of Model Parameter Changes on Contributing-Area Delineation

As previously discussed, the contributing areas were delineated by assuming a variable hydraulic conductivity. The variability was introduced into the model by assuming a lognormal hydraulic conductivity distribution in which the mean of the distribution was set at the value determined by the calibrated model. For each hydraulic conductivity zone, the distribution values were assumed to range from one order of magnitude greater than the mean to one order of magnitude less than the mean. In reality, it is impossible to know exactly what the actual value of hydraulic conductivity is for a certain part of the aquifer and the actual range of hydraulic conductivities in the area. To better understand how the probabilistic contributing areas would vary for a different set of hydraulic conductivity assumptions, some additional simulations were run. To test the effect of a change in the hydraulic conductivity range, two simulations were run: (1) the range was decreased to half an order of magnitude, and (2) the range was increased to two orders of magnitude (fig. 50). The decrease to half an order of magnitude resulted in a slightly thinner probabilistic contributing area that extended farther north than the original simulated probabilistic contributing area. The increase to two orders of magnitude resulted in an overall wider probabilistic contributing area that did not extend as far north as the original simulated probabilistic contributing area.

Two simulations were run in which the hydraulic conductivities were varied. In the first simulation, the hydraulic conductivities were reduced to 50 percent of the calibrated value; in the second simulation, hydraulic conductivities were increased by 100 percent of the calibrated value (fig. 51). The decrease in hydraulic conductivity resulted in a slightly larger probabilistic contributing area. The largest change occurred in the greater than 10-percent probabilistic contributing area, whereas the least change occurred in the greater than 80-percent contributing area.

Cross Sections of Probabilistic Contributing Areas

The probabilistic contributing areas for wells CW-6 and CW-25 were delineated in cross section (fig. 52). Well CW-6 is located where the Upper Floridan aquifer is about 1,200 ft thick; the open hole interval for the well is 144 ft and is located almost at the top of the aquifer. This well penetrates only about 12 percent of the aquifer, and its pumping rate is 1,409 gal/min. The highest probability of capture occurs near the open-hole interval; vertically, the probability of capture decreases with increasing depth of the aquifer. Well CW-25 is located where the aquifer is relatively thin (about 700 ft). The open-hole interval for the well is 145 ft and is located near the top of the aquifer. This well has a relatively high pumping rate of 2,600 gal/min. Because of the relatively thin aquifer and the high pumping rate, the probability of capture for this well (even the 60-percent probability contour) extends throughout the full thickness of the Upper Floridan aquifer.

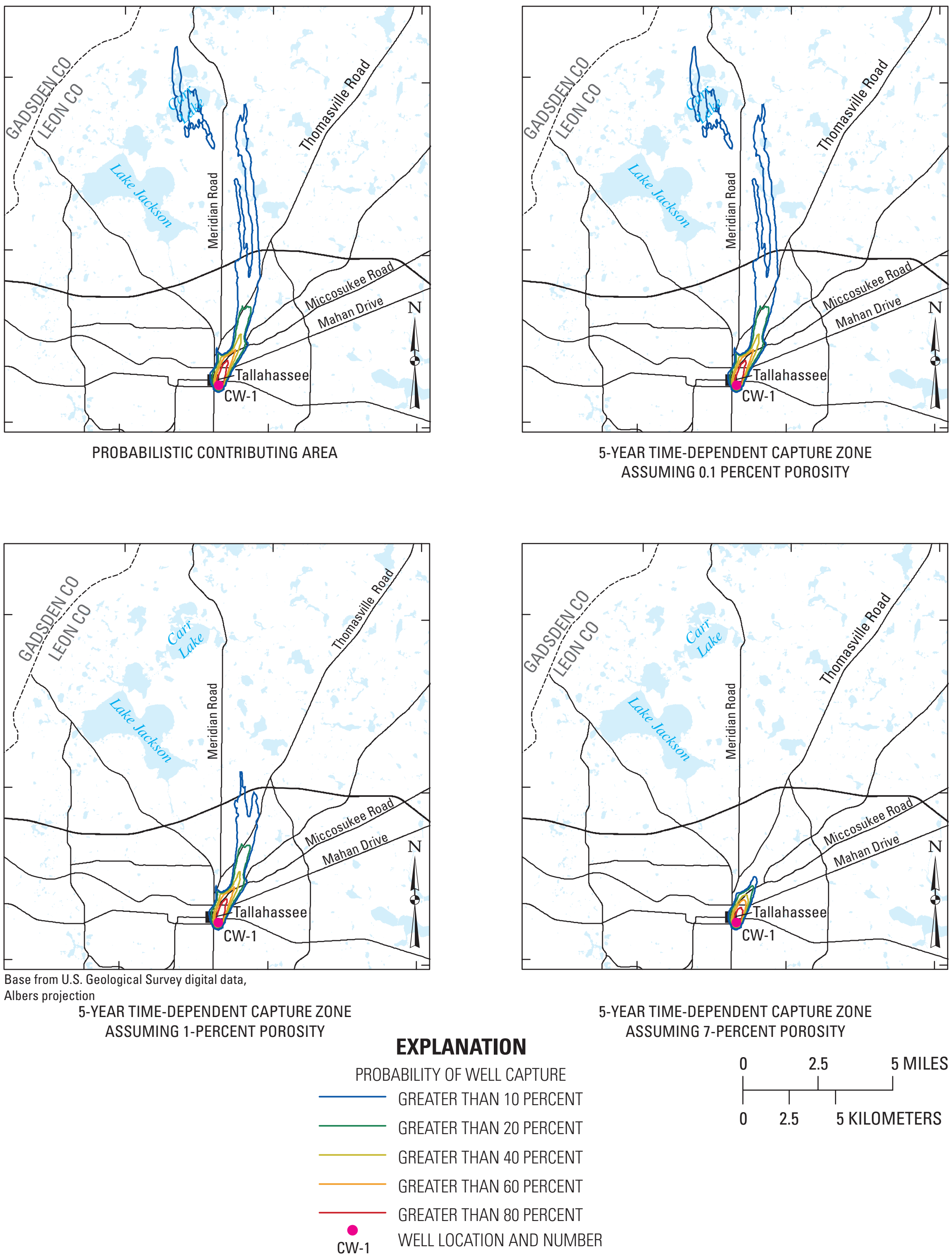

Figure 45. Probabilistic contributing areas and 5-year time-dependent capture zones for City of Tallahassee well CW-1, assuming various porosities for the Upper Floridan aquifer.

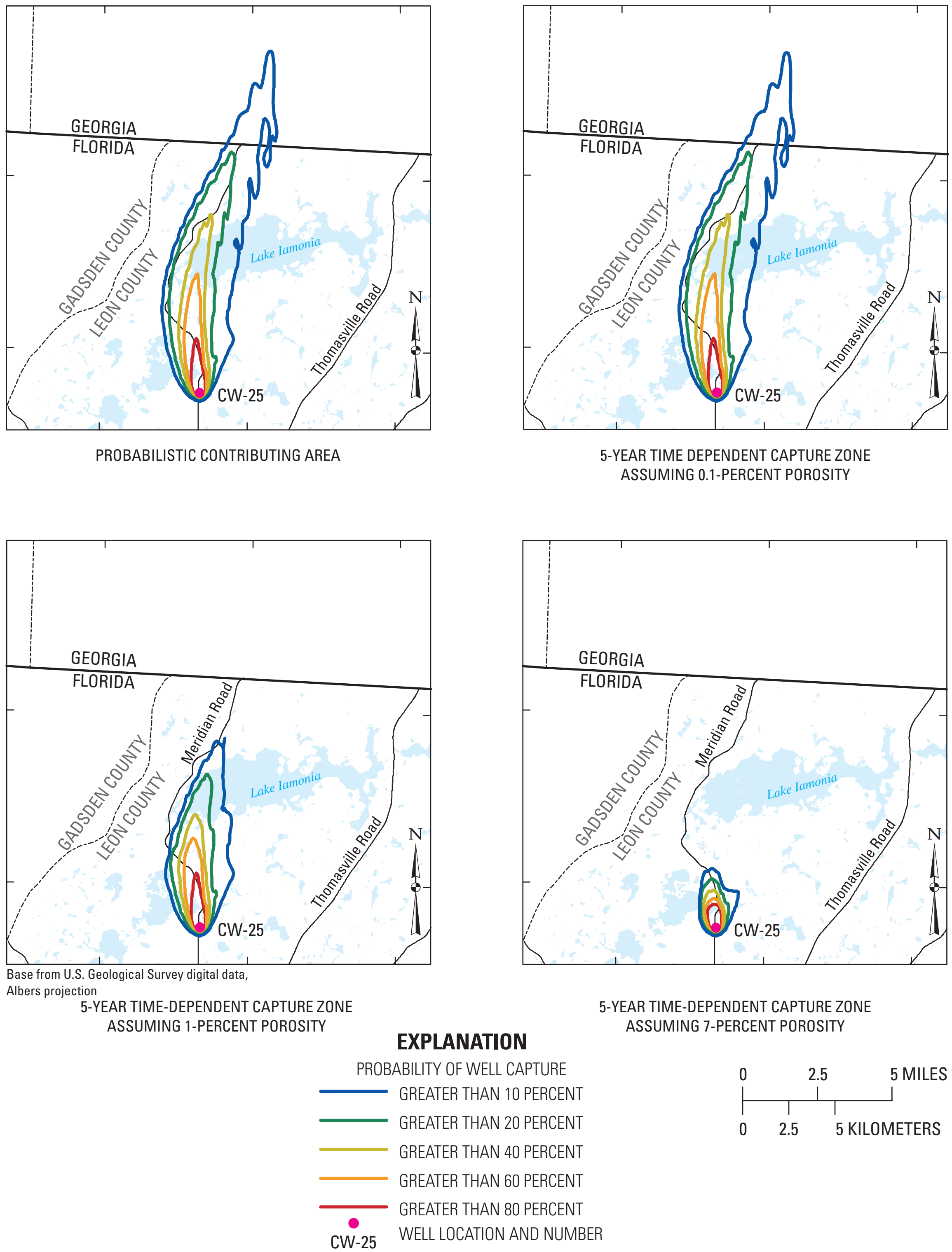

Figure 46. Probabilistic contributing areas and 5-year time-dependent capture zones for City of Tallahassee well CW-25, assuming various porosities for the Upper Floridan aquifer.

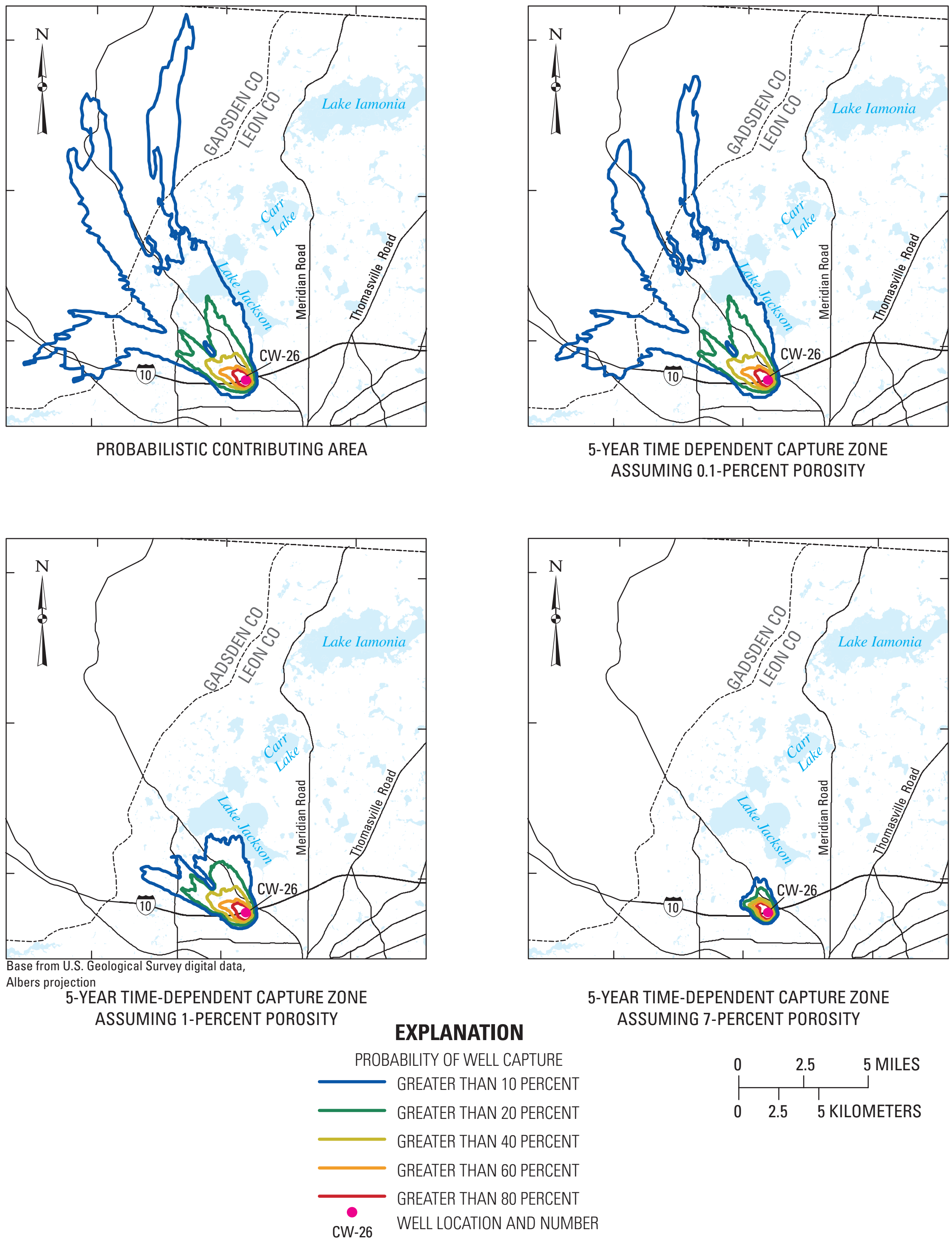

Figure 47. Probabilistic contributing areas and 5-year time-dependent capture zones for City of Tallahassee well CW-26, assuming various porosities for the Upper Floridan aquifer.

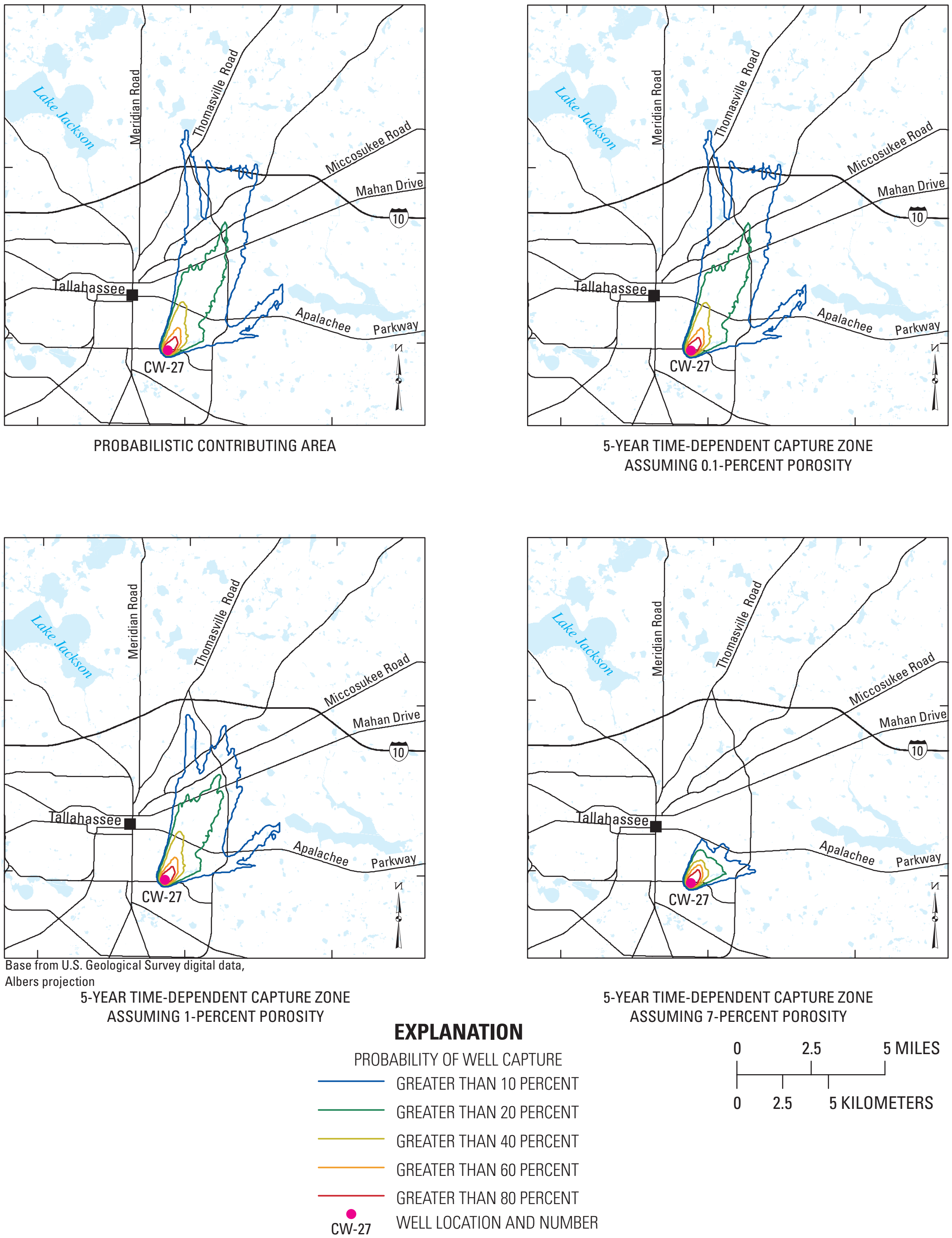

Figure 48. Probabilistic contributing areas and 5-year time-dependent capture zones for City of Tallahassee well CW-27, assuming various porosities for the Upper Floridan aquifer.

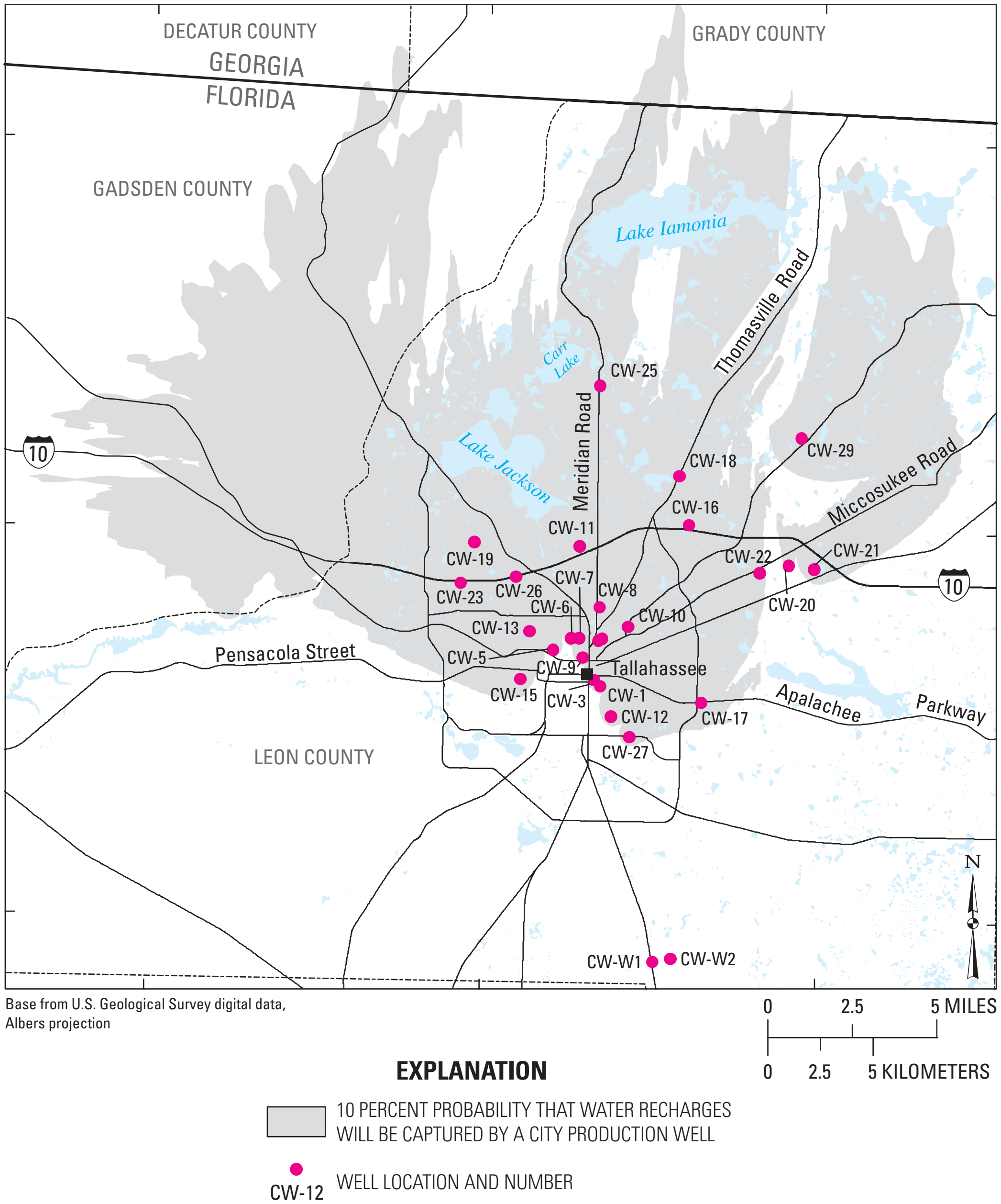

Figure 49. Probabilistic contributing area for all wells with greater than 10-percent probability of capture.

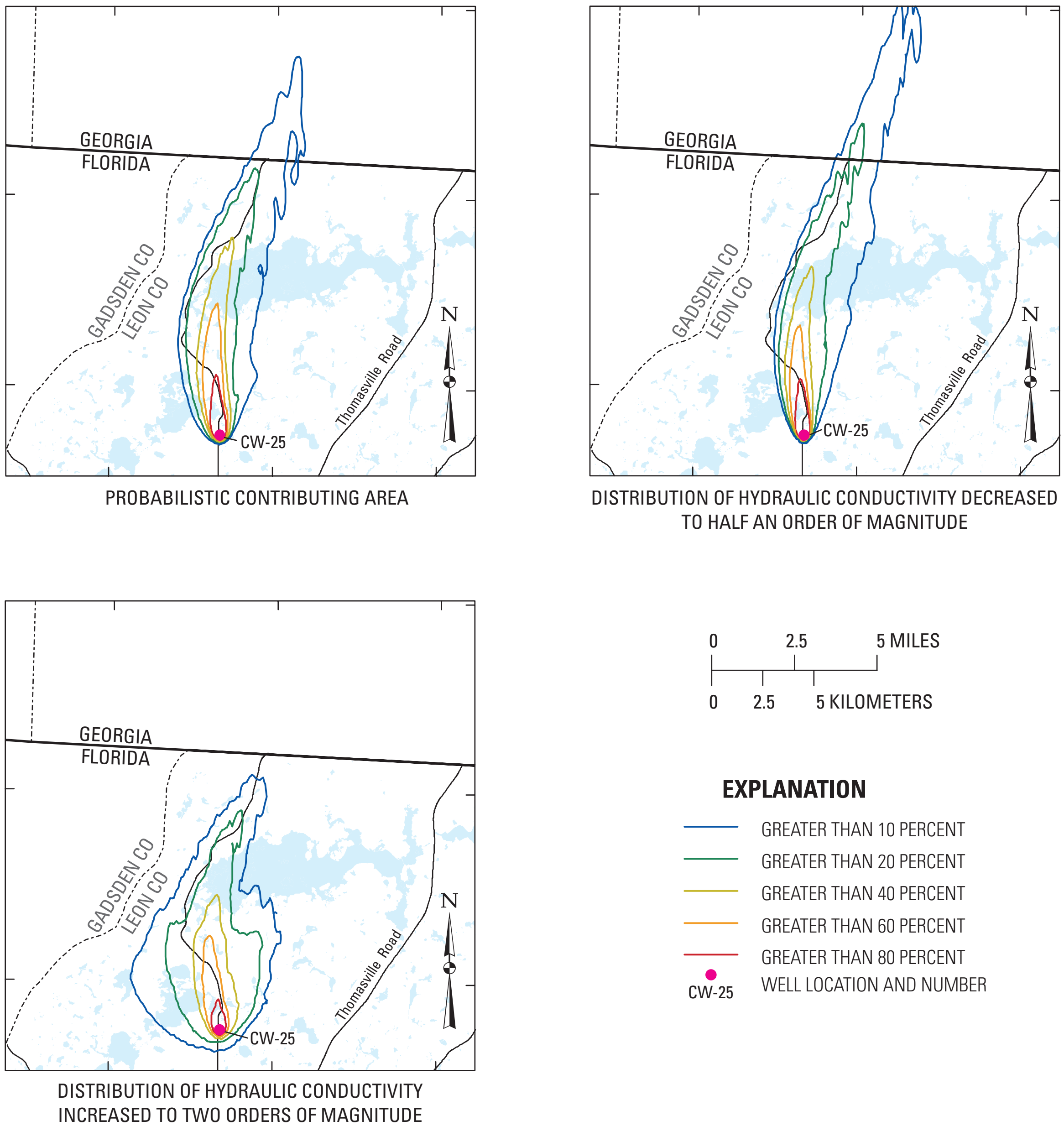

Figure 50. Probabilistic contributing areas for City of Tallahassee well CW-25, assuming various ranges of hydraulic conductivities.

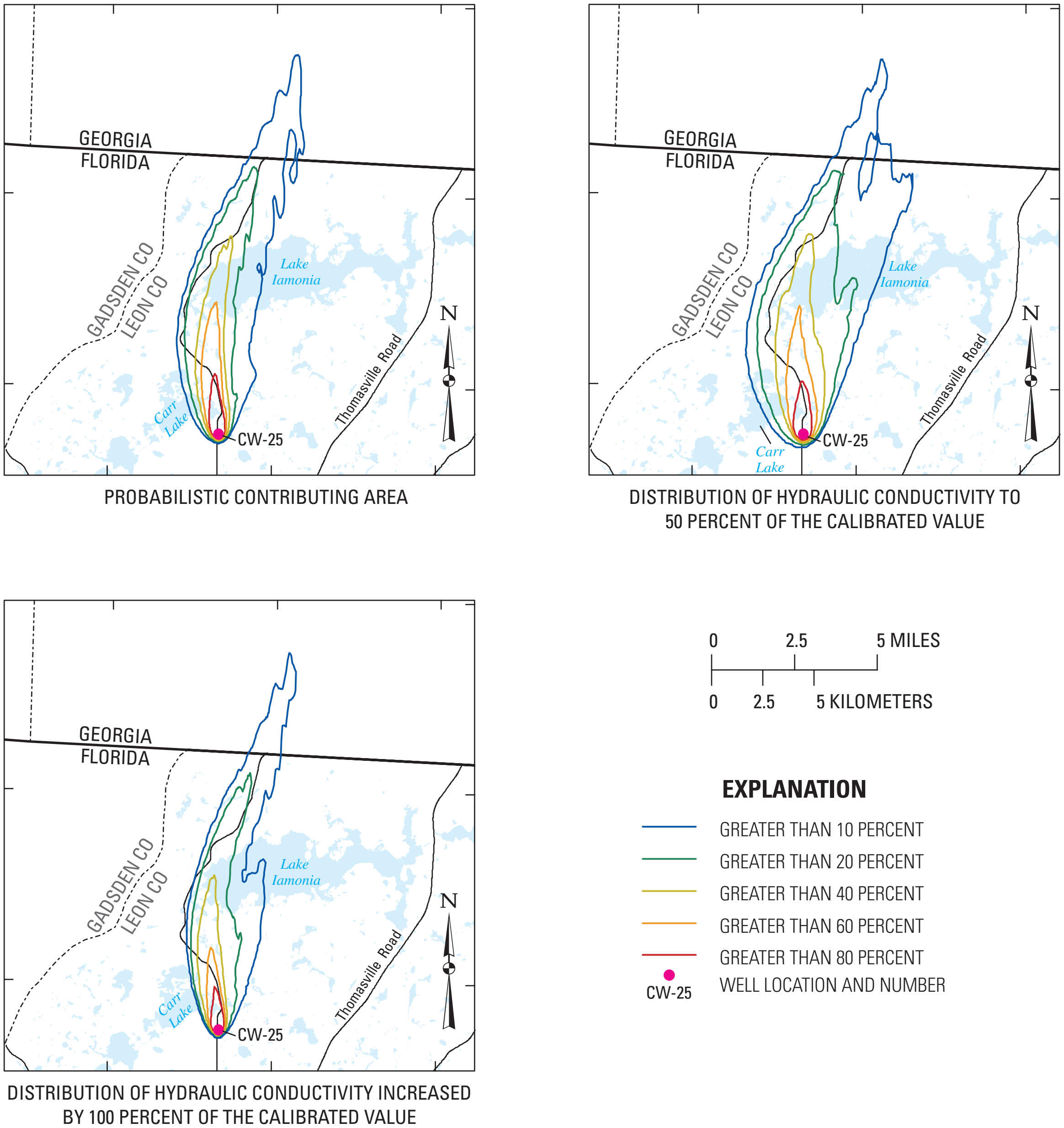

Figure 51. Probabilistic contributing areas for City of Tallahassee well CW-25, assuming different mean hydraulic conductivities.

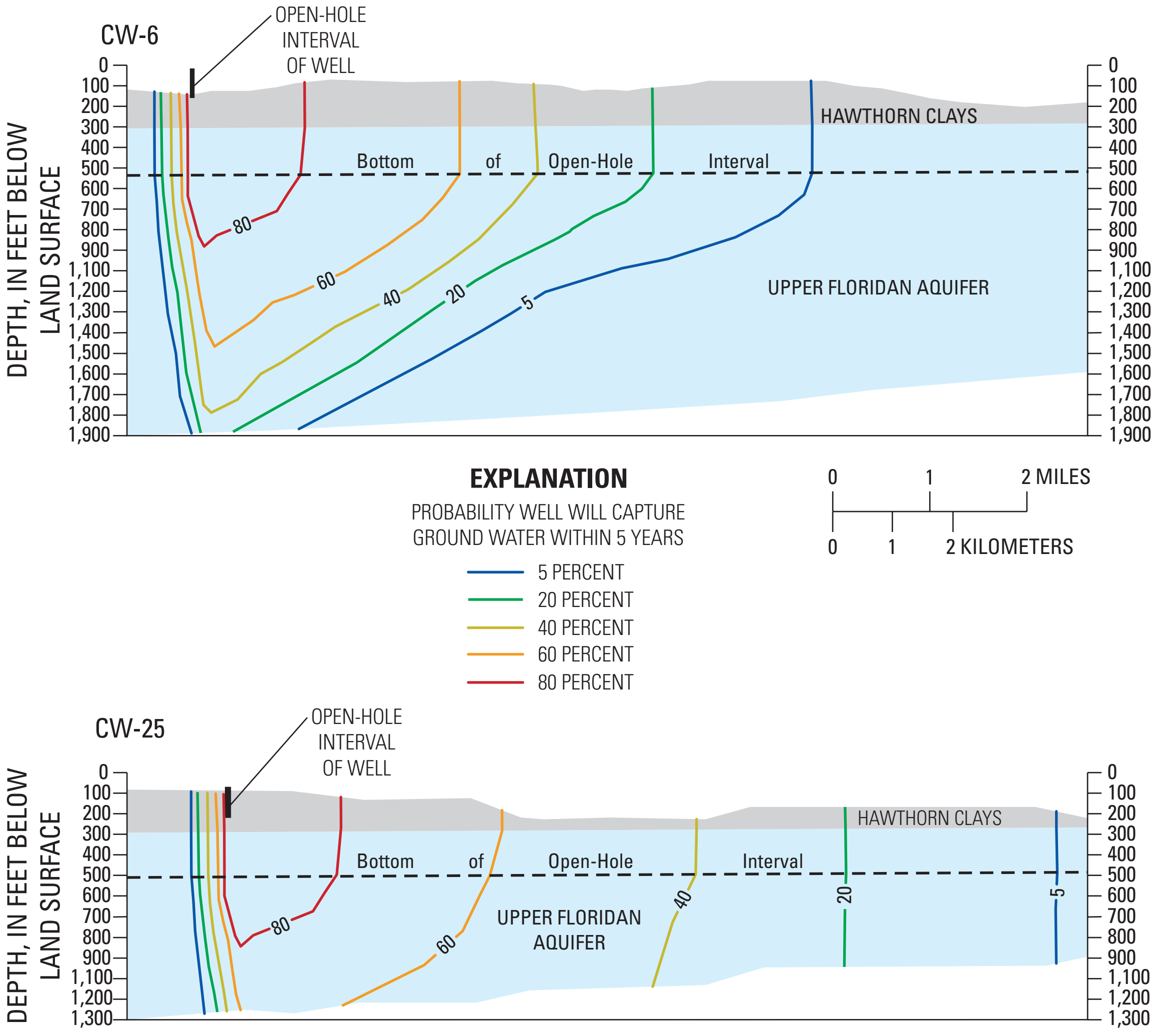

Figure 52. Probabilistic contributing areas for wells CW-6 and CW-25.

Limitations of Contributing-Area Delineation

The greatest source of potential error in delineating the contributing areas comes from the assumptions about effective porosity, hydraulic conductivity of the Upper Floridan aquifer, and recharge. The simulated probabilistic contributing areas assume uniform effective porosity and hydraulic conductivity within each of the individual zones shown in figure 16. The basis of this assumption is that the porosities and hydraulic conductivities beneath the City are the result of widespread secondary development (similar to that shown in caliper logs from the Lafayette Park deep well). If the secondary effective porosity development near a well has resulted in an extensively developed cave system, then the actual contributing area for a well could vary substantially from the predicted contributing area.

Model simulations assume steady-state conditions for the aquifer. Substantial increases in pumping within the study area could result in a long-term decline in aquifer water levels, and thus, steady-state conditions would not be appropriate. Long-term water levels, however, appear to be stable and steady-state conditions currently are present. Additionally, the size of the contributing area is highly dependent on recharge—the lower the recharge, the larger the contributing area.

Summary

Ground water from the Upper Floridan aquifer is the sole source of water supply for Tallahassee, Florida, and the surrounding area. The City of Tallahassee (the City) currently operates 28 water-supply wells; 26 are distributed throughout the City and 2 are located in Woodville, Florida. Most of these wells yield an ample supply of good quality water; however, water from some wells has low levels of tetrachloroethylene (PCE). The City removes the PCE from the water by passing it through granular-activated carbon units before distribution. To ensure that water-supply wells presently free of contamination remain clean, it is necessary to understand the ground-water flow system in sufficient detail to protect the contributing areas to these wells.

Ground-water samples were collected from four public-supply wells to determine the ages of the ground water (defined as the period of time that has passed since recharge occurred, or the traveltime). Generally, this period consists of the time it takes ground water to move through the water-table aquifer, Hawthorn clays, and Upper Floridan aquifer to the well. All of the wells are located within the Wakulla-Spring Creek recharge area. The water samples were analyzed for tritium (^3H), chlorofluorocarbons (CFCs), and sulfur hexafluoride (SF_6). Using data for three CFC compounds, apparent ground-water ages ranged from 7 years (well FP-1) to 31 years (well CW-11). For SF_6, apparent ages of ground water tended to be about 5 to 10 years younger than those from CFCs. Apparent ages based on the tritium/tritiogenic helium-3 ($^3H/^3He_{trit}$) method ranged from 26 (well FP-1) to 33 years (well CW-11). The $^3H/^3He_{trit}$ apparent ages are slightly older than those based on CFCs (within ±3 years) for wells CW-11 and CW-3, but are about 10 years older than CFC apparent ages for water from well FP-1. Water from all four wells had relatively high amounts (greater than 20 percent) of excess helium -4 (^4He) (greater than 20 percent), which may indicate a relatively deeper source for some portion of the water from the well. Although there are uncertainties and limitations associated with each age-dating method, it is worth noting that the three methods consistently indicate that the apparent age of ground water generally decreases from the northernmost site (well CW-25) to the southernmost site (well FP-1). This southward trend of decreasing ages is consistent with increasing amounts of recharge occurring as ground water moves from north to south.

Ground-water flow in the Upper Floridan aquifer was simulated using the U.S. Geological Survey modeling software MODFLOW. The largest model cells are 10,290 ft by 10,290 ft; the smallest cells are 400 ft by 400 ft, with each City well contained within its own small model cell. Layer 1 represents the water-table aquifer; layer 2 represents the Hawthorn clays; layer 3 represents the upper 200 ft of the Upper Floridan aquifer; and layer 4 extends from layer 3 to the bottom of the aquifer. The Upper Floridian aquifer was simulated with two layers to simulate withdrawals from City water-supply wells at their approximate open-hole intervals. After calibration, 183 simulated heads were within 10 ft of the 191 measured values and 112 of these values were within 5 ft. All simulated river gains were within 7 percent of the measured values.

The ground-water age data derived by geochemical and tracer analyses were used in combination with the flow model and particle tracking to determine an effective porosity for the Hawthorn clays and Upper Floridan aquifer. For each of the four wells in which age-dating samples were collected, the model was run 20 times and the effective porosity was systematically changed in both the Hawthorn clays and the Upper Floridan aquifer. The simulated effective porosities in the Hawthorn clays ranged from 12.5 to 35 percent, and the simulated effective porosities in the Upper Floridan aquifer ranged from 0.1 to 25 percent. Four simulations were run in which only the traveltime in the Upper Floridan aquifer was considered, which simulated the ground-water age where all of the recharge occurred through sinkholes and bypassed the clays. Eight combinations of porosities resulted in total traveltimes that fell within 3 years of the measured times. The effective porosities for the Upper Floridan aquifer that resulted in matches with measured porosities were averaged and produced an effective porosity of 7 percent; effective porosities for the Hawthorn clays that resulted in a match were averaged to produce an effective porosity of 22 percent.

Probabilistic contributing areas were determined for 26 City wells. For each probabilistic contributing area delineated, the model was run 100 times, and results were analyzed statistically. For each of the 100 runs, a different hydraulic conductivity for each of the zones was assigned to the Upper Floridan aquifer. The hydraulic conductivities were generated randomly assuming a lognormal probability distribution; the mean of the distribution was equal to the hydraulic conductivity from the calibrated model. After the 100 runs were completed, the data were analyzed to determine the probabilistic contributing area of each well using the following method: each particle's starting location was noted, and if, for example, on half the model runs a particle from a certain location was captured by a well, then that starting location was assigned a 50-percent probability of capture. This type of probability was calculated for each particle, and the probabilities for each starting location were contoured to determine probabilistic capture zones for each well.

The 5-year time-dependent capture zones (TDCZs), assuming effective porosities of 0.1, 1, and 7 percent, were delineated for four representative wells. Generally, the high probabilities of capture (greater than 40, 60, and 80 percent) were similar for all effective porosities, although the TDCZ delineated using a 7-percent porosity was slightly smaller; the low probabilities of capture (greater than 10 and 20 percent) showed a large range of variability.

Selected References

Applin, P.L., and Applin, E.R., 1944, Regional subsurface stratigraphy and structure of Florida and southern Georgia: Bulletin of the American Association of Petroleum Geologists, v. 28, no. 12, p. 1673-1742.

Böhlke J.K., 2002, Groundwater recharge and agricultural contamination: Hydrogeology Journal, v. 10, p. 153-179.

Busenberg, E., and Plummer, L.N., 1992, Use of chlorofluoromethanes ($CC_{13}F$ and $CC_{12}F_2$) as hydrologic tracers and age-dating tools: Example-The alluvium and terrace system of central Oklahoma: Water Resources Research, v. 28, p. 2257- 2283.

Busenberg, E., and Plummer, L.N., 2000, Dating young ground water with sulfur hexafluoride—Natural and anthropogenic sources of SF_6: Water Resources Research, v. 36, p. 3011-3030.

Busenberg, E., Weeks, E., Plummer, L.N., and Bartholemay, R.C., 1993, Age dating ground water by use of chlorofluorocarbons ($CC_{13}F$ and $CC_{12}F_2$), and distribution of chlorofluorocarbons in the unsaturated zone, Snake River Plain aquifer, Idaho National Engineering Laboratory, Idaho: U.S. Geological Survey Water-Resources Investigations Report 93-4054, 47 p.

Bush, P.W., and Johnston, R.H., 1988, Ground-water hydraulics, regional flow, and ground-water development of the Floridan aquifer system in Florida and parts of Georgia, South Carolina, and Alabama: U.S. Geological Survey Professional Paper 1403-C, 80 p.

Cook, P.G., and Böhlke, J.K., 1999, Determining time scales for groundwater flow and solute transport, *in* Cook, P.G., and Herczeg, A.L., eds., Environmental Tracers in Subsurface Hydrology: Boston, Kluwer Academic Publishers, p. 1-30.

Craig, H., 1961, Isotopic variations in meteoric waters: Science, v. 133, p. 1702-1703.

Davis, J.H., 1996, Hydraulic investigation and simulation of ground-water flow in the Upper Floridan aquifer of north-central Florida and southwestern Georgia and delineation of contributing areas for selected City of Tallahassee, Florida, water-supply wells: U.S. Geological Survey Water-Resources Investigations Report 95-4296, 55 p.

Deines, P., 1980, The carbon isotope composition of reduced organic carbon, in Fritz, P., and Fontes, J.S., eds., Handbook of Environmental Isotope Geochemistry: Amsterdam, Elsevier, v. 1A, p. 329-406.

Happell, J.D., Chanton, J.P., Top, Z., and Opsahl, S., 2006, CFC and $^3H/^3He$ age dating of water from Floridan aquifer springs: Journal of Hydrology, v. 319, no. 1-4, p. 410-426.

Harbaugh, A.W., Banta, E.R., Hill, M.C., and McDonald, M.G., 2000, MODFLOW-2000, the U.S. Geological Survey modular ground-water model—User guide to modularization concepts and the ground-water flow process: U.S. Geological Survey Open-File Report 00-92, 121 p.

Hazlett, T.J., and Kincaid, T.R., Loper, David, Davies, G.J., DeHan, Rodney, and McKinley, Casey, 2004, Realistic numerical modeling of ground-water flow based on quantitative site characterization in the Woodville Karst Plain of North Florida: Geological Society of America, 2004 Annual Meeting and Exposition, Abstracts with Programs, v. 36, no. 5, p. 31

Hendry, C.W., and Sproul, C.R., 1966, Geology and ground-water resources of Leon County, Florida: Florida Geological Survey Bulletin 47, 174 p.

Ho, D.T., and Schlosser, P., 2000, Atmospheric SF_6 near a large urban area: Geophysical Research Letters, v. 27, p. 1679-1682.

Huddlestun, P.F., 1988, A revision of the lithostratigraphic units of the Coastal Plain of Georgia, the Miocene through Holocene: Georgia Geological Survey Bulletin 104, 162 p.

Katz, B.G., 1992, Hydrochemistry of the Upper Floridan aquifer in Florida: U.S. Geological Survey Water-Resources Investigations Report 91-4196, 37 p.

Katz, B.G., Chelette, A.R., and Pratt, T.R., 2004, Use of chemical and isotopic tracers to assess nitrate contamination and ground water age, Woodville Karst Plain, USA: Journal of Hydrology, v. 289, no. 1 /4, p. 36-61.

Katz, B.G., Coplen, T.B., Bullen, T.D., and Davis, J.H., 1997, Use of chemical and isotopic tracers to characterize the interactions between ground water and surface water in mantled karst: Ground Water, v. 35, no. 6, p. 1014-1028.

Maddox, G.L., Lloyd, J.M., Scott, T.M., Upchurch, S.B., and Copeland, R. eds., 1992, Florida's ground-water quality monitoring network program: Background hydrogeochemistry: Florida Geological Survey Special Publication 34, 364 p.

McDonald, M.G., and Harbaugh, A.W., 1988, A modular three-dimensional finite-difference ground-water flow model: U.S. Geological Survey Techniques of Water-Resources Investigations, book 6, chap. A1, 528 p.

Michel, R.M., 1989, Tritium deposition in the continental United States, 1953-1983: U.S. Geological Survey Water-Resources Investigations Report 89-4072, 46 p.

Miller, J.A., 1986, Hydrologic framework of the Floridan aquifer system in Florida and in parts of Georgia, Alabama, and South Carolina: U.S. Geological Survey Professional Paper 1403-B, 91 p.

Plummer, L.N., and Busenberg, E., 1999, Chlorofluorocarbons, in Cook P.G., and Herczeg, A., eds., Environmental Tracers in Subsurface Hydrology: The Netherlands, Kluwer Academic Press, chap. 15, p. 441-478.

Pollock, D.W., 1989, Documentation of computer programs to compute and display pathlines using results from the U.S. Geological Survey modular three-dimensional finite-difference ground-water flow model: U.S. Geological Survey Open-File Report 89-381, 188 p.

Reilly, T.E., Plummer, L.N., Phillips, P.J., and Busenberg, E., 1994, The use of simulation and multiple environmental tracers to quantify groundwater flow in a shallow aquifer: Water Resources Research, v. 30, p. 421-433.

Schlosser, P., Stute, M., Dorr, H., Sonntag, C., and Munnich, K.O., 1988, Tritium/^{3}He dating of shallow groundwater: Earth Planetary Science Letters, v. 89, p. 353-362.

Schlosser, P., Stute, M., Sonntag, C., and Munnich, K.O., 1989, Tritiogenic ^{3}He in shallow ground water: Earth Planetary Science Letters, v. 94, p. 245-256.

Scott, T.M., 1988, The lithostratigraphy of the Hawthorn Group (Miocene) of Florida: Florida Geological Survey Bulletin 59, 148 p.

Solomon, D.K., Hunt, A., Poreda, R.J., 1996, Source of radiogenic helium-4 in shallow aquifers: Implications for dating young groundwater: Water Resources Research, v. 32, no. 6, p. 1805-1813.

Solomon, D.K., and Sudicky, E.A., 1991, Tritium and helium-3 isotope ratios for direct estimation of spatial variations in groundwater recharge: Water Resources Research, v. 27, no. 9, p. 2309- 2319.

U.S. Geological Survey, 1997 to present (2006), National field manual for the collection of water-quality data: U.S. Geological Survey Techniques of Water-Resources Investigations, book 9, chaps. A1-A9, v. 2, variously paged.